

INFORMATION TO USERS

This reproduction was made from a copy of a document sent to us for microfilming. While the most advanced technology has been used to photograph and reproduce this document, the quality of the reproduction is heavily dependent upon the quality of the material submitted.

The following explanation of techniques is provided to help clarify markings or notations which may appear on this reproduction.

1. The sign or "target" for pages apparently lacking from the document photographed is "Missing Page(s)". If it was possible to obtain the missing page(s) or section, they are spliced into the film along with adjacent pages. This may have necessitated cutting through an image and duplicating adjacent pages to assure complete continuity.
2. When an image on the film is obliterated with a round black mark, it is an indication of either blurred copy because of movement during exposure, duplicate copy, or copyrighted materials that should not have been filmed. For blurred pages, a good image of the page can be found in the adjacent frame. If copyrighted materials were deleted, a target note will appear listing the pages in the adjacent frame.
3. When a map, drawing or chart, etc., is part of the material being photographed, a definite method of "sectioning" the material has been followed. It is customary to begin filming at the upper left hand corner of a large sheet and to continue from left to right in equal sections with small overlaps. If necessary, sectioning is continued again—beginning below the first row and continuing on until complete.
4. For illustrations that cannot be satisfactorily reproduced by xerographic means, photographic prints can be purchased at additional cost and inserted into your xerographic copy. These prints are available upon request from the Dissertations Customer Services Department.
5. Some pages in any document may have indistinct print. In all cases the best available copy has been filmed.

**University
Microfilms
International**

300 N. Zeeb Road
Ann Arbor, MI 48106

1323055

SIMPSON, DAVID FRANK

GEOLOGY OF THE AMBLER 4B EXTENSION OF THE SMUCKER VOLCANOGENIC
MASSIVE SULFIDE DEPOSIT AMBLER DISTRICT, ALASKA

UNIVERSITY OF ALASKA

M.S. 1983

**University
Microfilms
International** 300 N. Zeeb Road, Ann Arbor, MI 48106

PLEASE NOTE:

In all cases this material has been filmed in the best possible way from the available copy. Problems encountered with this document have been identified here with a check mark .

1. Glossy photographs or pages _____
2. Colored illustrations, paper or print
3. Photographs with dark background _____
4. Illustrations are poor copy _____
5. Pages with black marks, not original copy _____
6. Print shows through as there is text on both sides of page _____
7. Indistinct, broken or small print on several pages
8. Print exceeds margin requirements _____
9. Tightly bound copy with print lost in spine _____
10. Computer printout pages with indistinct print _____
11. Page(s) _____ lacking when material received, and not available from school or author.
12. Page(s) _____ seem to be missing in numbering only as text follows.
13. Two pages numbered _____. Text follows.
14. Curling and wrinkled pages _____
15. Other _____

**University
Microfilms
International**

GEOLOGY OF THE AMBLER 4B EXTENSION OF THE SMUCKER
VOLCANOGENIC MASSIVE SULFIDE DEPOSIT
AMBLER DISTRICT, ALASKA

A
THESIS

Presented to the Faculty of the University of Alaska
in Partial Fulfillment of the Requirements
for the Degree of

MASTER OF SCIENCE

By
David F. Simpson, B. S.

Fairbanks, Alaska
December 1983

GEOLOGY OF THE AMBLER 4B EXTENSION OF THE SMUCKER
VOLCANOGENIC MASSIVE SULFIDE DEPOSIT
AMBLER DISTRICT, ALASKA

RECOMMENDED:

Samuel E. Swanson

Don Trigiton

Rain J. Nelson
Chairman, Advisory Committee

Richard B. Murray
Program Head

APPROVED:

M. Powell

Director of Geosciences

12/2/83

Date

W. S. Reubing
for Vice Chancellor for Research and Advanced Study

16 December 1983

Date

ABSTRACT

The Smucker volcanogenic massive sulfide deposit occurs at the western end of the Ambler district within the polymetamorphosed (amphibolite and greenschist) and polydeformed Brooks Range schist belt. The Ambler 4B extension of the Smucker deposit shows gross-scale original depositional features dissimilar from many classic volcanogenic massive sulfide deposits and detailed-scale metamorphic features similar to those seen in the surrounding host rocks.

The sulfide mineralization at Ambler 4B consists of blanket-like "Zone A" sulfides which are underlain by very irregular and lens-like "Zone B" sulfides. Zone B sulfides may represent a diffuse feeder system that deposited Zone A sulfides onto the sea floor.

Effects of the deformation observed in the sulfides includes the plastic and brittle deformation, annealing, and rotation of sulfides. Polyphase deformation of the sulfides is indicated by the presence of both relatively iron-poor and iron-rich sphalerite inclusions in pyrite porphyroblasts.

TABLE OF CONTENTS

	Page
ABSTRACT.	iii
TABLE OF CONTENTS	iv
LIST OF FIGURES	vii
LIST OF TABLES.	ix
LIST OF PLATES.	x
ACKNOWLEDGEMENTS.	xi
INTRODUCTION	1
PREVIOUS WORK	6
REGIONAL GEOLOGY.	9
LITHOLOGIC UNITS.	12
Terminology	12
Graphitic-Mica-Quartz Schist (Pzgm)	17
Graphitic Schist (Pzgs)	18
Calc-Schist (Pzcs).	20
Calc-Silicate Schist (Pzss)	21
Metabasite (Pzgt)	23
Calcareous Chlorite Schist (Pzcc)	24

TABLE OF CONTENTS - continued

	Page
Feldspathic mica-quartz schist (Pzmq)	25
Metarhyolite Tuff (Pzmt).	27
Microcline-mica-quartz schist (Pzbs).	29
STRATIGRAPHY.	31
Area 1 Stratigraphy.	33
Area 2 Stratigraphy.	38
Area 3 Stratigraphy.	38
STRUCTURE	40
D1 Deformation	40
D2 Deformation	42
D3 Deformation	47
D4 and D5 Deformation.	47
METAMORPHISM.	49
D2 Metamorphism.	49
D3 Metamorphism.	51
Retrograde Metamorphism.	55
SUMMARY OF DEFORMATIONAL EVENTS IN THE AMBLER DISTRICT.	56
SULFIDE MINERALIZATION.	58

TABLE OF CONTENTS - continued

	Page
Zone A Sulfides.	59
Zone B Sulfides.	64
Discussion of Ore Genesis.	69
METAMORPHISM OF THE SULFIDES.	72
Changes in Fabric.	72
Mobilization of Minerals	88
Changes in Mineralogy.	90
Mobilization of Elements	91
Summary and Scenario for Textural Development.	95
COMPARISON OF AMBLER DISTRICT DEPOSITS.	97
SUMMARY AND CONCLUSIONS	118
APPENDIX I.	123
REFERENCES CITED.	127

LIST OF FIGURES

Figure Number	Page
1 General Geology of the Ambler District	2
2 Juice Mountain and Ambler 4B	3
3 Geologic Map of Ambler 4B.	4
4 Stratigraphic Columns of Ambler 4B Lithologies	32
5 Stratigraphic Variations of the Felsic Units Along Strike	34
6 Contours of Poles to S1 Schistosity.	43
7 Contours of Poles to S2 Schistosity.	45
8 Contours of L2 Lineations.	46
9 Photomicrograph of D2 Hornblende Being Cut by D3 Glaucophane.	52
10 Photomicrograph of D3 Glaucophane Being Altered by Actinolite	54
11 Unfolded Cross-Section of DDH Ore Intercepts	60
12 Generalized Cross-Section of Zone A and Zone B Sulfide Horizons	61
13 Photograph of Symmetrically-Zoned Massive Sulfide Layer from Zone B.	66
14 Photomicrograph of Radiating Fractures in Pyrite Grains	74

LIST OF FIGURES - continued

Figure Number	Page
15 Photomicrograph of Fractured Pyrite Grains	75
16 Photomicrograph of an Annealed Mass of Pyrite Grains	76
17 Photomicrograph of Inclusions in Annealed Pyrite Grains	77
18 Photomicrograph of Rounded Pyrite Grains	79
19 Photomicrograph of Polygonized Pyrite Grains	80
20 Photomicrograph of Rounded Pyrite Grains	81
21 Logarithmic Plot of Pyrite Grain Size as a Function of Metamorphic Grade.	83
22 Plot of Average Pyrite Grain Size Versus Percent Total Sulfides	85
23 Frequency Distributions of Pyrite Morphology as a Function of Grain Size	87
24 Photomicrograph of Fractured Pyrite Grains Infilled by Galena	89
25 Activity of Oxygen vs. Activity of Sulfur.	92
26 Photomicrograph of Sphalerite Inclusions in Pyrite . .	93
27 Photomicrograph of Sphalerite Inclusions in Pyrite . .	94
28 Ambler District Stratigraphic Columns.	102

LIST OF TABLES

Table Number	Page
1 Correlation of Ambler District Lithologic Unit Names .	13
2 Distinguishing Features of Lithologic Units Exposed at Ambler 4B	14
3 Approximate Modal Abundances for Rocks Exposed at Ambler 4B.	16
4 Approximate Modal Abundances for Samples Collected from Pzmt and Pzmq, Traverses 1, 2 and 3	36
5 Deformational History of the Ambler 4B Area.	41
6 Metamorphic Mineral Parageneses.	50
7 Approximate Mineral Modal Abundances: Zone A and Zone B Sulfide Horizons.	63
8 X-Ray Data for Chlorite Samples.	68
9 Metamorphic Data for Deposits Presented in Figure 23	84
10 Geologic Features of Some Ambler District Sulfide Deposits	98
11 Summary of Geologic Features of Ambler District, Bathurst District, Abitibi Belt, Iberian Pyrite Belt, and Kuroko Massive Sulfide Deposits.	109

LIST OF PLATES

Plates	Page
I Geologic Map of Ambler 4B.	in pocket
II North-South Cross-Section.	in pocket

ACKNOWLEDGMENTS

This project was supported by Bear Creek Mining Company. I would like to thank Russell Babcock and Jay Hammitt of Bear Creek's Anchorage office for their continued support and for allowing me to release this information. My summer field associates, Mark Stevens, Monica O'Keefe, Betsy Turner, and Don Taylor, added much to this project through discussion. I would like to thank Murray Hitzman and Jeannine Schmidt for their help at the beginning of this study.

I am indebted to Rainer Newberry for helping make this project such an exciting endeavor. His advice and encouragement are deeply appreciated.

Samuel Swanson critiqued the manuscript and made valuable suggestions concerning many aspects of the study. My sincere appreciation is extended to Don Triplehorn, Jay Hammitt, and my father, Donald Simpson, for their review of the manuscript.

Lastly, I would like to thank Marcia Gennette for preparing the manuscript and for her friendship throughout this project.

Introduction

The Smucker deposit is a volcanogenic massive sulfide deposit that is located at the western end of the Ambler district approximately 300 miles (480 kilometers) north of Fairbanks, 150 miles (240 kilometers) east of Kotzebue, 185 miles (300 kilometers) west of the Pipeline Haul Road, and 18 miles (29 kilometers) northwest of Bornite, the Bear Creek Mining Company (BCMC) camp from which this study was mounted (Fig. 1). It occurs in a thick sequence of metapelitic and metavolcanic rocks. The Ambler 4B extension of the Smucker deposit was the main area studied (Plates I, II, Figs. 2, 3). The Ambler 4B extension includes both BCMC and GCO Minerals Company-Houston Oil and Minerals Exploration Company (GCO-HOMEX) claim blocks that cover most of the southeastern slopes of Juice Mountain (Plate I, Figs. 2,3) where the sulfide horizon outcrops. The Smucker deposit lies to the west-northwest of Juice Mountain and is currently held by the Anaconda Minerals Company (1983). Although most of the field work for this study was focused in the Ambler 4B area, work was not restricted to the BCMC-GCO-HOMEX claim block.

Field work was conducted between June 3 and August 25, 1982. Access to the area was provided by BCMC from Bornite by helicopter. Mapping was done on 1:2400 topographic maps and on 1:6000 color air photos. At Bornite, BCMC diamond drill holes

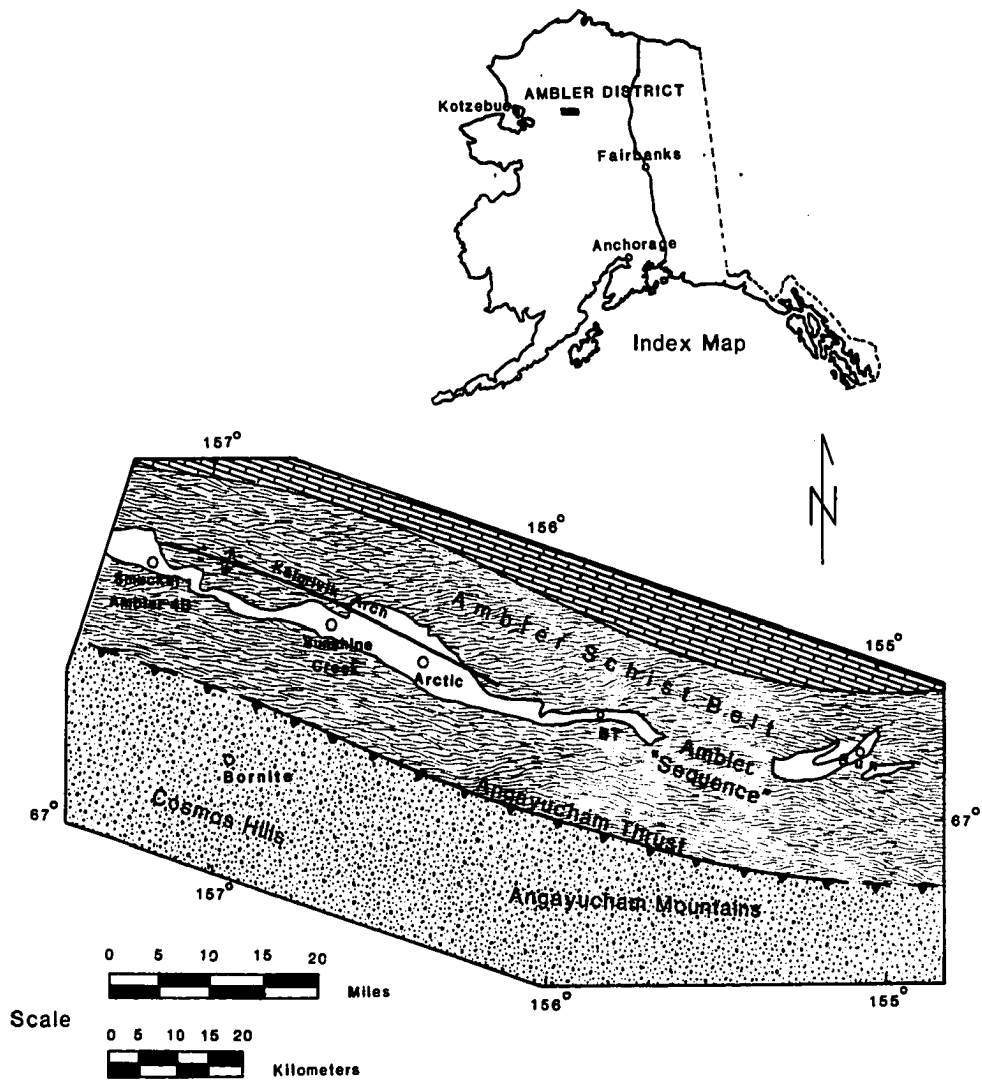


Figure 1. Index map of Alaska and generalized geologic map of the Ambler district. Generalized geologic map of the Ambler district modified from Hitzman and others (1982).

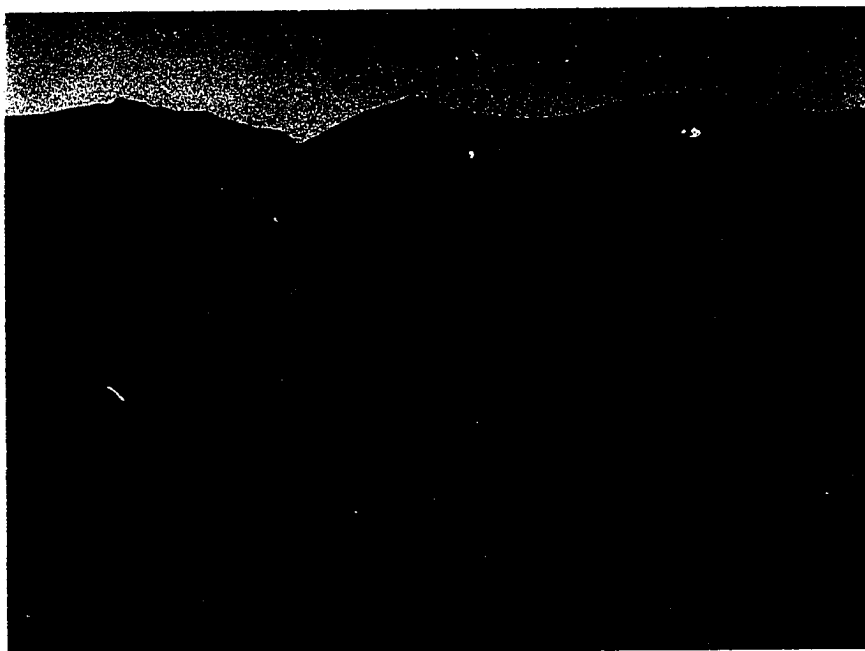


Figure 2. Looking West across Kalurivik Creek at Juice Mountain and Ambler 4B.

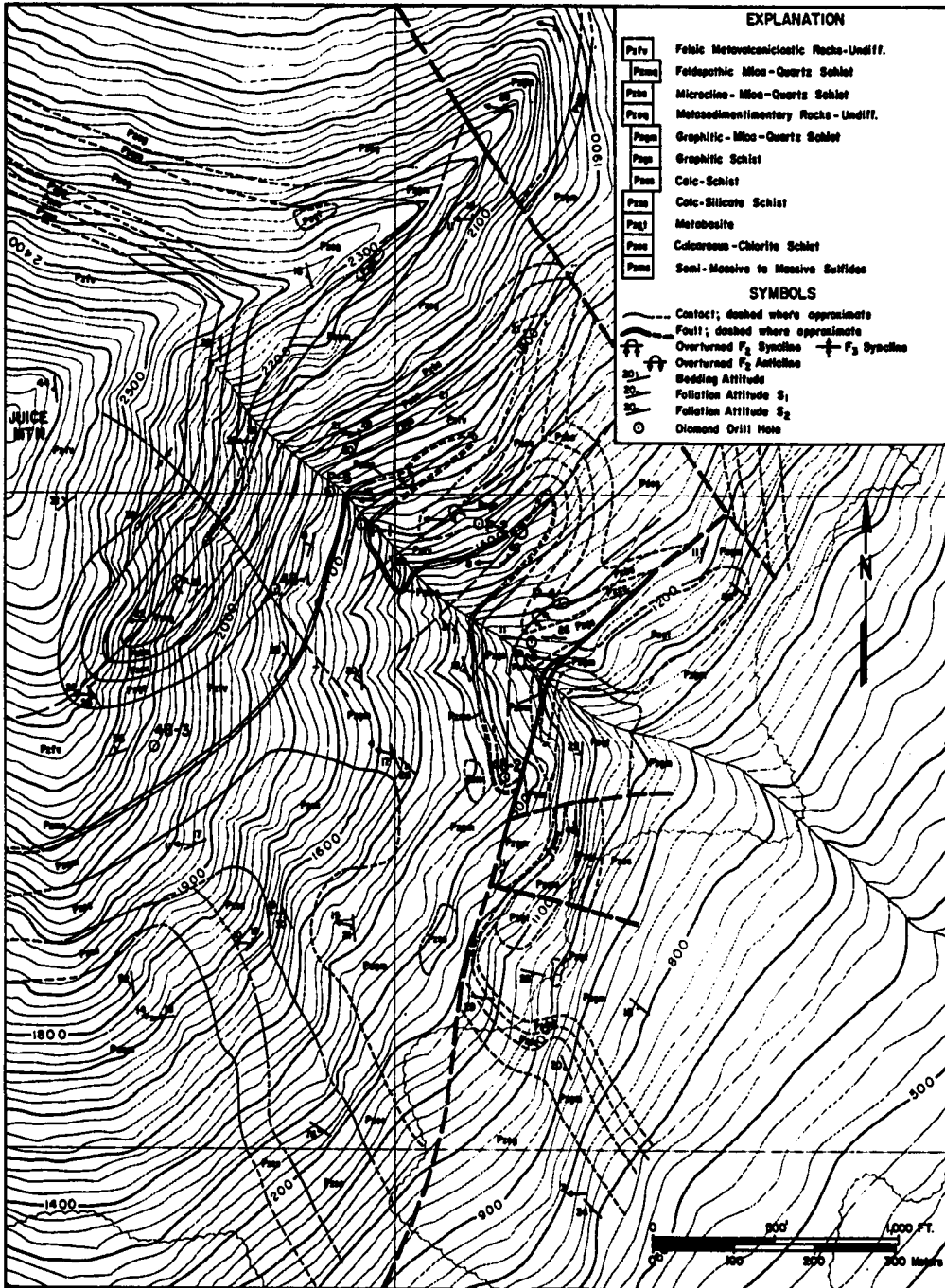


Figure 3. Generalized geologic map of Ambler 4B.

(DDH's) 1 and 2 were re-logged, and DDH-3 was logged. In October, 1982, in Anchorage, the author re-logged in detail ore intercepts from five GCO-HOMEX DDH's. Approximately 120 samples for thin section and 25 for polished section were collected in the field and from drill core.

The purpose of this investigation was two-fold. The first and major purpose was to define the structural deformation and metamorphism that affected the gangue rocks of the Ambler 4B area and to describe the effects on the massive sulfide mineralization. With this information in hand, the second purpose of this investigation was to compare the geology of the Ambler 4B area with other Ambler district massive sulfide deposits and then to compare Ambler district deposits with other massive sulfide districts on a worldwide basis.

Previous Work

Previous work in the Ambler district has been done by the United States Geological Survey (USGS) and the Alaska Division of Geological and Geophysical Surveys (ADGGS). This includes mapping (1:250,000 to 1:1,000,000) and geochemical sampling by Fritts, 1969, 1970a, 1970b; Fritts and others, 1972; Patton and others, 1968; Pessel and others, 1972, 1973; Pessel and Brosge, 1977; Brosge and Pessel, 1977; Grybeck, 1977a, 1977b; Grybeck and others, 1977; Grybeck and DeYoung, 1978; Mayfield and Grybeck, 1978; and Hitzman and others, 1982. Fritts (1969, 1970b) discussed the stratigraphy and structural history of the Cosmos Hills (Fig. 1), and briefly summarized the geology of the Angayucham Mountains (1970a) (Fig. 1). Wiltse (1975) discussed the geology of the Arctic deposit and proposed a volcanogenic origin for the sulfide deposits in the Ambler district. Gilbert and others (1977) discussed the petrology and structure of Ruby Ridge.

Numerous age dates have been published for Ambler district rocks. Turner (1973) and Turner and others (1978) report K-Ar geochronological data for rocks collected throughout the district, including data for Smucker rocks. The work of Turner (1973) and Turner and others (1978) defines two metamorphic events. Smith and others (1977, 1978) discussed evidence of a probable Devonian age for deposition of Ambler district rocks and sulfide deposits. Their evidence includes paleontological and Pb-isotope data.

Mining companies have been active in the Ambler schist belt since 1962. These include, at one time or another, the Bear Creek Mining Company (BCMC), GCO Minerals Company (GCO), Anaconda Minerals Company, and Sunshine, Cominco, and Noranda mining companies. The most recent publication by Hitzman and others (1982) is a 1:125,000 map of the Ambler district compiled from work done by Anaconda Minerals Company geologists between 1975 and 1980. Also presented by Hitzman and others (1982) are stratigraphic sections, cross-sections, a distribution of metamorphic facies, a summary and tabulation of geochronological and paleontological data, and chemical data for rocks of the district. Lead isotope ratios for a galena sample from the Smucker deposit are included in this report. They also suggest that the tectonic setting of the southwestern Brooks Range during Devonian time was one of a rifted continental margin with bimodal volcanism, associated exhalative mineralization along rift faults, accumulation of sedimentary sequences in grabens, and development of carbonate banks on horsts.

Previous work of particular importance to this study includes graduate work by Carden (1978), Hitzman (1978), Nelsen (1979), Kelsey (1979), Zdepski (1980), and Schmidt (1983). Carden (1978) made a comparative study of blueschists and greenschists in the Brooks Range and Kodiak-Seldovia schist belts. Hitzman (1978) studied the geology of the BT claim group (Fig. 1) and described six

periods of deformation (D1 to D6) and two periods of regional metamorphism (D2 and D3). He also discussed two zones of stratiform sulfide mineralization that occur on the BT claim block. Nelsen (1979) discusses the geology and blueschist petrology of the Western Ambler Schist belt. Kelsey (1979) studied the petrology of metamorphic rocks in the Arctic, Luk, and Lost areas. He was primarily interested in the petrology of the felsic metavolcanic rocks exposed in the three areas studied. Zdepski (1980) studied the stratigraphy, mineralogy, and zonal relations of the Sun massive sulfide deposit (Fig. 1). Sulfide mineralization studied by Zdepski (1980) consists of four stratiform banded, massive to semi-massive sulfide horizons. Schmidt (1983), in the most detailed and rigorous study to date of an Ambler district deposit, described the geology and geochemistry of the Arctic deposit (Fig. 1). She described the mineralogy, ore occurrences, alteration, mineral composition, genesis, and setting of the Arctic deposit.

Regional Geology

The regional geology of the southwestern Brooks Range can be divided into three west-northwest belts. These belts, from south to north, include the Cosmos Hills-Angayucham Mountains belt, the Ambler Schist belt, and rocks of the central Brooks Range (Fig. 1). The reader is referred to more detailed descriptions of the regional geology by Wiltse (1975), Nelsen (1979), Kelsey (1979), and Zdepski (1980).

The Cosmos Hills-Angayucham Mountains belt consists of upper Paleozoic to Middle Mesozoic mafic volcanic rocks, Devonian carbonates, phyllites, pelitic schists, and Cretaceous metasedimentary rocks (Hitzman and others, 1982). The Cosmos Hills-Angayucham Mountains belt is bounded on the north by the Angayucham thrust.

The Ambler Schist belt or Ambler Mineral district, as defined by Smith and others (1978), is bounded on the south by the Ambler Lowlands and on the north by the Walker Lake lineament. It is bounded on the west by the Redstone River and on the east by the Reed River (Hitzman and others, 1982). The Ambler Schist belt consists of a unit of metapelitic rocks 25,000 to 40,000 feet (7,600 to 12,000 m) in thickness that encloses a unit of metavolcanic and metasedimentary rocks 3,000 to 4,000 feet (900 to 1,200 m) in

thickness (Smith and others, 1977, 1978). The metavolcanic rocks host the sulfide deposits and are referred to as the "Ambler Sequence" by Hitzman and others (1982). Although some controversy exists as to the age of rocks in the Ambler district, a Devonian age, based on fossils identified in marbles within the district, is now generally accepted (Hitzman and others, 1982).

The major structural feature of the central and western Ambler district is the Kalurivik Arch (Fig. 1). It has been described as a simple anticlinorium by Pessel and others (1972) and as a nappe-like structure by Forbes and others (1973).

The Ambler district is bounded on the north by the Walker Lake lineament. It was originally described and mapped by Fritts and others (1972). The lineament has been described as a thrust fault by Pessel and others (1972), as an unconformity by Wiltse (1975), and as a facies change which is locally faulted by Smith and others (1978). The Walker Lake lineament is believed to be an unconformity to the west and a faulted unconformity to the east by Gilbert and others (1977), Hitzman (1978), and Turner and others (1978).

Rocks to the north of the Walker Lake lineament consist of generally north-dipping Paleozoic carbonate, quartzitic, and pelitic strata of the central Brooks Range. These rocks have been intruded

by plutons of most probable Devonian (Dillon and others, 1980) or possible Cretaceous (Grybeck, 1977a) age.

The sulfide deposits of the Ambler district can probably be classified as volcanogenic massive sulfide deposits (Hitzman and others, 1982). Features that Ambler district deposits have in common with other volcanogenic massive sulfide deposits include morphologies, metal zonation patterns, alteration styles, and associated host rock types.

Lithologic Units

Terminology

The terminology used in this study is one that has been developed in recent years by BCMC. This terminology is a compilation of the descriptive techniques used by Kelsey (1979), J. Schmidt, K. Hill, and BCMC geologists. Rock names are based on major minerals present in hand sample.

Recently, Ambler district rocks were more formally named by Hitzman and others (1982). As most of the work for this project was completed before this information was published, rock names and descriptions formulated at the beginning of this study will still be used. It should be noted that rock names used in this report correlate well with the more formalized names. Table 1 lists the lithologic names used in this report and Hitzman and others' (1982) names. Correlations are made when possible.

Distinguishing features of the rock units at Ambler 4B are summarized in Table 2, and Table 3 lists approximate modal abundances of the units.

In the following descriptions, helicitic crystals refer to crystals that have grown during metamorphism including oriented groundmass minerals. Helicitic structure refers to a straight or

TABLE 1. Correlation of Ambler District Lithologic Unit Names

Names Used in This Study	Names Presented by Hitzman and others (1982)
Graphitic-mica-quartz schist (Pzgm)	Anirak schist (Pzas)
Graphitic schist (Pzgs)	Anirak schist (Pzg)
Calc-schist (Pzcs)	Micaceous calc-schist (Pzsc)
Calc-silicate schist (Pzss)	Banded calc-silicate schist (Pzgn)
Metabasite (Pzgt)	Greenstone and metabasite (Pzg)
Feldspathic mica-quartz schist (Pzmq)	Felsic schist (Dsf)
Metarhyolite tuff (Pzmt)	Sparsely porphyritic rhyolite (Dr)
Microcline-mica-quartz schist (Pzbs)	Rhyolite porphyry (Dbs)

TABLE 2. Distinguishing Features of Lithologic Units Exposed at Ambler 4B

Unit	Grain Size	Fresh Color	Weathered Color	Outcrop Characteristics
Pzgm Graphitic-Mica- Quartz Schist	fine to medium	gray to green to brown	dark brown	resistant ridge former
Pzgs Graphitic Schist	fine to medium	brown to black	reddish-brown	resistant cliff former to poorly-exposed saddles
Pzcs Calc-Schist	fine	gray	light gray	moderately resistant
Pzss Calc-Silicate Schist	fine to medium	pale green to green	light green	resistant
Pzgt Metabasites	fine to medium	light green to green	dark green	highly resistant cliffs
Pzcc Calcareous Chlorite Schist	fine to medium	light green	olive green	moderately resistant
Pzmq Feldspathic Mica- Quartz Schist	fine to medium	light green to white	light brown to greenish gray	moderately resistant
Pznt Metarhyolite tuff	fine to medium	light green to gray to white	white to buff	very resistant
Pzbs Microcline-Mica- Quartz Schist	coarse	tan to light gray	gray to brown	moderately resistant

* Grain size: Fine = < 1 mm; Medium = 1 to 5 mm; Coarse = > 5 mm

TABLE 2. - continued

Talus	Megascopic Structural Elements	Microscopic Structural Elements	Nature of Contacts
fissile to blocky (depending on S1-S2)	well foliated	S1, S2, S3 well preserved	Gradational with: Pzgs, Pzcs, Pzcc; Sharp with: Pzgt, Pzss, Pzbs, Pzmq
fissile to platy	well foliated	S1, S2, S3 well preserved	Gradational with: Pzcs, Pzgm; Sharp with: Pzmt
platy	poor to moderately foliated	S1, S2 poorly preserved	Gradational with: Pzgm, Pzgs, Pzss, Pzgt; Sharp with: Pzbs, Pzgt, Pzmq
platy to blocky	banded, large amplitude isoclinal folds well preserved	S1, S2, S3 poorly preserved	Gradational with: Pzcs, Pzgt; Sharp with: Pzgm, Pzgt, Pzcc
blocky	poorly foliated, joints well preserved	S2, S3 poorly preserved	Gradational with: Pzcs, Pzss; Sharp with: Pzcs, Pzgm, Pzss, Pzmq
platy	well foliated	S1, S2, S3 well preserved	Gradational with: Pzgm; Sharp with: Pzss
platy	well foliated, large amplitude folds well preserved	S1, S2, S3 well preserved	Gradational with: Pzmt; Sharp with: Pzgt, Pzms, Pzcs, Pzgm
blocky	banded, joints and large amplitude folds well preserved	S1, S2, S3 poorly preserved	Gradational with: Pzmq; Sharp with: Pzgs
platy	well foliated	S1, S2, S3 well preserved	Sharp with: Pzgm, Pzcs

TABLE 3. Approximate Modal Mineral Abundances for Rocks Exposed at Ambler 4B. *

Unit	Quartz	Microcline	Albite	White Mica	Chlorite	Epidote-Clinzoisite	Garnet	Actinolite	Glaucophane	Calcite	Sphene	Zircon	Tourmaline	Graphite	Biotite	Apatite	Opales	Fe-Carbonate
Pzgm Graphitic-Mica- Quartz Schist	10-45	---	10-30	15-50	0-25	0- 2	--	---	--	0- 5	0-2	Tr	Tr	1-5	Tr	Tr	0-4	--
Pzgs Graphitic Schist	20-65	---	6-25	15-30	0-15	Tr	--	---	--	0- 2	0-3	Tr	--	5-8	Tr	Tr	0-5	--
Pzcs Calc-Schist	10-30	---	5-30	25-30	3-45	0- 2	--	---	--	15-25	0-2	--	Tr	Tr	---	Tr	Tr	--
Pzss Calc-Silicate Schist	1-30	---	2-35	0- 5	10-50	0-30	0-15	0-30	0-40	0-20	1-3	--	Tr	---	0-5	Tr	Tr	0-25
Pzgt Metabasites	1-20	---	1-20	0- 2	15-25	20-25	7-15	15-25	Tr	2-15	0-2	--	--	---	---	Tr	Tr	0- 5
Pzcc Calcareous Chlorite Schist	10-30	---	2-40	5-20	20-35	Tr	--	---	--	0-20	0-5	Tr	Tr	Tr	Tr	Tr	0-2	0-10
Pzmq Feldspathic-Mica- Quartz Schist	14-40	---	30-55	9-20	0-25	Tr	--	---	--	Tr	Tr	Tr	--	Tr	Tr	0-15	0-2	--
Pzmt Metarhyolite tuff	15-40	15-50	5-35	1-23	Tr	0- 3	--	---	--	Tr	0-2	Tr	--	---	0-1	Tr	0-3	--
Pzbs Microcline-Mica- Quartz Schist	15-30	15-45	30-35	10-15	Tr	Tr	--	---	--	Tr	1-2	--	--	---	---	Tr	0-1	--

* Table does not include mineral abundances for the sulfide horizon.

curved inclusion pattern which is a structural element of the rock older than the crystal, and which has been preserved during the growth of the crystal (Spry, 1969).

Graphitic-Mica-Quartz Schist

The graphitic-mica-quartz schist (Pzgm) comprises the most abundant rock type at Ambler 4B. In the past, this unit has been referred to as "country rock schist."

It is a fine- to medium-grained, gray- to green- to brown-colored, well-foliated rock. Weathered surfaces are usually a dark brown color. Outcrops are resistant and form ridges.

Structural elements preserved in the graphitic-mica-quartz schist include two foliations (S1 and S2) and, in some cases, a weak crenulation cleavage (S3). Smoky and white quartz pods and segregations to 10 cm are common. The segregations typically follow the S2 foliation.

In thin section, the graphitic-mica-quartz schist consists of a well-foliated rock. Quartz grains up to 2 mm in diameter have poorly sutured to moderately polygonized boundaries. White mica blades to 2 mm in length contain inclusions of trace amounts of graphite. Along with chlorite, white mica blades define two foliations (S1 and S2) observed in most samples. Polygonized mica

grains are common in noses of microfolds. Helicitic albite porphyroblasts to 1.8 mm often enclose older foliations. An contents from poorly developed albite twins range from An₃ to An₇. Sulfide phases include rare, euhedral pyrite grains and a red to yellow, translucent, anhedral mineral that is probably sphalerite.

The graphitic-mica-quartz schist occurs in contact with many of the other units at Ambler 4B (Table 2). In some areas, the graphitic-mica-quartz schist may grade laterally into the microcline-mica-quartz schist (Pzbs) (e.g., north of GCO DDH-5). Adjacent to the sulfide horizon (Pzms), the graphitic-mica-quartz schist is interbedded and gradational with graphitic schist (Pzgs) and feldspathic mica-quartz schist (Pzmq).

Because of the presence of aluminous minerals and graphite, the protolith of the graphitic-mica-quartz schist is thought to be a pelitic sedimentary rock (Hitzman, 1978; Kelsey, 1979).

Graphitic Schist

The graphitic schist (Pzgs) is a fine-grained, brown to black, well-foliated rock. Limonite stains the surface of weathered rocks to a reddish brown color. Outcrops range from resistant cliffs (above BCMC DDH-3) to poorly exposed outcrops in saddles along ridge crests (approximately 2425 feet (740 m) NE from Juice Mountain).

Structural elements preserved in the graphitic schist include two foliations (S1, S2) defined by mica plates and a weakly developed crenulation cleavage (S3). Isoclinally folded white mica and chlorite grains can be observed in hand samples and drill core. White and smoky quartz pods and segregations aligned parallel to S2 schistosity are common. Quartz "pressure shadows" occur behind large euhedral pyrite grains.

In thin section, the graphitic schist is similar to the graphitic-mica-quartz schist except that it contains several percent more graphite and ubiquitous euhedral pyrite. Thin bands to 4 mm of quartz and mica plates are often isoclinally folded with polygonization of micas and quartz common in the noses of folds. Anhedral to subhedral helicitic albite grains to 2 mm enclose graphite grains. Rare biotite occurs in the graphitic schist immediately adjacent to the sulfide horizon (Pzms). These biotite grains appear to coexist with chlorite. The chlorite is colorless to pale green and ranges from isolated blades to rosettes to 0.3 mm. As in the graphitic-mica-quartz schist (Pzgm), sphalerite occurs in trace quantities, particularly in the graphitic schist units associated with the sulfide horizon (Pzms). Pyrite cubes up to 0.75 cm are common and occur in both quartz-rich bands and more micaceous bands.

The protolith for the graphitic schist is probably a fine-grained carbonaceous sedimentary rock. The protolith for the

graphitic schist is probably very similar to that of the graphitic-mica-quartz schist.

Calc-Schist

The calc-schist (Pzcs) is a fine-grained, poor- to moderately-foliated, gray colored rock. Weathered surfaces are commonly covered by an orange colored (in the Fall) lichen or moss. Outcrops are only moderately resistant. Structural elements are poorly preserved and difficult to interpret in the field. Cross-cutting foliation relationships were obscure due to the fine-grained nature of the mica grains.

In thin section, weak foliations are defined by elongate anhedral calcite grains to 1.5 mm in length and by chlorite and white mica grains to 0.5 mm in length. Pale green chlorite occurs as blades and as felted masses. The felted masses may have replaced garnet. White mica grains occur as wide blades and are often randomly oriented within a sample. Helicitic and poikiloblastic albites to 1 mm in diameter are common and enclose S₂ foliations. An contents from poorly-developed albite twins range from An₆ to An₁₀. Opaque phases are rare.

Contacts between the calc-schist and other Ambler 4B rock units are often poorly exposed due to the weathering characteristics of the calc schist. In the area of the large metabasite (Pzgt)

boudins (Fig. 3), thin beds of calc-schist (Pzcs) occur in both sharp and in gradational contact with metabasite (Pzgt) and with calc-silicate schist (Pzss).

The protolith for the calc-schist is thought to be an impure limestone or calcareous sedimentary rock (Hitzman, 1978; Kelsey, 1979).

Calc-Silicate Schist

The calc-silicate schist is a fine- to medium-grained rock with pale green to green bands. The bands, varying in thickness from 0.5 cm to 10 cm, are composed of variable amounts of actinolite, clinozoisite-epidote, garnet, calcite, chlorite, and quartz. Band colors are due mainly to varying percentages of actinolite, clinozoisite-epidote, and pink garnet. Outcrops are resistant, and weathered surfaces are typically covered by the same orange (in Fall) lichen or moss as that described for the calc schist (Pzcs). Limonite-stained surfaces are common, and minor malachite stains were observed in several outcrops below BC MC DDH-3.

Large structural features, such as isoclinal folds, are well preserved in outcrops of the calc-silicate schists. Smaller-scale features, such as foliations and lineations, are difficult to interpret because of the general granoblastic nature of the minerals. Chlorite and white grains are usually very fine grained.

In thin section, the calc-silicate schist consists of poorly foliated to banded rocks. The banded rock, observed in one sample, consists of two bands of amphibole + chlorite + clinozoisite-epidote + calcite + accessory minerals. Contacts between bands are sharp. The minerals show a distinctly granoblastic texture. In the more schistose calc-silicate schist, foliations are indicated by oriented actinolite, clinozoisite-epidote, and chlorite grains. Poikiloblastic clinozoisite-epidote grains to 1 mm in length commonly contain inclusions of sphene, calcite, and quartz. Garnet grains to 1 mm in diameter show all degrees of alteration to chlorite. Both iron carbonate and calcite were present in one sample. Amphiboles include actinolite, hornblende, and glaucophane. The hornblende and glaucophane will be described in detail in the following chapter on metamorphism. Sphalerite was observed in one sample collected from an outcrop below BCMC DDH-3.

Contacts between the calc-silicate schist and graphitic-mica-quartz schist (Pzgm), calcareous-chlorite schist (Pzcc), and in rare cases metabasite (Pzgt) are sharp, while contacts with calc-schists (Pzcs) and metabasites (Pzgt) are gradational. In the area around the metabasite (Pzgt) boudins (Fig. 3), several thin beds of unmapped calc-silicate schist occur interbedded with calc-schist (Pzcs) and graphitic-mica-quartz schist (Pzgm).

The protolith of calc-silicate schist is thought to be an impure calcareous sedimentary rock (Hitzman, 1978; Kelsey, 1979). It is probable that this rock also contained a large component of mafic volcanic phases.

Metabasite

The metabasite (Pzgt) is a dense, fine- to medium-grained, very poorly foliated, light green to green rock. It commonly weathers to a dark green color. Outcrops are highly resistant and form cliffs. Structural features, with the exception of joints, are not preserved in the metabasite. At least two joint directions, with a spacing ranging from 15 cm to 1 meter, were observed in many outcrops. Metabasites exposed at Ambler 4B show no evidence of primary bedding or pillow structures like those described at Arctic (Wiltse, 1975).

In thin section, the metabasite is granoblastic to weakly foliated. Foliations are defined by pale green actinolite blades. These blades, from 0.1 to 1.2 mm in length, typically have serrate grain boundaries. Inclusions of white mica are common in larger actinolite grains. Glaucofanite, reported to occur in other Ambler district metabasites (e.g., Nelsen, 1975; Carden, 1978), was not identified in any samples. Helicitic and poikiloblastic albite grains from 0.1 to 2 mm in length are common. Inclusions consist of

garnet, quartz, calcite, sphene, clinozoisite-epidote, and actinolite. Clinozoisite-epidote grains are also poikiloblastic with similar inclusion assemblages. These grains give the metabasite its granoblastic texture. Poikiloblastic garnets with inclusions of sphene, clinozoisite-epidote, quartz, and calcite show all degrees of alteration to chlorite. Colorless to pale green chlorite occurs in apparent random orientation as blades to 0.5 mm long and as rosettes to 1 mm wide. Iron carbonate and calcite grains form anhedral masses to 2 mm. Opaque phases occur only in trace amounts.

The protolith of the metabasite is thought to be a mafic tuff or lava (Hitzman, 1978; Kelsey, 1979).

Calcareous Chlorite Schist

The calcareous chlorite schist (Pzss) is a fine- to medium-grained, well-foliated, light green rock. Outcrops are fairly resistant and form cliffs. Structural elements preserved in the calcareous chlorite schist include S1 and S2 foliations and S3 crenulations. Minor smoky quartz pods and segregations parallel S2 schistosity.

In thin section, the calcareous chlorite schist has a weakly granoblastic to well-foliated texture defined by chlorite and white mica plates. Isoclinally folded chlorite and white mica

plates are common. Colorless to light green chlorite forms blades to 4 mm in length and rosettes to 0.7 mm in diameter. Chlorite blades and rosettes typically include sphene, tourmaline, and trace quantities of graphite and appear to coexist with biotite. Fractured biotite blades to 0.4 mm long are rare. Quartz grains with poorly sutured to moderately polygonized boundaries give the rock a slightly granoblastic appearance. Poikiloblastic and helicitic albite grains to 3 mm long include sphene and white mica and are commonly elongate parallel to S₂ schistosity. Anhedral calcite poikiloblasts to 3 mm in diameter include white mica, chlorite, and sphene. Sphene grains to 0.9 mm in length are common and are elongate parallel to the major S₂ foliation. Euhedral opaque grains to 0.5 mm in length are probably pyrite.

The protolith of the calcareous chlorite schist is thought to be a mafic volcanic tuff with a large pelitic sediment component (Hitzman, 1978).

Feldspathic Mica-Quartz Schist

The feldspathic mica-quartz schist (Pzmq) is a fine- to medium-grained, well-foliated, light green to white to light gray rock. Weathered surfaces are typically a light brown to greenish gray color. Outcrops are fairly resistant, and scaly siderite pods and coatings are common. Structural elements preserved in the mica

quartz schist include S1 and S2 foliation and S3 crenulations. Parasitic folds with amplitudes up to 20 feet (6 m) are common in larger outcrops.

In thin section, the feldspathic mica-quartz schist is a well-foliated rock with common isoclinally folded micas. White mica blades to 2 mm contain inclusions of epidote, sphene, zircon, apatite, and traces of graphite. Chlorite blades to 3 mm in length contain inclusions of apatite and sphene. Color variations seen in hand samples are due to the presence of variable amounts of chlorite and white mica. Strained biotite grains to 0.3 mm in length occur in trace quantities and are closely associated with the sulfide horizon (Pzms). Poikiloblastic and helicitic albite grains to 2 mm in diameter contain inclusions of sphene, quartz, white mica, and apatite. These grains are typically elongate parallel to S2 foliation. Quartz grains to 0.5 mm in diameter have poorly sutured to well-polygonized boundaries and are commonly stretched. Mineralogic variations in the feldspathic mica-quartz schist associated with the sulfide horizon (Pzms) will be discussed in the following section on "Stratigraphy."

Thin interbeds of fine-grained, relatively pure quartz occur discontinuously throughout the main section of feldspathic mica-quartz schist. These beds range in thickness from 10 cm to 20 cm and are typically stained yellow to reddish brown because of the

oxidation of trace pyrite. In thin section, the beds are composed almost entirely of well-polygonized quartz grains to 0.3 mm in diameter. These beds may have been original chert beds, or they may have been products of submarine hydrothermal activity (either direct precipitates ("exhalites") or sub-surface replacements).

The protolith of the feldspathic mica-quartz schist is thought to be a submarine felsic tuff and reworked tuffaceous debris (Hitzman and others, 1982). Slight contamination by carbonaceous material has occurred in the feldspathic mica-quartz schist at Ambler 4B.

Metarhyolite Tuff

The metarhyolite tuff (Pzmt) is a banded, poorly-foliated, fine- to medium-grained, porphyritic rock. Bands, ranging in thickness from 1 cm to 3 m, range in color from light green to white to gray. Outcrops are very resistant, and weathered surfaces are white to tan. Structural features seen in the metarhyolite tuff include large-scale folds and a very weak foliation defined by oriented mica plates. Joints are common with a spacing between 5 cm and 1 meter.

In thin section, the metarhyolite tuff is a poorly-foliated, banded rock. Bands, ranging in thickness from 5 mm and up, consist of quartz-microcline-albite bands separated by quartz-

microcline-albite-mica bands. Variable amounts of white mica and chlorite are responsible for the color variations seen in hand sample. White mica and chlorite blades to .8 mm long are usually fractured and formed parallel to the compositional banding. Strained biotite grains to 0.2 mm long are rare. Quartz grains, elongate parallel to banding, have well-polygonized grain boundaries. Triple-point junctions of 120° are common. Trace sphene grains are included in micas and in poikiloblastic albite grains.

Feldspars present in the metarhyolite tuff include microcline and albite. Microcline phenocrysts to 2 mm in diameter, that show "gridiron" twinning, are very common. The grains are subhedral to euhedral with long direction often parallel to banding. Possible embayments in microcline grains are filled with very fine-grained quartz. Microcline is crosscut and altered by albite + quartz. Albite poikiloblasts to 2.5 mm in diameter include quartz, microcline, white mica and sphene. These crystals are typically elongate parallel to banding. Helicitic albites are also common. An contents from poorly developed albite twins range from An_2 to An_6 .

Contacts between the metarhyolite tuff and graphitic schist (Pzgs) and graphitic-mica-quartz schist (Pzgm) are sharp. Contacts with mica-quartz schist (Pzmq) are gradational. Lateral continuity

of the metarhyolite tuff along strike will be discussed in further detail in the following section on stratigraphy.

The protolith for the rock is thought to be a rhyolite tuff because of the presence of microcline phenocrysts (after sanidine ?), the high potassium content, the very siliceous nature, and the banded appearance. The mineralogic continuity of this unit along strike, to be discussed below, suggests that it was a tuff and not a rhyolite flow.

Microcline-Mica-Quartz Schist

The microcline-mica-quartz schist (Pzbs) is a tan to light gray, well-foliated, porphyritic rock. Weathered surfaces range from brown to gray. Outcrops are fairly resistant. Structural elements preserved in the microcline-mica-quartz schist include S1 and S2 foliations and S3 crenulations. No large folds were seen in any microcline-mica-quartz schist outcrops.

In thin section, the microcline-mica-quartz schist is characterized by round blastophenocrysts of microcline surrounded by a fine-grained groundmass of albite, quartz, white mica, and accessory minerals. The microcline is metamorphic in origin, having presumably inverted from sanidine. Microcline shows "gridiron" twinning and is altered by albite and white mica along fractures and around grain edges. Poikiloblastic and helicitic albite grains to

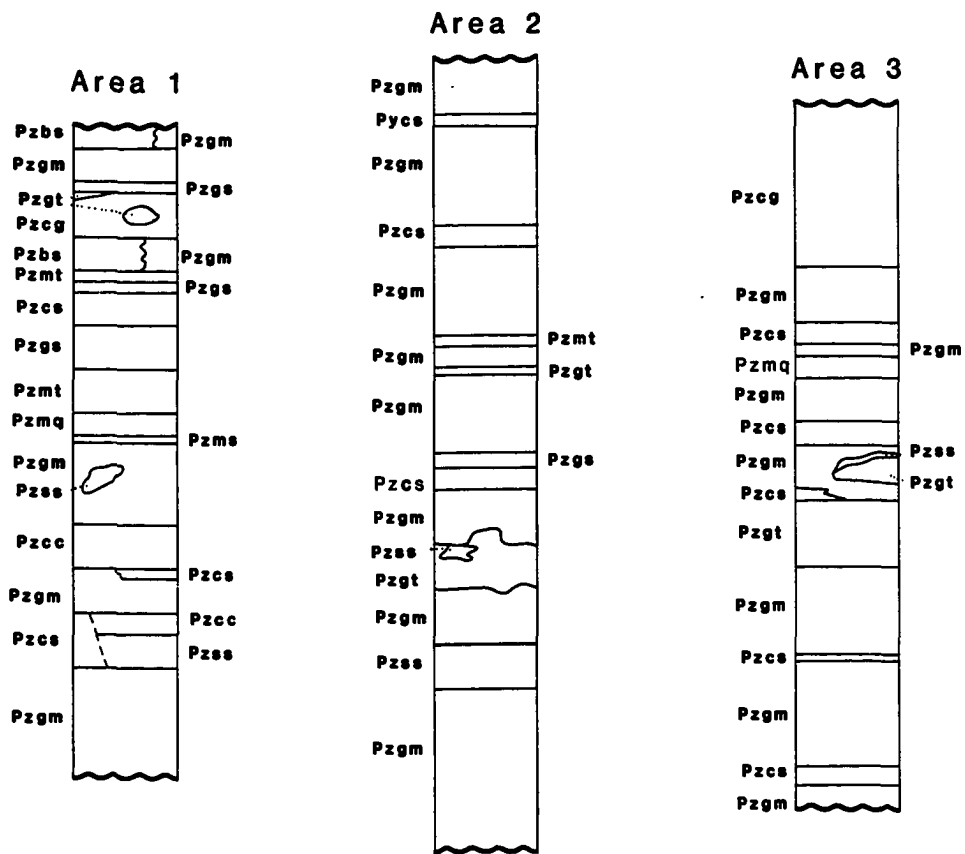
3.5 mm include white mica, quartz, and sphene. These grains are typically elongate parallel to the S2 foliation direction. Quartz grains to 0.8 mm in diameter are polygonized and elongate in the S2 foliation direction. White mica grains to 3.5 mm in length define S1 and S2 foliations. Skeletal, elongate sphene grains to 0.8 mm in length are common.

The protolith of the microcline-mica-quartz schist is thought to be a submarine ignimbrite. Marrs and others (1978) have suggested that the microcline-mica-quartz schist may represent a district-wide submarine ignimbrite eruptive event. This suggestion will be addressed in a latter section.

Stratigraphy

The rocks in the Ambler 4B area strike northeast-southwest to northwest-southeast, depending on large-scale folding. Dips range from northwest to west to southeast. During the course of this study, the stratigraphic up direction was not precisely determined. Sedimentary features, such as the drape structures, graded bedding, and load casts seen by Zdepski (1980) in sedimentary beds contained in greenstone, were not seen in any Ambler 4B rocks. Stratigraphic "up" assumed in this section is based on features observed in the sulfide horizon. These features will be discussed in detail in the following section on sulfide mineralization.

The Ambler 4B area will be divided into three different stratigraphic areas. Simplified stratigraphic sections that cover the three areas are shown in Figure 4. Area 1 covers the major area mapped during the study and includes the folded metavolcanic rocks (Pzmr), the massive sulfide horizon (Pzms), and enclosing metasedimentary rocks (Fig. 3). Area 2 covers the northeastern corner of the map area, which is separated from the main map area (Area 1) by a major northwest-southeast trending fault (Fig. 3). Area 3 covers the southeastern corner of the map area, which is in fault contact with the main map area (Area 1).



Ambler 4B Stratigraphy



stratigraphic up is assumed

Figure 4. Ambler 4B stratigraphy. Area 1: main map area including the sulfide horizon. Area 2: northeast corner of the map area. Area 3: southwestern corner of the map area.

Area 1 Stratigraphy

Area 1 stratigraphy includes all lithologic units seen at Ambler 4B. Most of the section is well exposed in the main northwest-southeast creek (Fig. 3). Detailed mapping and correlation of DDH intercepts shows that units in the approximate center of the section (Pzbs, Pzcs, Pzmt, Pzmq, Pzgm, Pzms) have been isoclinally folded on a large scale.

Only the metarhyolite tuff (Pzmt), feldspathic mica-quartz schist (Pzmq), and massive sulfide horizon (Pzms) were traceable through this folding. The metarhyolite tuff (Pzmt) forms resistant outcrops, and the feldspathic mica-quartz schist (Pzmq) and massive sulfide horizon (Pzms) have been intercepted by BCMC and GCO drilling.

In an attempt to see if any lateral variations occur within the metarhyolite tuff (Pzmt) and feldspathic mica-quartz schist (Pzmq), three sections were measured by tape and sampled along strike. Section 1 crosses BCMC DDH-3, Section 2 crosses BCMC DDH-2, and Section 3 crosses the lowermost exposure of the felsic units exposed in the main creek area (Fig. 3). Samples were collected for thin section analyses whenever a different (color or mineralogy) lithology was encountered.

A compilation of the results of the measurements is shown in Figure 5, and approximate modal abundances of minerals from

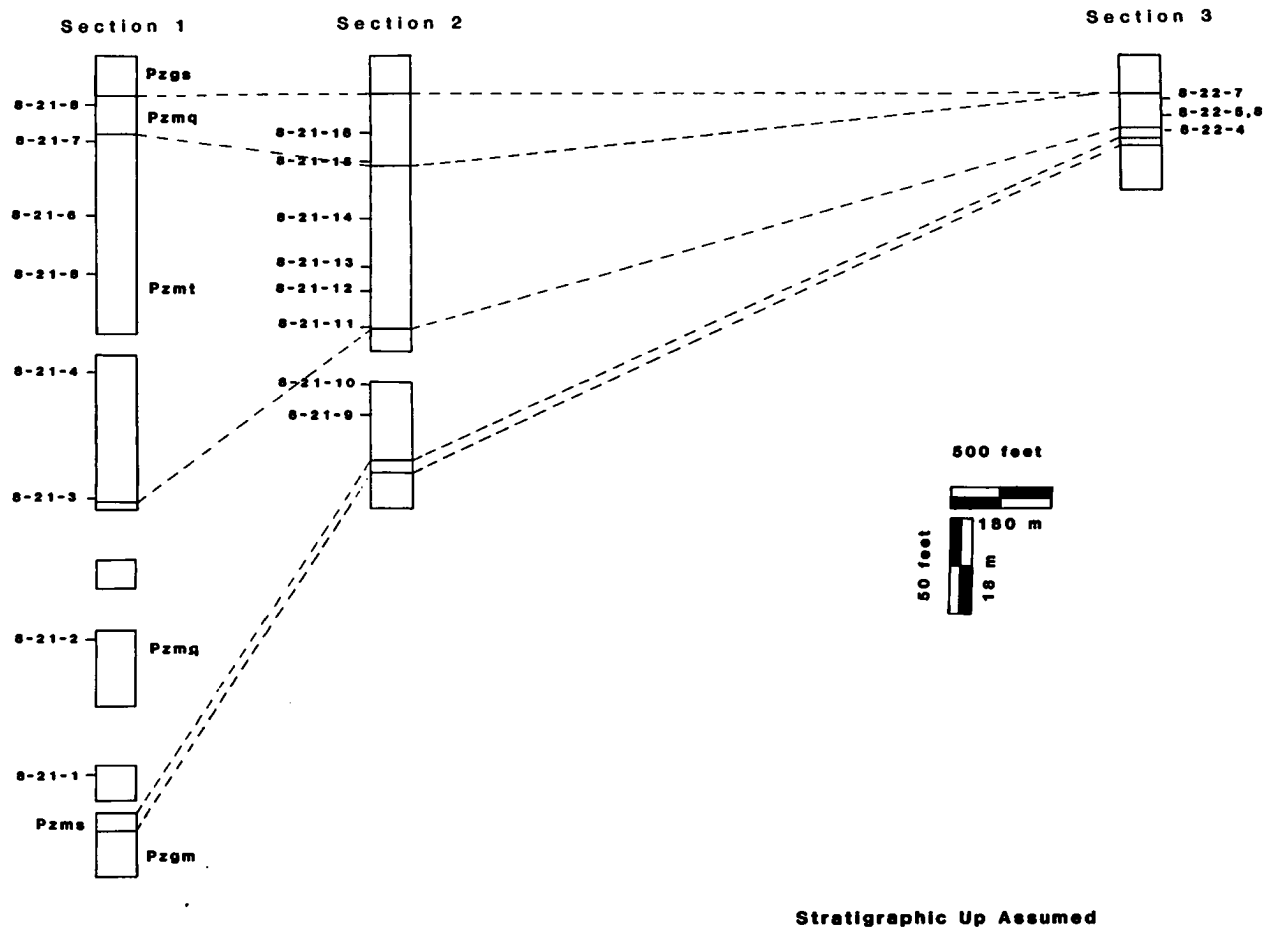


Figure 5. Stratigraphic variation of Ambler 4B felsic metavolcanic units along strike. Section 1: DDH 4B-3 area. Section 2: DDH 4B-1 area. Section 3: low in creek.

samples collected along the traverses are shown in Table 4. In Figure 5, the units have been unfolded. Section 1 is approximately 4,920 feet (1,500 m) along strike from Section 3. Also shown in Figure 5 is the approximate thickness of the sulfide horizon (Pzms) inferred from the nearest DDH intercept.

From Figure 5, it can be seen that the metarhyolite tuff (Pzmt) thins from approximately 200 feet (60 m) at Section 1 to approximately 16 feet (5 m) at Section 3. This represents an approximate 92 percent decrease in thickness. The feldspathic mica-quartz schist (Pzmq) thins from approximately 165 feet (50 m) along Section 1 to approximately 13 feet (4 m) along Section 3. This also represents an approximate 92 percent change in thickness along strike. A thin bed of feldspathic mica-quartz schist (Pzmq) occurs above (structurally) the metarhyolite tuff (Pzmt) in Sections 1 and 2. This horizon was not seen in Section 3. It is interesting to note that the massive sulfide horizon (Pzms) does not thin from Section 1 to Section 3. From Table 4, it is clear that the mineralogies of the units remain approximately constant along strike. Grain sizes also remain constant along strike.

Possible explanations for the thinning of the metarhyolite tuff (Pzmt) and feldspathic mica-quartz schist (Pzmq) along strike include the following: (1) a structural thinning due to isoclinal folding; (2) the felsic units depositionally lapping up onto the

TABLE 4. Approximate Modal Abundances for Samples Collected from Pzmt and Pzmq,
Traverses 1, 2 and 3

Sample No.	Quartz	Microcline	Albite	White Mica	Chlorite	Biotite	Epidote- Clinzoisite	Calcite	Sphene	Zircon	Apatite	Graphite	Opauques
8-21-1	25	--	55	20	--	--	Tr	--	Tr	Tr	Tr	Tr	Tr
8-21-2	14	--	55	20	--	--	Tr	--	Tr	--	15	Tr	1
8-21-9	29	--	55	15	--	--	Tr	--	Tr	--	Tr	--	1
8-21-10	29	--	50	20	--	--	Tr	--	Tr	--	Tr	--	1
8-22-4	25	--	45	30	--	--	Tr	--	--	--	Tr	--	Tr
8-21-8	30	--	50	19	--	--	Tr	--	Tr	Tr	Tr	--	1
8-21-15	40	--	50	9	--	--	Tr	--	Tr	--	Tr	--	1
8-21-16	30	--	45	25	--	--	Tr	--	Tr	--	Tr	--	--
8-21-3	26	50	20	3	--	1	Tr	--	Tr	Tr	Tr	--	Tr
8-21-5	20	43	30	5	Tr	--	Tr	--	2	--	Tr	--	Tr
8-21-6	20	55	20	3	--	--	Tr	2	Tr	Tr	Tr	--	Tr
8-21-7	30	30	35	5	--	--	Tr	--	Tr	--	Tr	--	Tr
8-21-11	40	40	15	5	--	--	Tr	--	Tr	--	--	--	Tr
8-21-12	30	45	21	4	--	--	Tr	--	Tr	--	Tr	--	Tr
8-21-13	35	43	20	2	--	--	Tr	--	Tr	Tr	Tr	--	Tr
8-21-14	30	40	20	5	Tr	--	Tr	2	Tr	--	Tr	--	3
8-22-5	35	40	3	2	--	--	Tr	3	Tr	--	Tr	--	Tr
8-22-6	30	45	22	3	--	--	Tr	--	Tr	--	Tr	--	Tr
8-22-7	30	35	30	4	--	--	Tr	--	1	Tr	Tr	--	Tr

8-21-1 through 8-21-16: Pzmq;

8-21-3 through 8-21-7: Pzmt

edge of a basin and; (3) a simple decrease in volcanic material away from its source. A simple structural thinning can be ruled out, as the sulfide horizon (Pzms) does not thin along strike. Of the latter two possibilities, both seem to be reasonable. Because of the constant mineralogic composition of the units along strike, it appears as if the units may have lapped up onto the edge of a basin during deposition. One might expect that compositional changes may occur, particularly in a silicic tuff away from its source.

Units above the felsic units and sulfide horizon (Pzms) have also been isoclinally folded, but outcrops are poor, making it difficult to accurately follow them through the folding. Directly north of GCO DDH-5 (Fig. 3), the microcline-mica-quartz schist (Pzbs) appears to grade laterally into the graphitic-mica-quartz schist (Pzgm). This is probably a facies change. Metabasite (Pzgt) beds and boudins occur sporadically and interlense with calc-schist (Pzcs) and thin calc-silicate schist (Pzss) horizons. Two large metabasite (Pzgt) boudins (at an elevation of approximately 2,300 feet (700 m) Fig. 3) are probably structural features, as beds of graphitic-mica-quartz schist (Pzgm) and calc schist (Pzcs) appear to "wrap" around them.

Units below the felsic rocks owe their apparent complicated stratigraphy to deformation. The isolated outcrops of calc-silicate schist (see Fig. 3) were probably structurally emplaced and isolated

during the major folding event. Based on field observations, the graphitic-mica-quartz schist (Pzgm) and calcareous chlorite schist (Pzcc) appear to have "flowed" plastically into the noses of the large folds. This hypothesis cannot be substantiated, because contacts are poorly exposed in the area.

Area 2 Stratigraphy

Area 2 stratigraphy is apparently fairly simple and needs little explanation. Lithologic units strike north-south and dip to the west. The relationship between Area 1 and Area 2 stratigraphy is not known, as displacement and movement on the faults is unknown.

Area 3 Stratigraphy

Stratigraphy in Area 3 is complex because of (1) east-west faulting and (2) the presence of large metabasite (Pzgt) bodies. The major stratigraphic complexities result from the different deformational characteristics of the metabasite (Pzgt) and the schistose rocks (Pzss, Pzgm, Pzcs, Pzmq). In many cases, the more ductile schistose rocks appear to have "flowed" plastically around the more rigid metabasite (Pzgt) during deformation, greatly altering the original stratigraphy. Field evidence of the plastic "flow" includes (1) the brecciation of schistose units around the metabasites, and (2) the disruption of earlier foliations in the schistose rocks in close proximity to the metabasites. After

folding, the units were faulted (see chapter below on "Structure"). In the extreme southeastern edge of the field area, the schistose units, away from metabasites (Pzgt), strike northwest-southeast and dip to the southwest where they become covered by vegetation in the valley.

Structure

At least five periods of deformation (D1 to D5) affected rocks of the Ambler 4B deposit (Table 5). D1, D2, and D3 were folding events, and D4 and D5 were faulting events. Regional metamorphism accompanied D2 and D3. The Ambler 4B deposit is one of the only sulfide deposits in the Ambler district where large amplitude folds are well exposed. F2 and F3 folds are easily identifiable in the field and in map pattern. Calc-silicate schists (Pzss), calc-schists (Pzcs), calcareous-chlorite schists (Pzcc), and graphitic-mica-quartz schists (Pzgm) provided most of the megascopic structural data, while graphitic schists (Pzgs), graphitic-mica-quartz schists (Pzgm), and feldspathic-mica-quartz schists (Pzmq) provided most microscopic structural data.

D1

The earliest period of deformation was an isoclinal folding event (F1). In the field, one F1 isoclinal fold was observed in the isolated outcrop of calc-silicate schist (Pzss) directly upslope from BCMC DDH-2 (see Fig. 3). The fold, with an amplitude of approximately 40 feet (10 m), was refolded by an F2-style fold.

F1 folding produced a compositional banding (S1) in metarhyolite tuff (Pzmt) and calc-silicate schist (Pzss) and possibly in the sulfide horizon. In feldspathic-mica-quartz schist

TABLE 5. Deformational History of the Ambler 4B Area

Deformation Phase	Fabric	Mesoscopic Folds or Faults	Lineations	Metamorphism
D1 (F1)	Compositional banding (S1) subparallel to bedding, generally NW-SE striking schistosity (S1) subparallel to bedding	Isoclinal folds poorly preserved	-----	-----
D2 (F2)	Generally NW-SE striking prominent axial planar schistosity (S2), often subparallel to S1	Large-scale isoclinal folds plunge 2° to 15° to the west, parasitic folds common	Lineations from feldspar and actinolite grains, aligned mica plates, noses of F2 parasitic folds, and from S1-S2 intersections	Greenschist to albite amphibolite
D3 (F3)	Crenulation cleavage (S3)	Open upright folds	L3 lineations from aligned mica and actinolite grains	Glaucophane-forming greenschist event
D4 *	Cataclastic texture in faults	High-angle normal(?) faults trend NW-SE	-----	Retrograde metamorphism
D5 *	Cataclastic texture in faults	High-angle normal(?) fault trends NE-SW, truncates ore horizon	-----	

* Age relationships between D4 and D5 faults are unclear due to poor exposure.

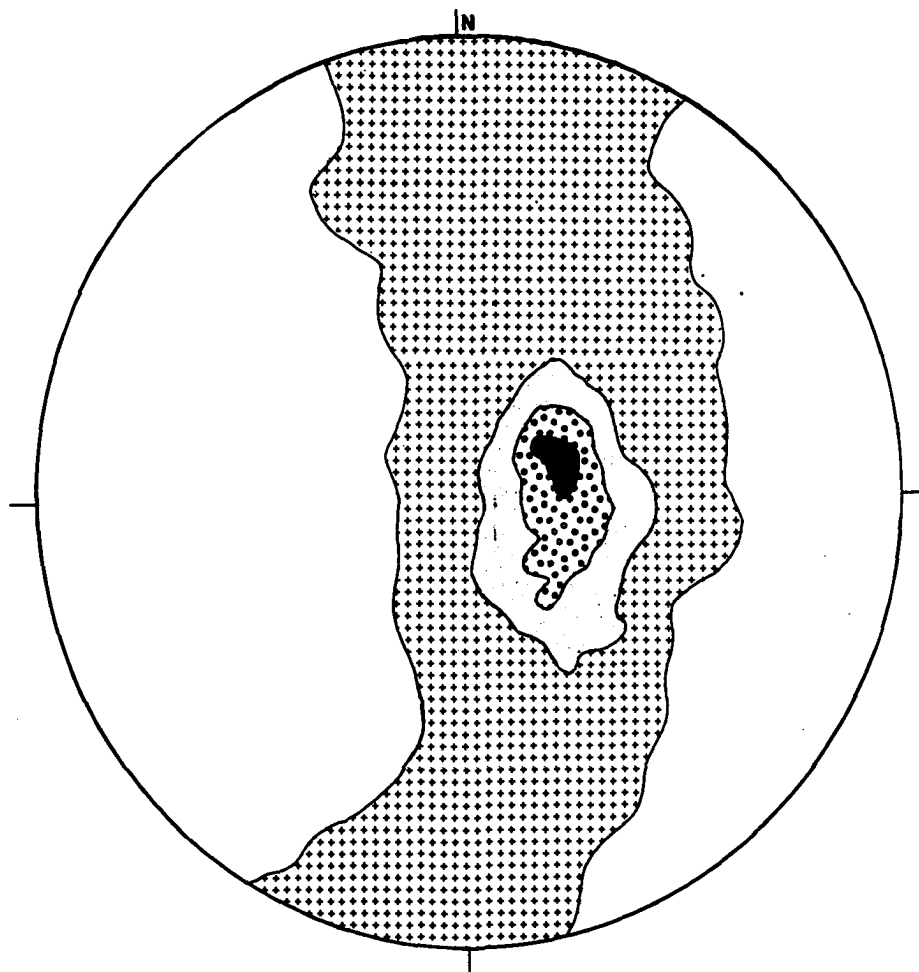
(Pzmq), graphitic schist (Pzgs), graphitic-mica-quartz schist (Pzgm), and calcareous-chlorite schist (Pzcc), a schistosity (S1) was developed. This schistosity (S1), defined primarily by aligned mica plates, was poorly exposed in outcrop due to the later overprinting of the D1 event by D2 and D3 events. S1 banding and schistosity are believed to have formed parallel to original bedding (S0).

Contours of poles to S1 schistosity are shown in Figure 6. From Figure 6 (for description of experimental methods, see Appendix I), it can be seen that S1 generally strikes northwest-southeast and dips shallowly to the southwest. The broadly developed girdle seen in Figure 6 is caused by the folding of S1 by F2 and F3 events.

D2

The second folding event (F2) is responsible for the major folding of the rocks at Ambler 4B. Five large F2 isoclinal folds are exposed on the Ambler 4B side of Juice Mountain (Fig. 3). They have amplitudes up to 2000 feet and plunge from 2° to 15° to the west. "S" and "Z" parasitic folds with amplitudes up to 30 feet are commonly developed on the flanks of the larger folds.

F2 folding and D2 metamorphism produced a penetrative axial planar schistosity (S2). S2 schistosity is the dominant planar element exposed in outcrop at Ambler 4B and is defined in the field



Percent Poles per one Percent Area



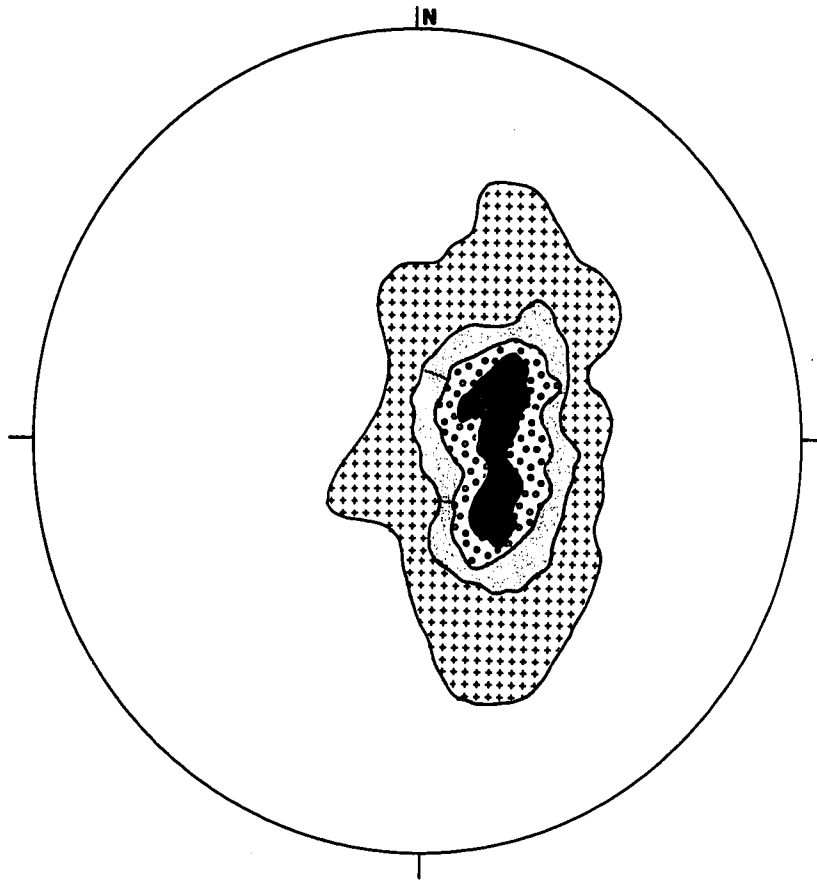
217 poles

Figure 6. Contours of poles to S1 schistosity.

by aligned mica plates. In thin section, F2 microfolds fold S1 schistosity. On the flanks of the large F2 folds, S2 is generally subparallel to S1. As an F2 fold nose is approached, the angle between S2 and S1 increases because of the folding of S1 until it eventually reaches 90° on the nose of the fold.

Contours of poles to S2 schistosity are shown in Figure 7. Most S2 schistosity strikes northwest-southeast and dips southwest, but a substantial portion of S2 strikes show northeast-southwest trends. This may be because of the slight divergence of the axial planar foliation, particularly in the noses of the large folds. F3 folding has also affected S2 schistosity. S1 and S2 orientations are similar and even overlap (Figs. 6 and 7). While they cannot be separated in Figures 6 and 7, they can be readily distinguished in the field because of their distinct crosscutting relationships.

Contours of L2 lineations are shown in Figure 8. In the field, L2 lineations were measured on elongate feldspar and actinolite grains, from the noses of F2 parasitic folds, and from S1-S2 intersections. From Figure 8, it can be seen that most L2 lineations plunge from approximately 2° to 20° in a west-southwest direction. L2 lineations that stray from the main cluster in Figure 8 have been reoriented by F3 folding.

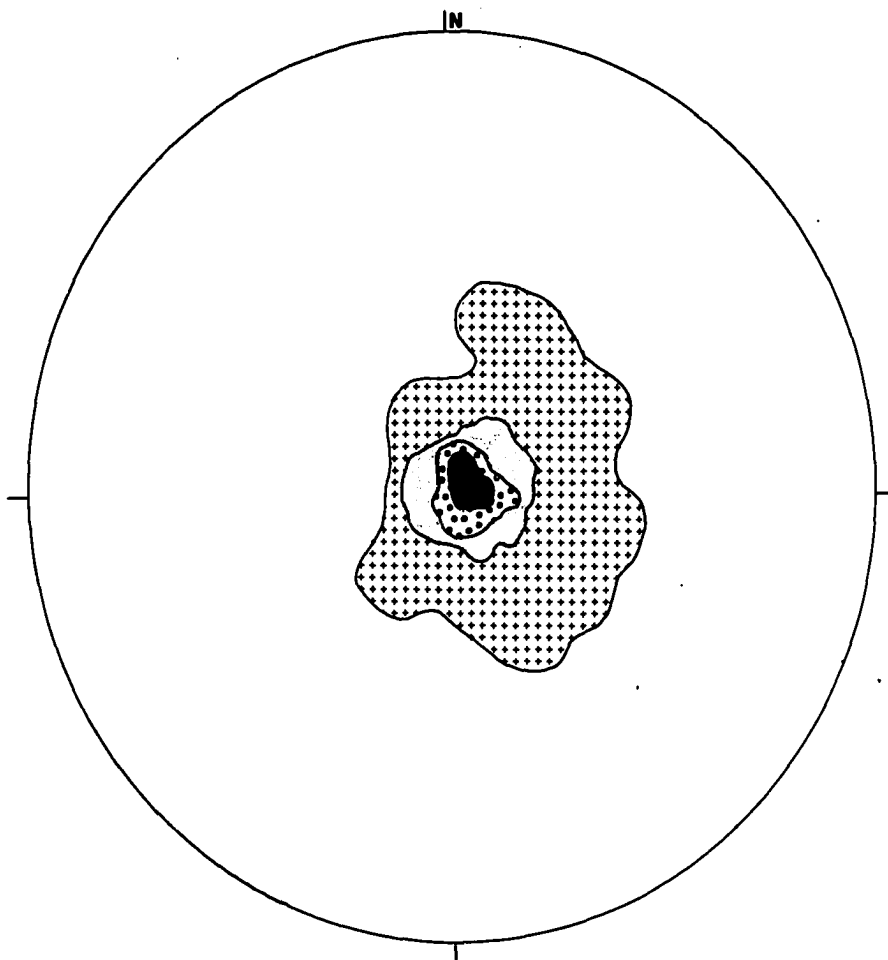


Percent Poles per one Percent Area



150 poles

Figure 7. Contours of poles to S2 schistosity.



Percent Poles per one Percent Area



93 poles

Figure 8. Contours of L2 lineations.

D3

One large F3 fold was mapped (Fig. 3). This fold with broad, open amplitude folds the largest of the F2 folds. F3 folding and D3 metamorphism produced weakly developed crenulation cleavage (S3) in graphitic schists (Pzgs), graphitic-mica-quartz schist (Pzmg), calcareous-chlorite schist (Pzcc), and feldspathic-mica-quartz schist (Pzmq). F3 crenulations are best seen in thin section. L3 lineations consist of aligned mica and actinolite grains. F3 effects seen in Figures 7 and 8 consist of a broad warping of S2 schistosity and L2 lineations.

D4 and D5

D4 and D5 are faulting events. The relationship between D4 and D5 faults is unclear, because exposures of the faults in the field are poor. Crosscutting relationships were not seen. Also, BC MC and GC O drilling has failed, with the exception of BC MC DDH-3, to intercept substantial fault zones.

D4 faults trend northwest-southeast and are thought to be high-angle normal faults. Fault zones are exposed along the ridge in the NE edge of the field area and directly south of BC MC DDH-2. They consist of poorly consolidated gouge and breccia zones up to 10 feet wide. Fine-grained quartz and black clay comprise the matrix material. Quartz pods to six inches commonly occur within the fault

zones, suggesting that the fault zones acted, at one time, as channels for the movement of fluids.

BCMC DDH-3 intercepted a seven-foot fault zone that is thought to be a D4 fault. The fault zone, not exposed on the surface, consists of a uniform black clay and gouge material with minor iron and copper staining.

The northeast-southwest trending fault in the area that truncates the sulfide horizon is a D5 fault. It is very poorly exposed on the surface, and its position on the map has been inferred. It is also thought to be a normal fault with a dip to the southeast. The fault is believed to dip to the south, because BCMC DDH-2 that intercepts the felsic units (Pzmt and Pzmq) and the sulfide horizon (Pzms) at depth does not encounter a fault zone. Also, GCO DDH-3 and DDH-4 do not intercept faults. If the dip of the plane of the fault is to the southeast, the dip must be greater than approximately 40° from horizontal. Otherwise, the fault would crop out in the metabasite cliff area below BCMC DDH-2 (see Plate II).

Metamorphism

Two periods of regional metamorphism have affected rocks of the Ambler 4B deposit. The first event (D2), which corresponds with F2 folding, was upper greenschist and locally amphibolite in grade. The second (D3) metamorphic event, which corresponds with F3 folding, was a greenschist event that locally produced glaucophane. Retrograde metamorphism followed D2 and D3 events.

D2 Metamorphism

Greenschist facies assemblages were developed during D2 metamorphism in many Ambler 4B rocks. Syntectonic metamorphism is indicated, because D2 mineral growth parallels F2 fold axial planes. A typical D2 assemblage found in metasedimentary and felsic metavolcanic rocks consists of quartz-albite-white mica-sphene \pm chlorite \pm epidote \pm calcite (Table 6). Biotite is found in trace amounts in the silicic metavolcanic units and in the massive sulfide horizon, which indicates a chlorite to biotite Barrovian zone of metamorphism (Turner, 1981). No garnets were observed in these rocks, but round clots of chlorite occur in graphitic-mica-quartz schists (Pzgm), in shapes that suggest that the chlorite may have pseudomorphed garnets.

Metabasites (Pzgt) and calc-silicate schists (Pzss) typically contain the greenschist assemblage: albite-actinolite-

TABLE 6. Metamorphic Mineral Parageneses

	Mafic Metavolcanic Rocks (Pzgt, Pzss)			Metasedimentary and Silicic Metavolcanic Rocks (Pzmq, Pzmt, Pzbs, Pzgm, Pzgs, Pzcs, Pzcc)		
	Greenschist to albite amphibolite (D2)	Glaucophane-forming greenschist (D3)	Retrograde alteration	Greenschist to albite amphibolite (D2)	Glaucophane-forming greenschist (D3)	Retrograde alteration
Quartz						
Albite						
Chlorite						
White Mica						
Biotite						
Actinolite						
Glaucophane						
Hornblende						
Garnet						
Epidote-Clinzoisite						
Sphene						
Carbonate						

chlorite-clinzoisite (epidote)-sphene-quartz ± garnet ± calcite ± iron carbonate (Table 6). D2 amphiboles are, largely, pale green actinolite. In some cases, blue-green actinolites (defined by pleochroic formula: x = yellowish-green, y = pale green, z = greenish blue) are present which could easily be mistaken for glaucophane. D2 garnets commonly contain inclusions of sphene, clinzoisite, and carbonate. Rotated garnets were not seen. In several cases, garnet grains were found to have isotropic cores and anisotropic rims, indicating that the garnets have undergone complex metamorphic growth histories.

In one calc-silicate schist (Pzss) sample (7-19-3), a blue-green D2 hornblende was observed (Fig. 9). This hornblende (defined by pleochroic formula: x = yellow-green, y = green, z = deep greenish-blue) occurs as subhedral to euhedral crystals to 8 mm long. These crystals are cut and altered by D3 glaucophane (described below). The hornblende shows no preferred orientation in the sample. The presence of hornblende indicates that albite-amphibolite grade metamorphism was reached, at least locally, during D2 (Winkler, 1979). Hornblende was not seen in any other samples.

D3 Metamorphism

Syntectonic metamorphism continued during D3. Tectonism is indicated by strained quartz, amphibole, and mica grains. Like that



Figure 9. Photomicrograph of D2 hornblende being cut by D3 glaucophane. Plane light. _____ 1.0 mm.

found by Hitzman (1978) at BT, mineral growth during D3 was, for the most part, mimetic to S2. However, white mica, quartz, actinolite, albite, and clinozoisite grains commonly formed at a high angle to D2 minerals. D3 mineral assemblages are similar to D2 assemblages except that (1) biotite and hornblende were not formed during D3, and (2) glaucophane was formed, locally, during D3 (Table 6).

Sample 7-19-3 contains D3 glaucophane (Fig. 9). The glaucophane (defined by low 2V and by pleochroic formula: x = colorless, y = lavender-blue, z = blue) cuts and alters the previously described D2 hornblende. The glaucophane ranges in grain size from 0.05 to 2.5 mm long and occurs in apparent random orientation in the sample.

Many glaucophane grains in sample 7-19-3 have pale green edges or cores, which may be actinolite, suggesting partial metamorphic re-equilibration (Fig. 10). This re-equilibration may have occurred at the end stages of D3 metamorphism or during the retrograde event. Minerals such as lawsonite and jadeite, indicative of blueschist facies metamorphism, were not seen in any Ambler 4B rocks.

D3 poikiloblastic albite and clinozoisite grains are common and often preserve relict D2 foliations. Minerals included in these grains include garnet, quartz, sphene, calcite, white mica, and



Figure 10. Photomicrograph of D3 glaucophane altered by actinolite. Plane light. _____ 0.1 mm.

amphibole (probably actinolite) grains. In all cases, minerals found as inclusions in albite and clinozoisite grains, and in rare cases garnet and calcite grains, are also found in the groundmass. The poikiloblastic grains do not preserve evidence of earlier high-grade metamorphic events.

Retrograde Metamorphism

Significant retrograde metamorphism followed D3. Chlorite and albite are the dominant minerals produced. Albite replaces white mica, and chlorite replaces garnet, actinolite, and biotite. Helicitic albite grains formed during retrograde metamorphism enclose F3 crenulations.

In many cases, minerals that were included in D3 poikiloblastic albite and clinozoisite grains show little effects of retrograde metamorphism. For example, garnet grains included in D3 albite grains commonly show euhedral crystal morphology, while those garnets in the groundmass show anhedral to subhedral morphologies. The garnets in the groundmass were subjected to higher degrees of retrograde alteration by chlorite.

Summary of Deformational Events in the Ambler District

Workers in the Ambler district are generally in agreement as to the nature of the structural geology throughout the district. Hitzman (1978) identified four folding events (F1, F2, F3 and F4), while Nelsen (1979), Kelsey (1979), and Zdepski (1980) identified three folding events. The first three folding events described by Hitzman (1978) and the three events described by the other authors are very similar to those observed during this study. The first event is a poorly preserved isoclinal event, the second is a major isoclinal event with resultant prominent axial planar schistosity, and the third is an open, upright folding event responsible for the development of a crenulation cleavage. Hitzman's (1978) fourth event (F4) is an open, upright folding event with a resultant crenulation cleavage.

Although descriptions of structural features are similar across the Ambler district, descriptions of metamorphic histories differ across the district. Workers in the Ambler district can be divided into two schools based on their descriptions of metamorphic histories. Carden (1978) and Nelsen (1979) describe initial blueschist events, which are then followed by greenschist events. Kelsey (1979) placed mineral assemblages in Nelsen's (1979) final greenschist facies event, and Zdepski (1980) described the rocks at Sun as having undergone complex metamorphic histories that ended in greenschist facies metamorphism.

Hitzman (1978) and this author, on the other hand, describe an initial greenschist to albite amphibolite grade metamorphic event that is followed by a high pressure low grade event. Hitzman (1978) describes the final metamorphism as a blueschist event, while the event as described in this study was termed a glaucophane-forming greenschist event. As in this study, Hitzman (1978) was able to identify the initial albite amphibolite grade metamorphism in only a few samples.

Sulfide Mineralization

The ore deposit at Ambler 4B is a Zn-Pb-Cu massive to semi-massive sulfide horizon (Pzms). The deposit also contains significant values of silver. The overall geometry of the sulfide horizon is that of a uniform blanket-like body. On the basis of surficial mapping of outcrops and by inferring data from two BCMC and five GCO diamond drill holes, the sulfide zone has a continuous strike length of at least 5,500 feet (1,500 m). The horizon is folded up into space and eroded on the western edge of the map area and is truncated by the D5 fault on the eastern edge of the map area (see Fig. 3). The downdip, down plunge extension of the horizon, covered by Anaconda Minerals Company claims, was not studied during this investigation, but it is known to be extensive. Published Anaconda Minerals Company diamond drill hole intercepts indicate that the sulfide horizon has been intercepted at least twice in holes 2,500 feet (762 m) apart on the Smucker side of Juice Mountain (DDH-3, 27.6 feet (8.4 m) assaying 8.8% Zn, 2.6% Pb, 2.9 oz./ton Ag; and DDH-5, 10.5 feet (3.2 m) assaying 2.3% Zn, 1.2% Pb, 15.75 oz./ton Ag, 0.06 oz./ton Au) (E/MJ, 1978).

The thickness of the sulfide horizon along strike on the Ambler 4B side of Juice Mountain has been tested by BCMC and GCO drilling (see Fig. 3 for drill hole locations). BCMC and GCO diamond drill holes and the sulfide zone intercepted by the holes in

an unfolded cross-section are shown in Figure 11. All drill holes are vertical. It should be noted that, because of the highly folded nature of the sulfide horizon, GCO DDH's 1, 2, and 5 intercepted the horizon twice. From Figure 11, it can be seen that the thickness of the sulfide horizon varies from 2.5 feet (1 m) in GCO DDH-1 intercept #1, to 23 feet (7 m) in GCO DDH-5 intercept #2. Overall, though, the sulfide horizon maintains a relatively constant thickness between 3 and 7 feet (1 and 3 m) along strike. The thickness of the horizon does not appear to vary along strike at either end of the deposit.

On the basis of the detailed logging of GCO DDH's 1, 2, 3, 4, and 5, the sulfide horizon was subdivided into an upper Zone A and a lower Zone B. Figure 11 lists the approximate thicknesses of Zone A and Zone B intercepted in the drill holes. Figure 12 is a generalized section that summarizes important features of Zone A and Zone B horizons.

Zone A Sulfides

Zone A sulfide layers occur in sharp contact with the overlying feldspathic mica-quartz schist unit (Pzmq) and has been intercepted by all drill holes. The thickness of Zone A decreases from approximately 8 feet (2.5 m) in GCO DDH-5 intercept #1 to approximately 0.8 feet (0.25 m) in GCO DDH-4, the lowermost drill

Ore Zone Variations Along Strike

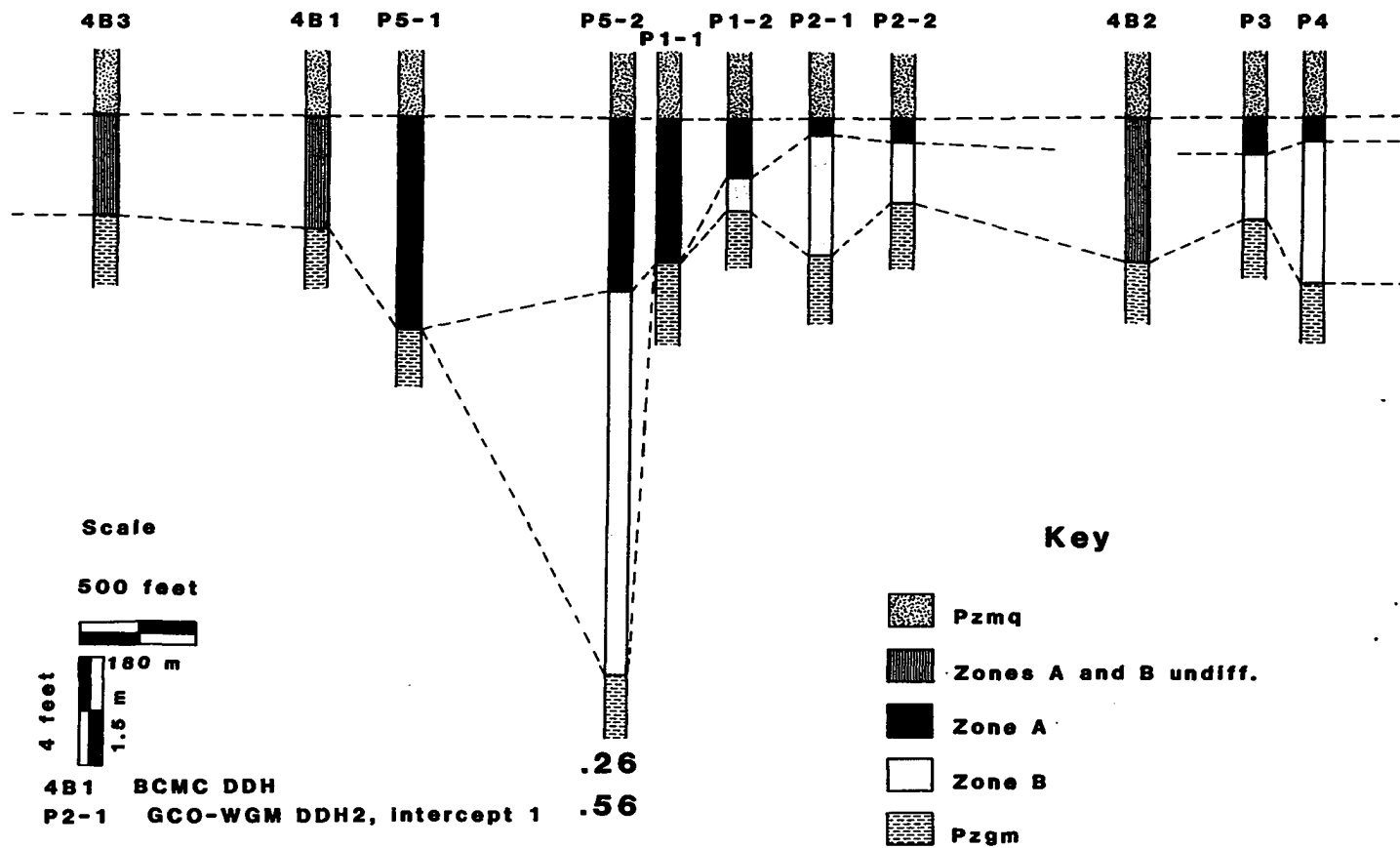


Figure 11. Unfolded cross-section and ore zone variations along strike.

Generalized Section of Zone A and Zone B Mineralization

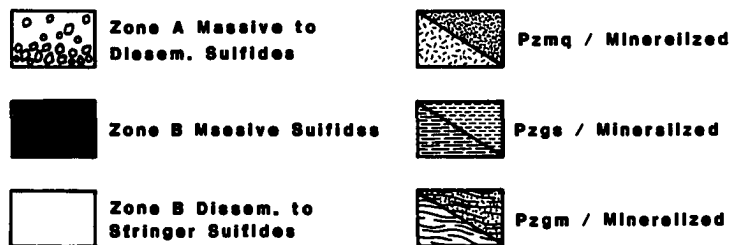
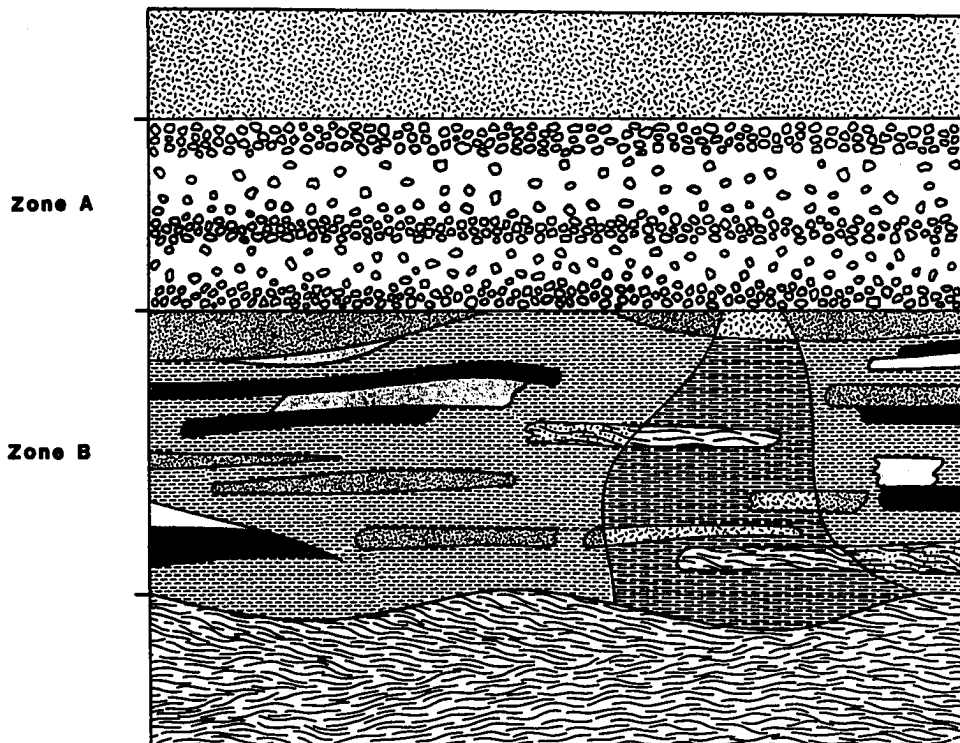


Figure 12. Generalized section, not to scale, of Zone A and Zone B mineralization.

hole on the property. The contact between Zone A sulfides and the underlying Zone B sulfides is also sharp.

Zone A consists of three distinct massive sulfide layers, from 0.1 feet (0.03 m) to 1.5 feet (0.46 m) in thickness, which are traceable in drill core along the strike length of the deposit. The massive sulfide layers are separated by quartz-rich layers with semi-massive and disseminated sulfides. The massive sulfide layers grade into the quartz-rich layers over distances usually less than 5 mm and give the rock a somewhat banded appearance (Figure 12).

Gangue minerals of Zone A include quartz, pyrite, and carbonate, with trace amounts of pyrrhotite, chlorite, biotite, white mica, and apatite. Approximate modal abundances of ore and gangue minerals for both Zones A and B are listed in Table 7. Pyrite grains 0.1 mm to 0.7 mm in diameter are common and contain inclusions of quartz, biotite, and white mica, as well as ore minerals (see below). Strained carbonate occurs as anhedral masses and is confined to the more massive sulfide zones. Biotite and colorless chlorite occur in and immediately adjacent to the more massive layers and appear to coexist. Kinked biotite and chlorite are common and usually occur parallel to the main sulfide layering. Barite and cymrite, common Ambler district gangue minerals, were not seen in any Ambler 4B rocks.

TABLE 7. Approximate Mineral Modal Abundances: Zone A and Zone B Sulfide Horizons

	<u>Zone A</u> Massive Zones	<u>Zone A</u> Disseminated Zones	<u>Zone B</u> Massive Zones	<u>Zone B</u> Disseminated in Quartz Matrix*
Pyrite	20-40	3-30	60-65	10-23
Sphalerite	15-30	4-16	20-35	Tr- 4
Chalcopyrite	10-20	2-20	---	0-13
Galena	3-10	Tr- 2	3- 5	Tr- 1
Arsenopyrite	Tr- 4	0- 2	2- 7	0- 1
Tennantite	0- 1	0- 1	0-Tr	0- 1
Pyrrhotite	0- 3	0- 4	---	0- 2
Marcasite	---	0- 3	---	0-Tr
Bornite	0-Tr	0-Tr	---	0-Tr
Covellite	---	0-Tr	---	0-Tr
Quartz	10-15	45-70	5-10	70-85
Calcite	5-15	0- 5	---	0-Tr
White Mica	0- 3	0-Tr	Tr	Tr- 3
Chlorite	2- 5	1-10	---	---
Biotite	Tr	2-15	---	---
Epidote	---	Tr	---	---
Apatite	---	0-Tr	---	---

* Does not include sulfides found in Pzgs, Pzgm, and Pzmq

Ore minerals of Zone A include sphalerite, chalcopyrite, and galena and trace amounts of arsenopyrite, tetrahedrite-tennantite, marcasite, covellite, and bornite (Table 7). The ore minerals are uniformly distributed between massive sulfide layers and the more quartz-rich, disseminated sulfide layers. The minerals are generally less than 1 mm in diameter, but anhedral masses of chalcopyrite and sphalerite to 5 mm, which appear to represent aggregates of grains, often occur in the quartz-rich, less sulfide-rich layers. Galena, tetrahedrite-tennantite, bornite, and covellite also occur as anhedral crystals and arsenopyrite exhibits subhedral to euhedral crystal morphology. Chalcopyrite, galena, sphalerite, and bornite are found as trace inclusions in annealed pyrite grains. Iron content of sphalerite from both Zone A and Zone B, defined by X-ray diffraction analysis, ranges from 4 to 6 mole percent Fe. Within Zone A, no vertical or lateral mineral or metal zonation trends were observed along strike. This lack of observed zonation is probably due to limited sampling and assay data.

Zone B Sulfides

Zone B consists of massive sulfides to disseminated sulfides in a quartz-rich matrix interbedded with graphitic schists (Pzgs) and minor feldspathic mica-quartz schists (Pzmq) that contain disseminated sulfides (Fig. 12). Zone B sulfide layers, intercepted by all DDH's except GCO DDH-5 intercept #1, ranges in thickness from

1.2 feet to approximately 14 feet and do not thin at either end of the deposit. The massive to disseminated sulfide layers range from 1 mm to 1 foot and are not traceable along strike between drill holes. The layers typically contain sharp contacts with surrounding schistose rocks, giving the rock a banded appearance (Fig. 12). In some cases, more massive, sulfide-rich layers often show a symmetric banding with, for example, pyrite + sphalerite-rich edges and pyrite-rich cores. An example of a symmetrically-zoned layer from Zone B is shown in Figure 13. In Zone B, disseminated sulfides are more common than massive sulfides, both in the schistose rocks and in the quartz-rich bands. In GCO DDH-5 intercept #2, few massive sulfide layers were encountered; however, assay data shows that the interval is mineralized.

Gangue minerals in Zone B include pyrite, pyrrhotite, and all the minerals that have been described as occurring in the feldspathic-mica-quartz schist (Pzmq) and graphitic schists (Pzgs) (Table 7). Gangue minerals found within the quartz-rich massive to disseminated sulfide bands include pyrite and quartz and trace amounts of pyrrhotite, white mica, and carbonate. Only those gangue minerals found within these siliceous bands are listed in Table 7. Pyrite grains are typically euhedral and range in size from 0.1 to 0.3 mm. In the more siliceous layers, strained white mica grains formed parallel to mineral banding, and trace amounts of anhedral carbonate occur in contact with quartz.

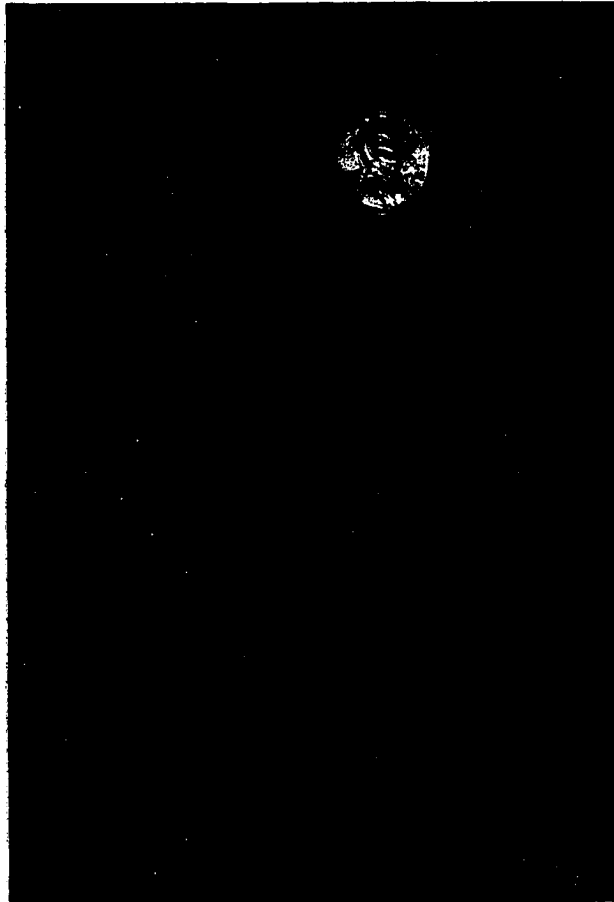


Figure 13. Symmetrically zoned massive sulfide layer from Zone B.

Micas found within the schistose rocks of Zone B have a distinctly "soapy-greasy" feel. They consist of coexisting colorless to pale green chlorite and white mica. These micas formed parallel to mineral banding and have been strained and folded. X-ray diffraction analysis of the chlorite from Zone B indicates that it may be similar to an Fe-Mg chlorite from the Besshi Mine, Japan described by Thorez (1975) (Table 8). X-ray data for several chlorite samples, including a sample collected from Zone B (D2-3), are listed in Table 8. From Table 8, it can be seen that the chlorite from Zone B exhibits slightly different X-ray properties than most Ambler 4B chlorites and that the chlorite from Zone B is similar to the chlorite from the Besshi Mine. Optically, the chlorites from Ambler 4B are very similar. However, the chlorite from Zone B, in several cases, has a slightly darker green color (plain light). The distinctive appearance and distribution of chlorites found in Zone B schistose rocks suggest that they may be alteration-related.

Ore minerals found within Zone B include sphalerite and chalcopyrite with trace amounts of galena, arsenopyrite, tetrahedrite-tennantite, bornite, and secondary(?) marcasite (Table 7). Grain sizes and morphologies are similar to those as described for the ore minerals of Zone A. As in Zone A, vertical and lateral mineral zonation trends along strike were not observed.

TABLE 8. X-ray Data for Chlorite Samples

SAMPLE NO.	^o "d" SPACING (In Å)									
	001		002		003		004		005	
8-3-3	14.51	W	7.12	S	4.74	S	3.53	S	2.82	W
7-10-2	14.48	S	7.13	S	4.74	S	3.54	S	2.83	W
8-16-1	14.59	W	7.12	S	4.73	S	3.53	S	----	-
D2-3	14.11	W	7.09	S	4.74	S	3.55	S	2.84	W
11b	14.2	M	7.1	S	4.72	M	3.54	S	2.83	W

Explanation

Peak intensity: W = Weak, M = Medium, S = Strong

8-3-3: Chlorite from typical calcareous chlorite schist

7-10-2: Chlorite from typical calcareous chlorite schist

8-16-1: Chlorite from typical metabasite

D2-3: Chlorite from Zone B Pzgm, possible alteration

11b: Fe, Mg Chlorite from Besshi mine, Japan (Data from Thorez, 1975)

Discussion of Ore Genesis

The continuous, blanket-like nature and the vertically gradational and alternating massive sulfide to disseminated sulfide changes within Zone A suggest that it may have been formed by the relatively quiescent deposition of sulfides from a metalliferous brine somewhat distal from its source or from fluids which emanated in a non-explosive manner. These fluids may have been similar to the metalliferous brines being discharged by present day "black smokers" (for description, see Bostrom and others, 1972). Features suggestive of a more proximal source, such as a highly copper mineralized stringer zone or vent, slump features, turbidites, breccia zones, or clastic grains, were not observed during this study, although deformation and recrystallization could have destroyed such textural features. Zone A sulfides may have been deposited onto a broad, flat submarine basinal plane composed primarily of pelitic and calcareous sediments with lesser volcanic and volcanoclastic rocks.

The lack of continuity along strike of the massive sulfide pods, the symmetrically-zoned sulfide layers, and the presence of Fe-Mg chlorite in enclosing and interbedded sedimentary and volcanoclastic rocks suggest that Zone B sulfides were deposited under different conditions than Zone A sulfides. Textures such as the symmetrically-zoned sulfide-rich layers are suggestive of a

replacement origin. The time of deposition of Zone B sulfides was probably synchronous with the time of Zone A deposition. Metal-rich fluids, from which Zone A sulfides were deposited on the sea floor may have circulated beneath the sediment-water interface through the porous and permeable sediments depositing sulfides and locally altering the enclosing rocks along poorly-defined bedding. Local chemical environments were probably a factor in the amount of sulfide deposition, resulting in the very lensey nature of the massive sulfide mineralization. These massive sulfide layers may reflect zones of upward movement of large amounts of fluid, i.e., diffuse feeder zones.

It is suggested that Zone A sulfides were deposited from a diffuse feeder zone (Zone B), rather than from a "point-source" vent. The three traceable massive sulfide layers of Zone A probably represent three different hydrothermal pulses. The upward gradational change between massive sulfide to disseminated sulfide for each of these pulses suggests that the initial metalliferous brine was metal rich, resulting in the deposition of massive sulfides. As hydrothermal activity continued, the brine became increasingly depleted in metals, resulting in the deposition of very siliceous layers with only minor disseminated sulfides. Alternatively, a hydrothermal pulse of metalliferous brine into the ocean may have resulted in the preferential settling of the heavy

(sulfide-rich) components relative to the light (silica-rich) components. The thinning of Zone A sulfide layers along strike may have been caused by the brine lapping up onto the edge of the basin. Structural thinning as a result of folding can be ruled out, as Zone B sulfides do not show any thinning along strike.

Metamorphism of Sulfides

It has been shown that the rocks in the area of the Ambler 4B deposit have been subjected to at least two regional metamorphic events. Samples from the sulfide horizons show considerable textural evidence that they, too, have been subjected to these regional metamorphic events.

Vokes (1969) divides the effects of the regional metamorphism in sulfide deposits into the following categories: (1) changes in fabric, (2) mobilization of minerals, (3) changes in mineralogy, and (4) mobilization of elements. These categories will be used as a basis of discussion to describe the metamorphic textures observed in the sulfides from Ambler 4B.

Changes in Fabric

Changes in the fabric of Ambler 4B sulfides include the following: (1) the brittle and plastic deformation of sulfides, (2) the annealing of sulfide grains, (3) the recrystallization of sulfides, (4) the rotation of sulfide grains during recrystallization, and (5) a general increase in sulfide grain size with metamorphism. As pyrite is, by far, the most ubiquitous sulfide mineral present at Ambler 4B, it lends itself well to a study of these factors.

Pyrite grains in both Zone A and Zone B show textures suggestive of brittle deformation. This deformation ranges from radiating fractures between pyrite grains that have collided (Fig. 14) to fracturing of pyrite grains (see Fig. 15). In Zone A and Zone B, brittle deformation of pyrite occurred in the more massive sulfide zones where collisions between adjacent pyrite grains occurred during deformation. Where pyrite grains have fractured, later annealing processes have often taken place.

Annealed pyrite grains are very common. These range from single pyrite grains that have fractured and then annealed (Fig. 15) to masses of many pyrite grains, which, as a result of deformation, have come into contact and annealed with other pyrite grains (Fig. 16). During the annealing process, other sulfide and gangue minerals were often caught between pyrite grains and incorporated into the new mass. Inclusions in annealed pyrite grains include sphalerite, galena, and quartz and trace amounts of chalcopyrite, bornite, white mica, and biotite (Fig. 17). Pyrite grains with inclusions of other sulfide and gangue minerals are most common in the more massive layers in Zone A, but examples of pyrite grains containing inclusions were seen in all areas of the sulfide horizon.

The process of annealing is tied closely to that of recrystallization. During the recrystallization of sulfide grains, boundary adjustments occur so as to reduce surface area and to



Figure 14. Photomicrograph of rounded and fractured pyrite porphyroblasts. Groundmass minerals include sphalerite (gray), chalcopyrite (yellow), galena (white), and quartz (black). Sample from Zone A sulfides. Reflected light.
_____ 0.2 mm.



Figure 15. Photomicrograph of a fractured pyrite grain. Groundmass minerals include chalcopyrite (yellow), sphalerite (gray), galena (white), and quartz (black). Sample from Zone B sulfides. Reflected light.
_____ 0.2 mm.



Figure 16. Photomicrograph of annealed pyrite grains.
Groundmass mineral is quartz. Sample from Zone B
sulfides. Reflected light. _____ 0.1 mm.



Figure 17. Photomicrograph of a rounded and rotated pyrite porphyroblast. Appendages are suggestive of counter-clockwise rotation. Pyrite contains inclusions of sphalerite (gray), galena (white), and quartz (black). Sample from Zone A sulfides. Reflected light.
_____ 0.2 mm.

adjust surface tension (Lawrence, 1972). Evidence of the recrystallization of pyrite grains at Ambler 4B includes the general euhedral nature of most pyrite grains and the presence of polygonized of pyrite grains. Polygonized pyrite grains at Ambler 4B are common, particularly in the more sulfide-rich layers in Zone B (Fig. 19).

In Zone A massive sulfide zones, rounded and rotated pyrite grains are common (Figs. 14, 17, 18, 20). These grains range in size from 0.3 to 1 mm and typically contain curved inclusion "trains" suggestive of rotation during the annealing and recrystallization of the pyrite grain. Inclusions are commonly found near the edges of these rounded grains.

Rounded grains found in Zone A massive sulfide zones often contain small appendages or "arms" that suggest that recrystallization of the grains took place contemporaneously with deformation (Figs. 17 and 18). Areas behind appendages are filled by sphalerite and galena. Approximately 360 pyrite grains in 4 polished sections were counted to see if a rotation direction could be determined using the appendages. In all four samples, from different positions along strike in Zone A, the number of pyrite grains showing clockwise rotation was approximately equal to those showing counterclockwise rotation. In these samples, many round pyrite grains showed no evidence of rotation. Minor subhedral and



Figure 18. Photomicrograph of a rounded and rotated pyrite porphyroblast. Appendages on pyrite porphyroblast are suggestive of clockwise rotation. Pyrite contains inclusions of sphalerite (gray) and quartz (black). Groundmass minerals include sphalerite, chalcopyrite (yellow), galena (white), and quartz. Sample from Zone A sulfides. Reflected light. _____ 0.2 mm.



Figure 19. Photomicrograph of polygonized pyrite grains.
Sample from Zone B massive pyrite layer. Groundmass
minerals include galena (gray) and quartz (black).
Reflected light. _____ 0.2 mm.



Figure 20. Photomicrograph of rounded pyrite porphyroblasts. Groundmass minerals include sphalerite (gray), chalcopyrite (yellow), galena (white), and quartz (black). Sample from Zone A sulfides. Reflected light.
_____ 0.2 mm.

trace euhedral pyrite cubes also occur in Zone A massive sulfides with the rounded, rotated grains.

Average pyrite grain sizes range from approximately 0.1 mm to 0.7 mm. Figure 21 is a logarithmic plot, modified from Templeman-Kluit (1970), that shows average fine pyrite and average coarse pyrite as a function of increasing metamorphic grade. Table 9 lists data from mines by Templeman-Kluit (1970) that was used in Figure 21. Templeman-Kluit (1970) found a positive correlation between increase in metamorphic grade and pyrite grain size. The grain sizes of Ambler 4B pyrites indicate a biotite zone Barrovian metamorphic grade.

Pyrite grain size versus percent total sulfides shows interesting relationships (Fig. 22). From Figure 22, it can be seen that, in general, as percent total sulfides increases, pyrite grain size also increases. This may be due to the fact that recrystallizing pyrite grains in the more massive sulfide horizons were able to grow to larger sizes due to the more abundant availability of elemental components (Fe, S). In Figure 22, two points plot far above (high percent sulfides) the field containing the majority of sample points. These represent samples taken from the very massive pyrite layers in Zone B. The fine-grained nature of these samples probably indicates that, during recrystallization, growth and crystal nucleation were hampered by the close packing of

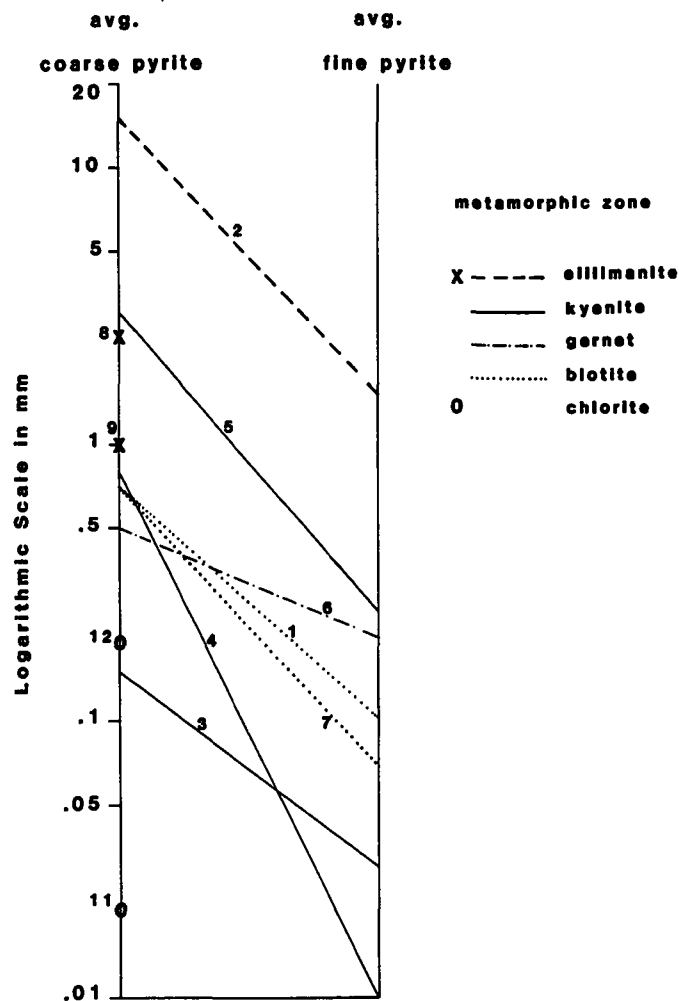


Figure 21. Logarithmic plot of pyrite grain size for different metamorphic grades from various metamorphosed massive sulfide deposits. Lines connect average coarse pyrite grain size and average fine pyrite grain size from the sulfide deposits listed in Table 9. The style of line (dots, dashes...) refers to the metamorphic grade that the deposit has been subjected to. Notations (X or O) along the average coarse pyrite axis refer to grain size and metamorphic grade for deposits where only one grain size is reported. In general as metamorphic grade increases so does pyrite grain size. Ambler 4B pyrite grain sizes (line 1) plot closely with other deposits that have been subjected to similar metamorphism. Data for deposits 2 through 12 has been modified from Templeman-Kluit (1970).

TABLE 9. Metamorphic Data for Deposits Presented in Figure 23

Deposit	Age	Lithology	Index Mineral	Retrograde Effects	Average Coarse Pyrite	Average Fine Pyrite
1. Ambler 4B, Alaska, U. S. A.	Devonian(?)	Felsic and graphitic schist	Biotite-chlorite	Extensive chlorite	.7 mm	.1 mm
2. Bleikvassil, Norway	Ordovician(?)	Mica quartz schist	Kyanite	Minor chlorite	15(?) mm	1.5 mm
3. Helmtjonnho, Norway	U. Ordovician	Schist amphibolite	Garnet	Minor chlorite	.15 mm	.03 mm
4. Nordgruve, Norway	L. Ordovician	Chlorite schists	Biotite-garnet	Extensive chlorite	.8 mm	.007 mm
5. Faro, Y. T., Canada	Proterozoic or Cambrian	Biotite schist	Biotite-garnet	-----	3 mm	.25 mm
6. Vangorda, Y. T., Canada	Ordovician	Phyllite	Chlorite-biotite	-----	.5 mm	.2 mm
7. Anaconda Caribou, N. B., Canada	Ordovician	Phyllite	Chlorite	Chlorite after chloritoid	.7 mm	.07 mm
8. King Fissure, B. C., Canada	unknown	Calc-silicate schist	Sillimanite	Minor sericite	2.5 mm	N. A.
9. It, in B. C., Canada	unknown	Calc-silicate schist	Sillimanite	Minor sericite	1 mm	N. A.
10. Rodkier-Gruve, Norway	Mid-Ordovician	Greenschist	Chlorite	-----	.2 mm	N. A.
11. Heath Steele, N. B., Canada	Mid-Ordovician	Chloritic tuff	Chlorite	-----	.02 mm	N. A.
12. Nordkjetten, Norway	Cambro-Ordovician	Phyllite	Biotite	-----	.7 mm	N. A.

Data from Tempelman-Kluit (1970)

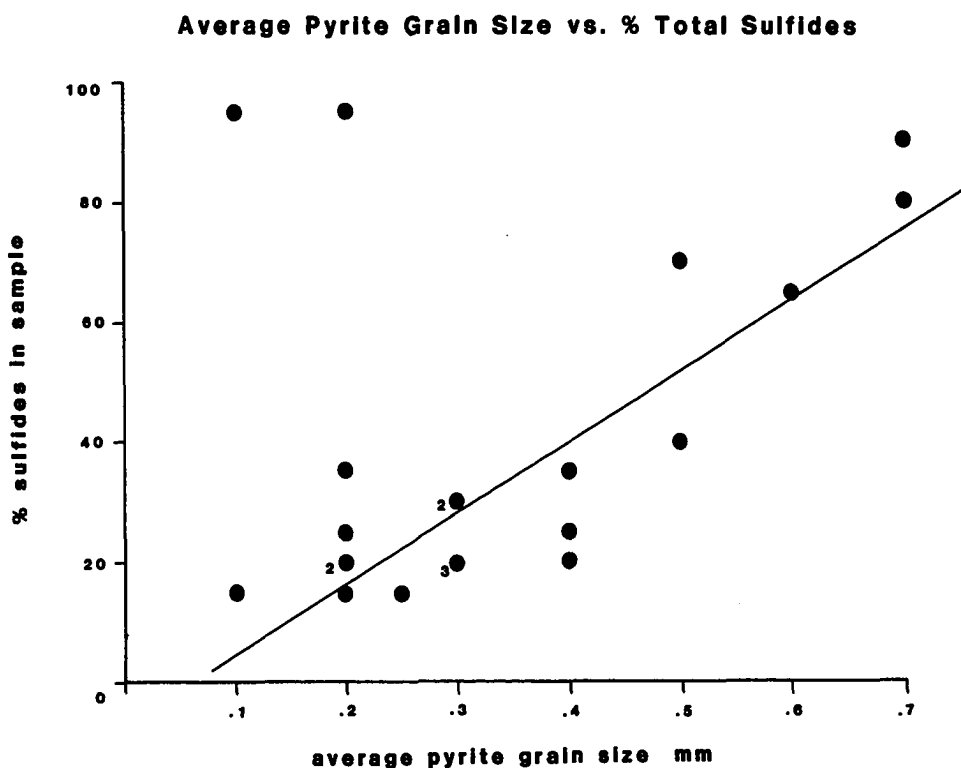


Figure 22. Average pyrite grain size vs. % total sulfides. For a particular sample average pyrite grain size and % total sulfides were estimated. Points with a number (2 or 3) indicates that more than one sample occupies the point on the graph. In general larger pyrite grain sizes occur in the more massive sulfide horizons. The two sample points that fall in the upper left-hand corner of the graph are exceptions. These samples were taken from very massive pyrite layers in Zone B. Pyrite grains in these layers could not achieve large grain size during metamorphism and recrystallization due, probably, to close original grain packing.

pyrite grains. Polygonized pyrite grains are common in the two samples. Pyrite grains in layers containing an intermediate percent total sulfides, on the other hand, were able to achieve larger grain size, because they did not have to compete for space/nucleation sites with other pyrite grains.

Pyrite morphology as a function of grain size also shows significant relationships. Four frequency distributions of pyrite morphologies as a function of grain size are shown in Figure 23. In 18 samples, 1,350 pyrite grains were described on the basis of their degree of roundness and grain size. From Figure 23, it can be seen that as pyrite grain size increases, the degree of rounding also increases. Similarly, the percentage of euhedral pyrite grains decreases with increasing grain size. This relationship between pyrite morphology and grain size may be due to the fact that the larger grains are more susceptible to deformation and shearing. In any event, the relationships indicate that pyrite morphology is a function of metamorphism and not original texture. Zone A and B sulfides are not separated on Figure 23, but in general, the finer-grained Zone B pyrites occur in the size range of 0 to 0.4 mm, and more coarse-grained Zone A pyrites occur in the size range of 0.4 mm and greater. Most pyrite grains in Zone B are euhedral cubes, while Zone A pyrites show a broader range in crystal morphology.

Sphalerite, chalcopyrite, and galena also show changes in fabric due to metamorphism. These minerals behaved, in varying

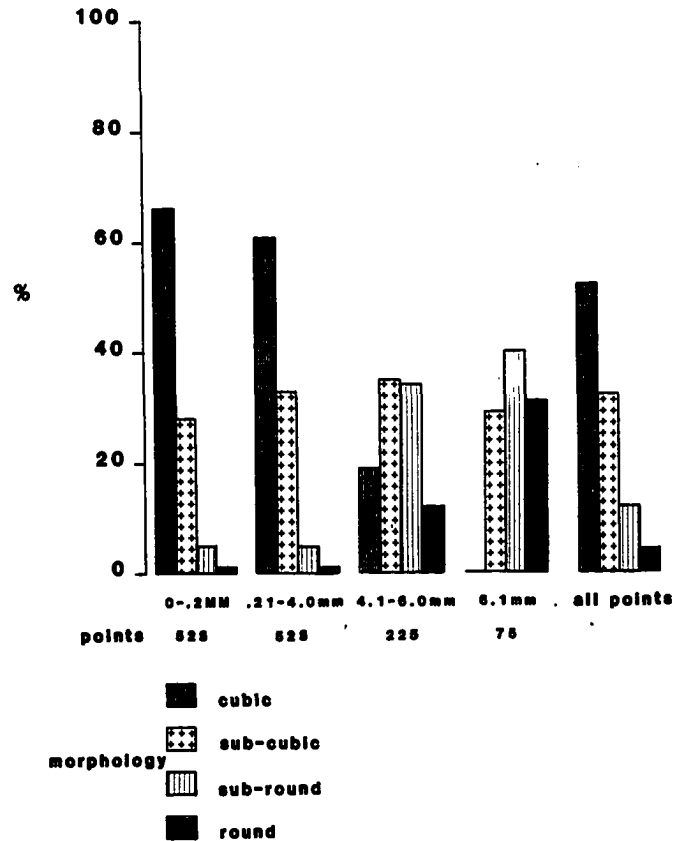


Figure 23. Frequency distributions of pyrite morphology as a function of grain size. Pyrite grains were counted from Zone A and Zone B samples and morphology and size were noted. Euhedral cubic pyrite grains are typically fine grained, while more rounded and deformed pyrite grains are usually coarser grained. The larger grains were probably more susceptible to rounding during deformation and recrystallization than the finer grains.

degrees, plastically and appear to have "flowed" around more brittle pyrite and arsenopyrite grains. Galena, in particular, filled in fractures in pyrite and sphalerite grains. A fractured pyrite grain that has been infilled by galena is shown on Figure 24. Several periods of infilling of galena into fractures in pyrite grains can be seen in some cases, indicating that multiple periods of deformation and metamorphism have occurred.

The major gangue mineral, quartz, also shows varying degrees of deformation and recrystallization. Quartz morphology varies, in some cases over the space of a few mm, from poorly sutured boundaries to a well polygonized nature to stretched, elongate, blade-like forms. Metamorphic textures in quartz are most easily observed in the less sulfide-rich, quartz-rich layers in Zones A and B.

Mobilization of Minerals

The mobilization of minerals such as galena, chalcopyrite, and sphalerite by plastic flow over distances less than approximately one millimeter is common in Ambler 4B sulfides. Such small-scale movement has already been described, i.e., the infilling of galena into fractures in pyrite and sphalerite. Evidence of large-scale movements of minerals, such as the mobilization of minerals into the noses of folds, was not observed macroscopically



Figure 24. Photomicrograph of galena (gray) being forced into a small fracture in a pyrite (yellow) porphyroblast. Sample from Zone A sulfides. Reflected light.
_____ 0.05 mm.

or microscopically. GCO DDH's 1 and 5 intercept the sulfide horizon near the nose of a major fold, and it is evident that a structural thickening of the sulfide horizon or mobilization of sulfide minerals into the fold nose has not occurred on a large scale.

Changes in Mineralogy

Mineralogic changes accompanied the deformation and metamorphism of Ambler 4B sulfides, but reactions are difficult to interpret because of the low abundance or total lack of many of the sulfide phases in a typical sample. Reactions between bornite, chalcopyrite, and pyrite, and pyrrhotite and pyrite were observed in Ambler 4B sulfides.

The reaction that occurred between bornite, chalcopyrite, and pyrite is fairly obvious. Bornite and bornite-chalcopyrite inclusions occur in trace quantities in pyrite porphyroblasts. No bornite was observed outside of pyrite grains. This relationship suggests that previously included chalcopyrite grains reacted to form bornite + pyrite. A rise in sulfur fugacity with metamorphism within a pyrite grain would drive the reaction ($5\text{CuFeS}_2 + \text{S}_2 == \text{Cu}_5\text{FeS}_4 + 4\text{FeS}_2$).

Pyrrhotite is also present in trace amounts at Ambler 4B. The formation of pyrrhotite occurs commonly during metamorphism by the de-sulfurization of pyrite ($\text{FeS}_2 == \text{FeS} + 1/2 \text{S}_2$).

The occurrence of both bornite-pyrite and pyrrhotite-pyrite indicates local domains of both high (bornite-pyrite) and low (pyrrhotite-pyrite) sulfur fugacity, suggesting a lack of widespread equilibrium during metamorphism. The fields for these possible reactions are illustrated in Figure 25, a log activity O_2 - log activity S_2 diagram.

Mobilization of Elements

The mobilization of elements also accompanied the metamorphism of Ambler 4B sulfides and can be best observed in pyrite-sphalerite relationships. Minor low iron, yellow sphalerites (approximately 4 mole % Fe) to more abundant higher iron, red sphalerites (approximately 6 mole % Fe) are found in both Zones A and B. Mole % Fe was calculated in the manner described by Barton and Toulmin (1966) with X-ray diffraction data from a sphalerite sample. Inclusions of sphalerite are common in annealed pyrite grains with yellow sphalerite found in cores and red sphalerites along grain edges (Figs. 26, 27). The iron-poor sphalerites in pyrite cores were presumably once iron rich like the sphalerite included around grain edges. An increase in sulfur fugacity with metamorphism within a pyrite grain would result in a decrease in the iron content of sphalerite resulting in a change in color from red to yellow. The presence of iron-poor yellow sphalerites and iron-rich red sphalerites as inclusions in annealed pyrite grains

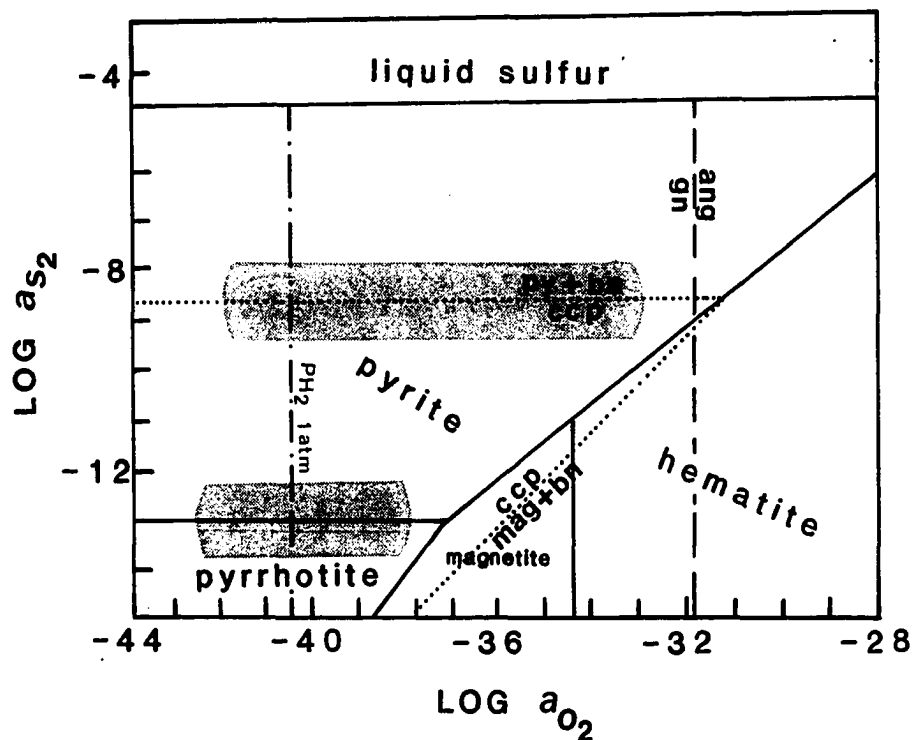


Figure 25. Log activity sulfur vs. log activity oxygen. Highlighted fields are those indicated by assemblages observed in Ambler 4B sulfides. The presence of both bornite-pyrite and pyrrhotite-pyrite indicates local domains of both high (bn-py) and low (po-py) sulfur activity suggesting a lack of widespread equilibrium during metamorphism. Abbreviations: py=pyrite; po=pyrrhotite; gn=galena; ang=anglesite; ccp=chalcopyrite; bn=bornite; mag=magnetite. The diagram, from Barnes (1979) is calculated for 250°C and an H₂O pressure of 40 bars.



Figure 26. Photomicrograph of sphalerite inclusions in a pyrite porphyroblast. Note the presence of relatively low-iron sphalerite (yellow) in the core and higher-iron sphalerite (orange) around the rim of the pyrite porphyroblast (black). Groundmass minerals include sphalerite (orange), pyrite, and quartz. Sample from Zone A sulfides. Plane light. _____ 0.2 mm.

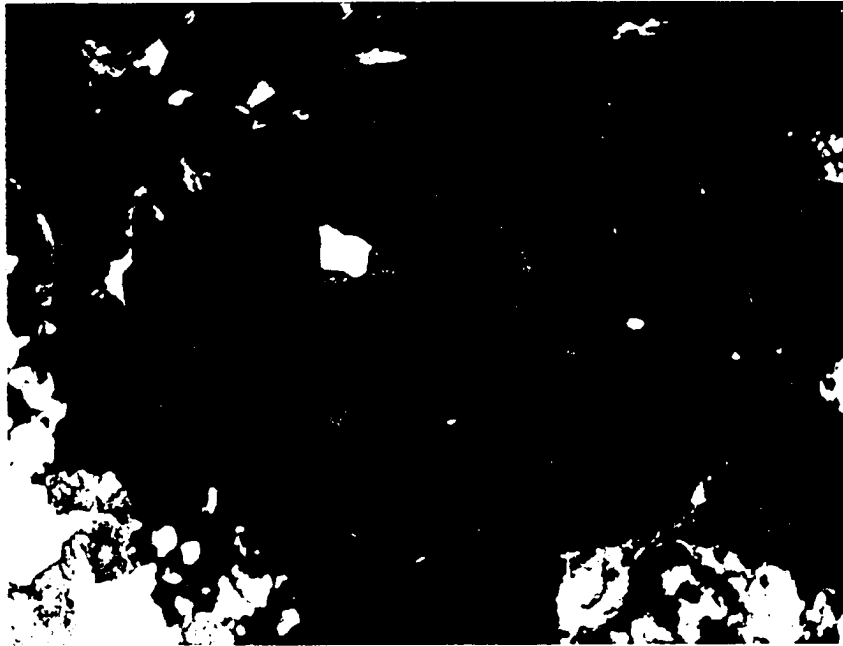


Figure 27. Photomicrograph of sphalerite inclusions in a pyrite porphyroblast. Note the presence of relatively low-iron sphalerite (yellow) in the core and higher-iron sphalerite (orange) around the rim of the pyrite porphyroblast (black). Groundmass minerals include sphalerite (orange), pyrite, and quartz. Sample from Zone A sulfides. Plane light. _____ 0.2mm.

suggests, again, that the sulfides have been subjected to at least two periods of metamorphism.

Summary and Scenario for Textural Development

Gangue rocks in the Ambler 4B area have been subjected to a greenschist-amphibolite grade of regional metamorphism (D2) and then to a glaucophane-forming greenschist event (D3). The sulfides also show evidence of at least two deformational events. The following is a simplified scenario for the development of the metamorphic textures observed in the sulfides.

D2 greenschist to amphibolite grade metamorphism caused the brittle deformation, recrystallization, and annealing of pyrite grains. Galena flowed plastically into fractures in pyrite grains and, along with trace quantities of red high-iron sphalerite and chalcopyrite, was included into annealed pyrite grains.

D3 greenschist metamorphism then occurred. During metamorphism, high-sulfur fugacities within annealed pyrite grains caused the following: (1) the transformation of chalcopyrite to bornite + pyrite and (2) a decrease in the iron content of sphalerite with resulting red to yellow color change. The brittle deformation and contemporaneous rotation, recrystallization, and annealing of pyrite grains continued. Galena "flowed" plastically into fractures in pyrite and sphalerite grains and was, again,

incorporated into annealed pyrite grains along with red iron-rich sphalerite and trace amounts of chalcopyrite. Following metamorphism, pyrrhotite altered to supergene marcasite.

D2 and D3 metamorphism caused the inclusion of both iron-poor and iron-rich sphalerites and bornite in annealed pyrite grains to occur. Retrograde effects were not observed in the sulfide phases.

Thus, the present sizes, morphologies, and mineralogies of sulfides at Ambler 4B are a result of deformation and metamorphism. Also, textures observed in the sulfides can be related to metamorphic grades observed in the silicate minerals. Original sedimentary textures in the sulfide horizon have been nearly obliterated by this metamorphism and deformation. Sedimentary features still recognizable include the relative stratigraphic localization of sulfides and the average sulfide-to-gangue percentage. These features are still recognizable, because the metamorphism and deformation did not result in the large-scale movement of minerals.

Comparison of Ambler District Deposits

With the preceding detailed description of the sulfides at Ambler 4B, a comparison of Ambler district deposits can now be made. The Arctic, BT, and Sun deposits will be briefly described, and then the stratigraphy of the deposits will be summarized. Major features of the deposits are listed in Table 10, and stratigraphic columns are presented in Figure 28. Finally, Ambler district deposits will be compared very briefly to other volcanogenic massive sulfide districts, including the Kuroko deposits, Japan, the Archean (Abitibi belt) deposits, Canada, the Iberian pyrite belt, Spain and Portugal, and the Bathurst district, New Brunswick, Canada.

The Arctic deposit, discovered in 1966, is the largest of the massive sulfide deposits known in the Ambler district (40 million tons; 4.0% Cu, 5.5% Zn, 1.0% Pb, 1.5 oz./ton Ag, .019 oz./ton Au) (Schmidt, 1983). At Arctic, multiple stratiform sulfide lenses from 1 to 60 feet (0.3 to 18.3 m) in thickness occur in chlorite-talc and graphitic schists and are separated by unmineralized schists (Smith and others, 1977). The deposit occurs in a thick sequence of metarhyolites, and rapid facies changes between the metarhyolites and chlorite-talc and graphitic schists are common. Schmidt (1983) reports that depletion of alkalies and enrichment of Ba, F, and Mg are the major chemical changes of pervasive alteration developed symmetrically around the fissure vent

TABLE 10. Geologic Features of Some Ambler District Sulfide Deposits

Deposit	Metals	Structure	
		Folds	Faults
Ambler 4B	Zn Pb Cu Ag (Au)	F1 Isoclinal, poorly exposed F2 Isoclinal, responsible for prominent schistosity, amplitudes to 2000 feet, fold ore horizon F3 Open upright folds produce crenulation cleavage	2 sets of high-angle faults, age relationship unknown, truncate ore horizon
Arctic	Cu Zn Ag Pb (Au)	F1 Intrafolial folds F2 Folds produce main foliation F3 Folds are gentle	Two generations of thrust faults recognized: 1. Low-angle thrusting parallels F1(?) axial planes 2. High-angle thrusting displaces the earlier thrust
BT *	Cu Zn Pb Ag	F1 Isoclinal recumbent folds F2 Folds produce dominant schistosity F3 Open upright folds F4 Open upright folds	Post metamorphic, high-angle reverse faults and steeply-dipping strike-slip faults
Sun	Zn Pb Cu Ag	F1, F2, F3 folds present F2 Folds produce dominant schistosity	27 of 37 DDH's intercept post metamorphic faults, major faults, three faults exposed on surface

* Includes the BT zone and the Jerril Creek horizon

TABLE 10. - continued

Metamorphism	Stratigraphic Localization of Ore	Sulfides
D2 Greenschist to albite amphibolite D3 Greenschist, local glaucophane-forming Retrograde metamorphism	Ore horizon at contact between meta-rhyolite tuff and graphitic schist, Interbedded with mica quartz schist Most of section composed of metasediments Mafic metavolcanic rocks are above and below ore horizon	Pyrite Sphalerite Chalcopyrite Galena Arsenopyrite Tennantite Pyrrhotite Marcasite Bornite Covellite
Low-grade greenschist	Ore occurs in a thick sequence of meta-rhyolites and graphitic schists Ore is confined to chlorite-talc and graphitic schists Rapid facies changes between schists and rhyolites are common	Pyrite Sphalerite Chalcopyrite Bornite Tennantite Galena Pyrrhotite Arsenopyrite Cubantite (Native Cu)
D2 Greenschist to albite amphibolite D3 Blueschist Retrograde metamorphism	BT zone: Ore occurs in muscovite-quartz and graphitic-muscovite quartz schist; two layers of mineralized schist separated by 2.5 - 3 m of unmineralized schist Jerri Creek zone: Ore occurs intercalated in a microcline-mica-quartz schist Metarhyolite - hanging and footwall	Pyrite Chalcopyrite Sphalerite Galena Tennantite Eucalrite(?) Stephenite(?) Enargite
Greenschist assemblages overprint earlier blueschist facies assemblages	Ore occurs in interfingering volcanoclastic and graphitic quartzite and schists	Pyrite Sphalerite Tennantite Galena Chalcopyrite Bornite Enargite Arsenopyrite Pyrrhotite (Magnetite)

TABLE 10. - continued

Gangue Minerals	Orebody Morphology	Ore Textures
Quartz Calcite White Mica Chlorite Biotite Epidote Apatite	Blanket-like sulfide horizon exposed continuously along strike for approximately 1500 m, thickness from 1-9 m Zone A: Three massive sulfide layers separated by quartz-rich layers Zone B: Massive sulfides are lensey	Sulfides show evidence of poly-deformation Rotated, recrystallized, and annealed pyrite grains contain inclusions of yellow and red sphalerite Chalcopyrite appears to replace galena
Quartz Calcite Dolomite Barite Fluorite Phengite Talc Phlogopite	Multiple stratiform sulfide horizons separated by unmineralized schist Individual sulfide bodies vary from 1 - 20 m in thickness	Annealed and recrystallized sulfides, poikiloblastic pyrite grains rare Complex, fine-grained intergrowths of chalcopyrite, sphalerite, minor galena and occasional tennantite
Quartz Muscovite Hyalophane	BT zone: Two beds approx. 1.5 m thick trace 2000 m Jerri Creek zone: Lateral extent of approx. 1 km	BT zone: Euhedral pyrite porphyroblasts up to 0.5 cm contain inclusions of bornite; sphalerite is a reddish color Jerri Creek zone: Disseminated sulfide grains rarely exceed 8 mm
Quartz Ferroan-calcite Ferroan-dolomite Cymrite Barite	Three distinct sulfide horizons are elongate and lenticular; approx. 8000 feet of strike length; massive sulfides grade laterally into semi-massive sulfides interbedded with volcanoclastic or pelitic sediments	Average ore is granular and recrystallized; pyrite crystals are euhedral and range from 1-2 1-2 mm; sphalerite ranges from brown to black

TABLE 10. - continued

Zonation	Alteration	References
No apparent mineralogic or compositional zonation	Possible chloritic alteration in Zone B	
Zn and Zn-Pb-Ag show zonation relative to Cu Metal ratios cyclic and sometimes inconsistent	Underlying chloritic and talc-bearing schist may represent a metamorphosed alteration pipe Horizontally stratified sequence of alteration: barian-phengite, Fe-rich talc, barian fluorophlogopite, magnesian chlorite	Wiltse (1975) Smith and others (1977) Kelsey (1979) Schmidt (1983)
BT zone: Cu / Pb+Zn+Ag decrease laterally from chloritic alteration zone and metarhyolite	Chloritic alteration below BT zone	Hitzman (1978)
Weak vertical and lateral zonation with Pb+Zn increasing with respect to Cu away from proposed fumarolic center Pyrrhotite occurs in hanging and footwall rocks	Talcose chloritic schists occur below massive sulfide horizons Schists contain abundant pyrrhotite and chalcopyrite	Smith and others (1977) Marrs and others (1978) Zdepski (1980)

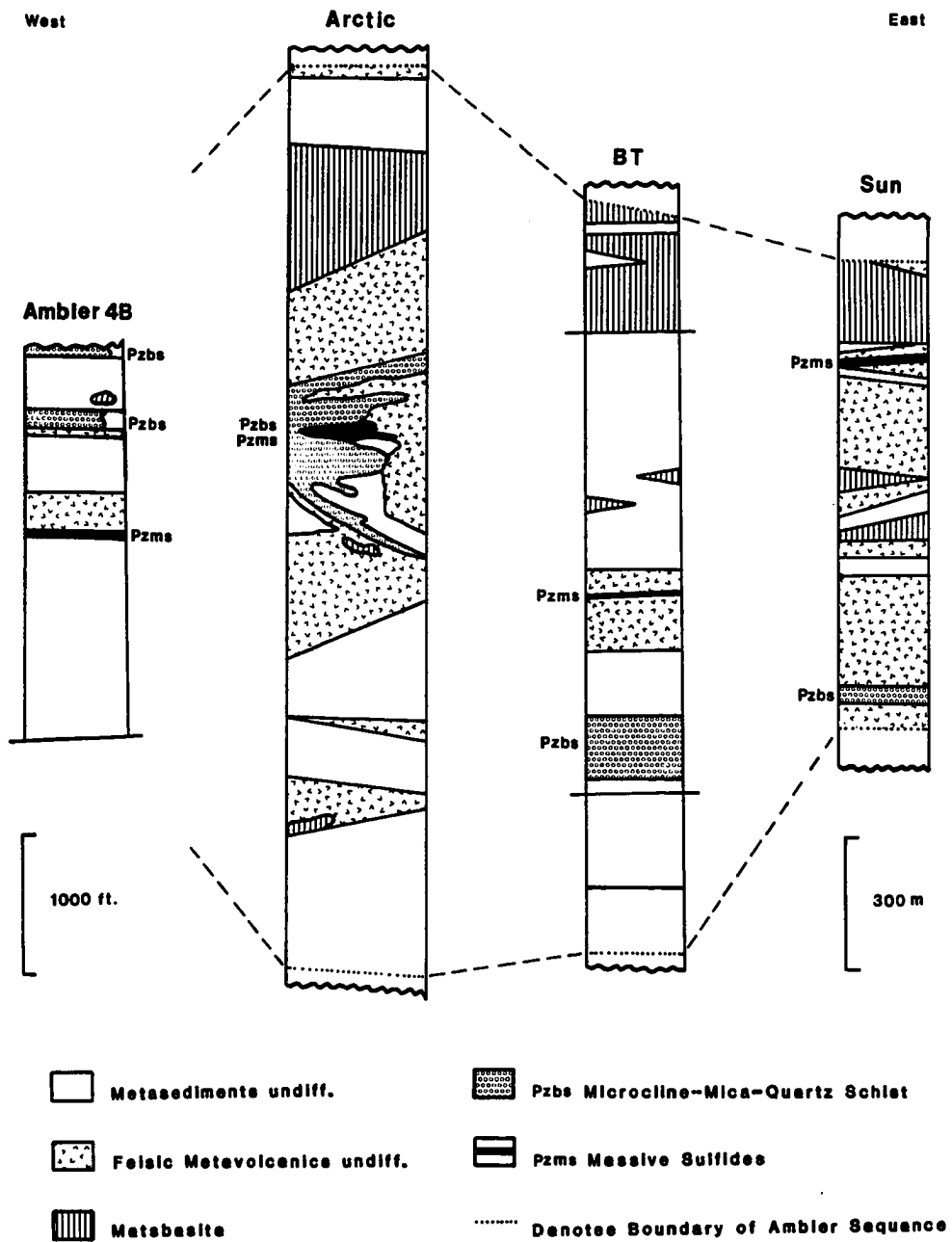


Figure 28. Ambler district stratigraphy. Columns modified from Schmidt (1983), Hitzman (1980), and Zdepski (1980).

at Arctic. The Arctic deposit is the only deposit in the Ambler district where a vent has been found. Schmidt (1983) describes a horizontally zoned sequence of alteration types composed of barian phengite, F-rich talc, barian fluorophlogopite, magnesian chlorite, quartz, carbonates, albite, and cymrite/celsian.

The main similarity between the Arctic and Ambler 4B deposits is that the mineralization occurs stratigraphically in areas of graphitic schists and metarhyolites. Also, the possible alteration-related chlorite present at Ambler 4B may be similar to the chlorites at Arctic. The sulfide horizon at Ambler 4B is much thinner than the Arctic deposit, but its strike length is much greater.

Sulfide mineralization on the BT claim block, described by Hitzman (1978), includes the BT and the Jerri Creek zones. The BT zone consists of two 5-foot- (1.5 m) thick layers of mineralized schist, which are separated by unmineralized pelitic schist (Hitzman, 1978). These layers have been traced laterally over a distance of 6,500 feet (2,000 m) by drilling. Hitzman (1978) reports that metarhyolite forms the hanging and footwall of the ore horizon and that richest base metal mineralization stratigraphically overlies the metarhyolite. The mica-quartz schist and graphitic schist, intercalated with metarhyolite underlying the deposit, contain 2 to 20 modal percent chlorite and minor talc, which are thought to be alteration related (Hitzman, 1978).

Hitzman (1978) reports that the Jerri Creek horizon consists of several beds of massive sulfide to 1 cm in thickness, which occur in a microcline-mica-quartz schist unit. These beds have a lateral extent of at least 1 km and, according to Hitzman (1978), are probably economically unimportant.

Similarities between mineralization at BT and at Ambler 4B are, once again, that mineralization is associated with metarhyolites, mica-quartz schists, and graphitic schists, and that chlorite has been identified as a possible alteration mineral. Also, the BT deposits are very thin and blanket-like and probably most closely resemble Ambler 4B Zone B sulfides.

Zdepski (1980) reports that massive sulfide ores at Sun occur in quartz-mica schist and quartz-graphite schist, which are closely associated with metarhyolites. He reports that individual massive sulfide layers grade laterally over short distances to semi-massive sulfides mixed with quartz-mica schists or quartz-graphite schists. The ore occurs as four mineralized horizons, three of which are traceable for a considerable distance (8,000 feet) (2,450 m) in strike length. The upper horizon is a zinc-lead rich bed, the middle horizon a copper-rich bed, and the lower horizon a copper-zinc rich bed (Zdepski, 1980). He reports that mineral and metal zonation occurs on small and large scales. Individual beds have sphalerite tops, galena \pm tennantite \pm barite centers, and

chalcopyrite + bornite, galena, and tennantite bases. On a large scale, metal zonation consists of high zinc and lead in upper horizons and high copper values in middle horizons. Zdepski (1980) also describes a talc-chlorite schist that underlies the sulfide horizon. He suggests that this schist horizon is an alteration blanket.

Similarities between the Sun deposit and Ambler 4B, once again, include the close spatial association of massive sulfide with feldspathic mica-quartz schist and graphitic schist, the occurrence of a chloritic alteration zone, the fact that the deposit is thin and broad with a large strike length, and that a vent has not been identified. Sun massive sulfide horizons most closely resemble Ambler 4B Zone B sulfides.

In summary, Ambler district massive Zn-Pb-Cu sulfide horizons occur in graphitic schists and felsic mica quartz schists, which are closely associated with metarhyolites. Traditionally, these deposits have been divided into two types based on orebody morphology: proximal and distal. Proximal deposits, such as the Arctic deposit, consist of multiply-stacked ore horizons in close proximity to a vent; and distal deposits, such as Ambler 4B-Smucker, BT, and Sun, consist of uniform, blanket-like deposits of sulfides apparently without an underlying vent. Metal zonation in proximal deposits shows a vertical and horizontal decrease in Cu/Pb+Zn away

from the metal source. Distal deposits are characterized by more irregular metal zonation patterns. Ore deposits are typically underlain by a chlorite or chlorite-talc alteration zone, and, with the exception of the Arctic deposit, zones with both alteration and high Cu grades have not been identified.

An alternative explanation for the deposit morphologies is that deposits like Ambler 4B, BT, and Sun represent sulfide deposition over a diffuse, rather than a "point-source" (vent) area. It seems unlikely that vents such as the well-developed and recognized Arctic vent could have been missed during the long and extensive exploration history of the Ambler district. As previously discussed for Ambler 4B sulfides, hydrothermal fluids may have moved up through the poorly consolidated, predominantly sediment-rich stratigraphies in a diffuse manner. If the fluids did broach the surface, they probably did not emanate in an explosive manner. Fluids or brines that did reach the surface could have been discharged from a great number of sites that may have included submarine features such as a series of fissures or faults, lithologic contacts, or channel ways through more permeable sedimentary units. Deposition of sulfides below the sediment-seawater interface or from a number of sites would explain the irregular metal zonation patterns in deposits such as Ambler 4B, BT, and Sun.

The stratigraphic setting of the sulfide deposits is also important in making a comparison of the deposits. Generalized stratigraphic sections for Ambler 4B and Arctic, modified from Schmidt (1983), BT modified from Hitzman (1980), and Sun modified from Zdepski (1982) are shown in Figure 30. The Ambler 4B section only includes those units in Zone A, and therefore probably does not represent the complete stratigraphic column.

It is apparent from Figure 30 that correlating stratigraphies among the deposits is problematic, because few units are extensive enough to trace more than a few kilometers. The one unit that may be traceable is the microcline-mica-quartz schist, and Marrs and others (1978) suggest that this unit represents a district-wide ignimbritic eruptive event. The position of the sulfide deposits within the stratigraphic columns relative to the position of the microcline-mica-quartz schist show interesting relationships across the district. The sulfide deposits at Ambler 4B occur below the microcline-mica-quartz schist; at Arctic, the sulfides occur essentially within the same stratigraphic horizon as the microcline-mica-quartz schist; at BT, the sulfides occur above the microcline-mica-quartz schist; and at Sun, the sulfides occur a great distance above the microcline-mica-quartz schist. This indicates that Ambler district massive sulfides were not deposited at the same time, and suggests a progressive younging in ages of

deposits from west to east across the district. This feature might be best explained by fissure-related fluid emanations rather than by fluid emanations related specifically to emplacement of a particular rhyolite tuff.

With these features concerning type of feeder system and host stratigraphy in mind, plus the facts that mafic volcanic rocks are commonly found in the district, and that the deposits are approximately Devonian in age (Hitzman and others, 1982), rift related (Hitzman and others, 1982), highly deformed and have been subjected to at least two regional metamorphic events and a retrograde event, the Ambler district massive sulfide deposits can be compared to other massive sulfide districts on a worldwide basis.

Geologic features of the Ambler district, the Bathurst district, the Abitibi belt, the Iberian pyrite belt and the Kuroko deposits are compared in Table 11. These districts were chosen for comparison, because the deposits in them are similar in some ways to Ambler district deposits.

The Miocene Pb-Zn-Cu Kuroko deposits of Japan described by Lambert and Sato (1974) have only a few features that are similar to the Ambler district deposits. The Kuroko deposits are found in the so-called Green Tuff region. Ore bodies are restricted to Middle Miocene rocks and were deposited over a very brief period of time

TABLE 11. Summary of Geologic Features of Ambler District, Bathurst District, Abitibi Belt, Iberian Pyrite Belt, and Kuroko Massive Sulfide Deposits

District and Location	Examples of Deposits	Age	Metals	Tectonic Environment
Ambler District Brooks Range, Alaska	Smucker (Ambler 4B) Sunshine Creek Arctic BT Sun	Devonian	Zn Pb Cu (Ag) (Au)	Rifted continental margin
Bathurst District New Brunswick, Canada	Caribou Wedge Heathe Steele Brunswick #12 Brunswick #6	Ordovician	Zn Pb Cu (Ag) (Au)	Resurgent caldera complex(?)
Abitibi Belt Superior Province, Canada	Millenbach Vauze Horne Quemont Orchan Mattagamí Lake Kidd Creek	Archean	Cu Zn Au Ag	
Iberian Pyrite Belt Spain and Portugal	Planes - San Antonio Rio Tinto Lousal La Zarza Tharsis Cerro Colorado	Carboniferous	Fe Cu Pb Zn (Au) (Ag)	Island arc subduction
Kuroko Deposits Green Tuff Belt, Japan	Kosaka Hanaoka Furutobe Matsuki	Miocene	Zn Pb Cu (Ag) (Au)	Island arc subduction

TABLE 11. - continued

Deformation and Metamorphism	Volcanic Rocks	Sedimentary Rocks	Stratigraphic Setting of Ore Deposits
Polyphase deformation and regional metamorphism	Bimodal tholeiitic basalts and high K ₂ O rhyolites Felsic tuffs and submarine ignimbrites	Pelitic, chemical, and calcareous sediments	Ore deposits associated with felsic domes and flows Typically interbedded with pelitic and felsic tuffaceous rocks
Polyphase deformation and regional metamorphism	Early felsic and latter mafic volcanic rocks Rhyolites are porphyritic and non-porphyritic, K ₂ O : Na ₂ O from .94 to 1.75	Continental derived include arkoses and graywackes Manganiferous and jaspilitic tuffaceous rocks in hanging wall	Metasediments, including sericite-chlorite schists and slates above felsic volcanic centers
Relatively undeformed Polymetamorphosed	Tholeiitic basalt and rhyolite, show calc-alkaline trends due to hydrothermal alteration	Magnetite iron formations, cherts Sediments rare	Ore deposits associated with regional felsic volcanic centers Deposits within or at top of acidic or mafic units
Highly deformed Recumbant folds, thrust faults common	Felsic volcanic rocks Mafic volcanic are minor	Carbonaceous slates Manganiferous jaspers and slates	Ore found in carbonaceous black slate and felsic tuff above felsic volcanic centers
Undeformed Zeolite facies metamorphism	Rhyolites, dacites (domes, flows, breccias, and tuffs) Andesites and basalts minor	Mudstones and siltstones Ferruginous cherts	Stratiform ore localized on flanks of rhyolite domes Overlain by acid tuffs and mudstones Stringer ore in footwall felsic volcanic rocks

TABLE 11. - continued

Orebody Morphology	Zonation	Alteration	References
Two types: 1) Multiply stacked stratiform lenses 2) Blanket-like deposits	Zn+Pb over Cu within individual horizons In some deposits (Ambler 4B), zonation not observed	Barian-phengite, Fe-rich talc, barian fluorophlogopite, Mg-chlorite associated with Type 1 Type 2 deposits	Smith and others (1977) Hitzman (1978) Zdepski (1980) Hitzman and others (1982) Schmidt (1983)
Stratabound lenses or "cigars" within semi-continuous sheetlike mineralized horizons	Lateral and vertical Pb+Zn over Cu Often obscured due to deformation	Chlorite and sericite schists Very limited stratigraphic distribution Confined mostly to footwall zones, chloritic, mineralized stringer zones	Davis (1972) Harley (1979) Jambor (1979) Franklin and others (1981)
Stratabound lenses and stringer zones commonly vertically stacked	Classic Zn over Cu	"Dalmatianite" = fine-grained aggregates of chlorite, sericite, or anthophyllite Cordierite often present Chlorite-sericite below stratiform ores	Simmons (1973) Spence and de Rosen-Spence (1975) Spence (1975) MacGeehan (1978) Riverin and Hodgson (1980)
Very large stratiform beds Stringer zones common Individual deposits often contain multiple pipes	Increase in Cu relative to Pb+Zn towards base of deposits	Cu-poor stockworks are sericitized Cu-rich stockworks are silicified and chloritized Sericite and chlorite in footwall volcanics	Strauss and Madel (1974) Williams and others (1975) Franklin and others (1981)
Oval-shaped, zoned, massive stratiform ores Stockworks and stringer zones in footwall rhyolites	Distinct vertical zonation from high Cu/Cu+Zn+Pb stockworks to low Cu/Cu+Zn+Pb ratios away from pipes	Four distinct zones Quartz, sericite, montmorillonite, and magnesium chlorite most common minerals	Kajiwara (1973) Urabe (1974) Lambert and Sato (1974) Ueno (1975) Urabe and Sato (1978)

(0.2 million years; Ueno, 1975). Also, volcanic rocks comprise most of the Kuroko stratigraphic columns. Features in common with Ambler district deposits include the general association of ore with felsic volcanic rocks, and the classic Pb and Zn over Cu zonation in proximal deposits. Features that are not in common include the great age difference, differences in tectonic environment (the Kuroko deposits are subduction related), the undeformed and unmetamorphosed nature of the Kuroko deposits, the large volcanic component of Kuroko stratigraphy, the absence of ferruginous cherts in the Ambler district, and differences in alteration style. Four alteration zones have been identified around the "average" Kuroko deposit, the most prominent of which is a quartz sericite alteration in the pipe area. This alteration is clearly different from the chlorite or chlorite-talc alteration seen below Ambler district deposits. Also, the Kuroko deposits were discharged from high, Cu-mineralized vents, while some Ambler district deposits may have been deposited as parts of a diffuse feeder system.

The Archean Cu-Zn-(Au-Ag) deposits of the Abitibi greenstone belt, Superior Province, Canada have several features that are comparable to Ambler district deposits (Table 11). These relatively undeformed, polymetamorphosed deposits are associated with felsic volcanic centers and are restricted to certain volcanic units (Amulet rhyolite, Amulet andesite) within a narrow

stratigraphic interval. Ore deposits occur within or at the top of felsic or mafic units, and sedimentary rocks are of minor abundance (Spence and de Rosen-Spence, 1975). Sedimentary rocks include iron formations and cherts. The deposits are zoned with pyrite and sphalerite overlying copper- and pyrrhotite-rich ore (Spence, 1975). Alteration consists of pipelike feeder zones of chloritic and sericitic alteration or anthophyllite, depending on the host rock (Spence and de Rosen-Spence, 1975). Features of these deposits that are similar to Ambler district deposits include the highly metamorphosed nature of the deposits and the presence of chloritic alteration below many of the deposits. Features that are not similar include the much larger mafic volcanic component, the absence of Pb in the Abitibi belt deposits, the absence of sedimentary iron formations in the Ambler district deposits, differences in possible feeder systems, differences in metal zonation patterns, and differences in the amount of volcanic rock within stratigraphies.

The massive Fe-Cu-Pb-Zn sulfide deposits of the Iberian pyrite belt, Spain and Portugal, also have some geologic features in common with Ambler district deposits. The deposits are Carboniferous in age and are island arc-subduction related (Williams and others, 1975) or possibly rift related (Schmidt, pers. comm., 1982). The deposits are highly folded and faulted and occur in

carbonaceous black slates and felsic tuffs above felsic volcanic centers without intermediate or mafic composition volcanics (Williams and others, 1975). The deposits are always limited to submarine, explosive, felsic volcanism and are confined to the vicinity of extrusive centers. Manganiferous jaspers and slates and manganese horizons are commonly found above the ore horizons (Strauss and Madel, 1974). Williams and others (1975) report that the deposits are zoned with Zn+Pb over Cu and that pipes containing both sericitic and chloritic alteration can often be found extending below the stratiform ores into the felsic volcanic rocks.

Similarities between the Iberian pyrite deposits and Ambler district deposits include the stratigraphic localization of ore in graphitic sedimentary rocks and felsic tuffs above felsic volcanic rocks, the classic zonation with Pb and Zn over Cu in proximal deposits, the large ratio of lateral extent to thicknesses of the deposits, and the presence of chloritic alteration. However, Ambler district deposits are not associated with manganiferous or siliceous horizons like those found in the Iberian deposits, were not deposited at the same time, and some deposits, such as Ambler 4B, may have different-type feeder systems than the Iberian pyrite deposits.

The massive Zn-Pb-Cu sulfide deposits of the Bathurst district, New Brunswick, Canada have more characteristics in common

with the Ambler district deposits than any of the previously mentioned districts (Table 11). These deposits are Ordovician in age and are thought to have formed in a resurgent caldera complex (Harley, 1979). Rocks include both felsic and mafic volcanics and continentally derived sediments. The deposits are restricted stratigraphically to the Tetagouche Group volcanic-sedimentary complex. The Tetagouche Group is divided into five main lithologic units, which show an evolution from initial continent-derived sedimentation, through early felsic volcanic and later dominantly mafic volcanic episodes and finally to more immature clastic sedimentation (Harley, 1979). The ore deposits are stratigraphically restricted to the period of felsic volcanism. Manganiferous and siliceous tuffaceous rocks are also common. These rocks have been subjected to polyphase deformation and regional metamorphism (Davis, 1975). Ore deposits are found in sericite-chlorite schists and slates above felsic volcanic rocks and typically contain the Pb-Zn over Cu zonation (Harley, 1979). Alteration consists of chloritic and sericitic schists, which are usually found in the footwall rocks with limited stratigraphic distribution (Jambor, 1979). Jambor (1979) reports that only a few of the deposits contain underlying mineralized and altered stringer zones that are probably feeder pipes.

Bathurst district deposit features that are similar to Ambler district deposits include the rift-related, tensional

tectonic environment, the stratigraphic localization of ore in graphitic and felsic schists associated with metarhyolite, the highly deformed and metamorphosed nature of the deposits, the metal zonation over proximal deposits, and the presence of chloritic alteration below the ore bodies. One feature not in common is that the Bathurst district deposits typically contain manganiferous and siliceous tuffaceous rocks in the hanging wall sequence (Jambor, 1979). Ambler district deposits do not contain these manganese- and iron-rich beds anywhere in their stratigraphies. Other main differences include type of feeder system and the fact that Ambler district sulfide deposition occurred over long periods of time.

In comparing these deposits, it is important to note the aspects in which the deposits differ from one another, i.e., types and styles of underlying feeder systems, stratigraphic settings, relative amounts of sediment within stratigraphies, and tendency towards well-developed metal zoning. These features have presumably been subject to the effects of such unknowns as water depth, wall rock permeability and composition, structural setting, degree and involvement of magmatic and pore fluids, rates of ore fluid discharge, water discharge temperatures, densities, salinities, and sulfidation-oxidation states. Given the number of possible variables involved and the lack of geologic control known for these variables, it would be premature to comment in detail on the effects

of these variables on features observed. However, some regularities appear to be present: volcanogenic massive sulfide deposits in sediment-dominant stratigraphic settings tend to be more blanket like and not funnel shaped; chloritic alteration is more common in sediment-dominant deposits; and there is an association of felsic volcanism seen in all the deposits, although the nature of that association appears to vary. Deposits associated with rift-like settings appear to show sediment-dominant stratigraphies and many common alteration types and morphologies.

Summary and Conclusions

Rocks in the Ambler 4B area consist of mafic and felsic metavolcanic rocks, a thick sequence of metasedimentary rocks, and a massive sulfide horizon. The Zn-Pb-Cu massive sulfide horizon (Pzms) and felsic metavolcanic rocks are traceable along strike for approximately 5,000 feet (1,500 m).

Based on the detailed logging of DDH ore intercepts, the massive sulfide horizon was divided into Zone A and Zone B sulfide horizons. Zone A sulfides consist of three massive sulfide layers that are traceable along strike, and that are vertically separated gradationally by quartz-rich interbeds with semi-massive and disseminated sulfides. Zone A sulfides are thought to represent a blanket-like submarine deposit of sulfides from a metalliferous brine discharged from a number of sites as opposed to a "point-source" (vent). Zone B sulfides, on the other hand, have textures that are different from Zone A sulfides. Zone B massive sulfide layers are not traceable along strike, in some cases are symmetrically zoned and occur interbedded with sulfide-bearing graphitic schist (Pzgs), graphitic-mica-quartz schist (Pzgm), and feldspathic mica-quartz schist (Pzmq). These schists contain an Fe-Mg chlorite, based on X-ray and optical data, which is thought to be alteration related. This evidence suggests that Zone B sulfides may have been of a replacement origin. It is suggested that

mineralized fluids, similar to those that deposited Zone A sulfides, travelled through permeable beds of pelitic rocks and tuffs below the sediment-seawater interface depositing local massive sulfides by replacement, and mineralizing and altering the enclosing sedimentary rocks as part of a diffuse feeder system.

The rocks of the Ambler 4B area have been subjected to two isoclinal folding events (F1, F2), an upright open folding event (F3), and two periods of faulting (D4, D5). F2 folds are large-scale folds and are responsible for the major deformation and folding of the sulfide horizon. Axial planes of F2 folds strike northeast-southwest to northwest-southeast and dip shallowly in a generally westward direction. These folds plunge to the west from 2° to 15°. One large F3 fold, seen in outcrop, folded an F2 fold. D4 and D5 faults at Ambler 4B are poorly exposed and have been inferred from drill hole and outcrop information. They are thought to be high-angle normal faults.

Two periods of regional metamorphism, corresponding with F2 and F3 fold events, affected rocks at Ambler 4B. The first period of syntectonic metamorphism (D2) was an upper greenschist facies event. The presence of D2 hornblende indicates that metamorphism reached amphibolite facies, at least locally, during D2. The second syntectonic metamorphic event (D3) reached greenschist facies. This event locally produced glaucophane. In one sample, D3 glaucophane

can be seen cutting D2 hornblende. Retrograde metamorphism followed D3 metamorphism. The metamorphism described in this report for rocks of the Ambler 4B area is similar to that described by Hitzman (1978) for rocks of the BT claim area.

D2 and D3 metamorphism also affected the sulfides at Ambler 4B. Effects of metamorphism seen in the sulfides, in polished section, include changes in fabric, small-scale mobilization of minerals, changes in mineralogy, and a mobilization of elements. Changes in fabric include brittle and plastic deformation of sulfides, annealing of sulfide grains, recrystallization of sulfides, rotation of sulfides during recrystallization, and increase in grain size with metamorphism. The mobilization of minerals is characterized by the infilling of pyrite and sphalerite fractures by galena. A large-scale remobilization of minerals did not occur at Ambler 4B. Mineralogical changes include galena-chalcopyrite, bornite-chalcopyrite-pyrite, and pyrrhotite-pyrite relationships. These relationships suggest that conditions of both high and low sulfur fugacity existed during metamorphism, which in turn suggests a lack of widespread equilibrium during metamorphism. The local-scale mobilization of elements can be seen in the differing iron contents of sphalerite as inclusions in annealed pyrite grains and sphalerite in the groundmass. All of the metamorphic effects can be accounted for by the metamorphic grades observed in the silicate minerals.

Original sedimentary features of the sulfides have been virtually destroyed during metamorphism and deformation. Still recognizable sedimentary features include the relative sulfide to gangue percentage and the stratigraphic localization of sulfides.

Based on the above detailed study of the Ambler 4B extension of the Smucker deposit, other massive sulfide deposits in the Ambler district were compared. In general, Ambler district massive sulfide deposits occur in highly deformed and polymetamorphosed graphitic schists and felsic mica-quartz schists that are closely associated with units of metarhyolite. Mafic metavolcanic rocks are also common in the district. The sulfide deposits can be divided into two types based on deposit morphology. One type, of which the Arctic deposit is an example, consists of multiply-stacked sulfide horizons in close proximity to a point-source vent. The other type, of which the Ambler 4B deposit is an example, consists of very broad and uniform blanket-like deposits over a "diffuse-source" feeder system.

Major differences between Ambler district massive sulfide deposits and Kuroko, Archean, Iberian pyrite belt, and Bathurst district deposits include the much greater percentage of sedimentary rock within Ambler district stratigraphies, differences in underlying feeder systems, and tendency towards well-developed metal zoning in the Kuroko, Archean, Iberian, and Bathurst district

deposits. These differences may be in part due to the absence of a single feeder system in the Ambler district deposits. Also, and importantly, Ambler district sulfide deposits were not formed at the same time, as was common in many other districts.

APPENDIX I

APPENIDX I

EXPERIMENTAL METHODS

Petrography of Lithologic Units

Tables 2, 3, 4, 5, 7

Standard petrographic methods were used. Approximate mineral modal abundances based on the very detailed thin- and polished-section analysis of numerous samples from a particular lithologic unit.

Structural Data - Stereo Nets

Figures 5, 7, 8

Structural information, collected in the field, computer processed, and plotted in the University of Alaska Honeywell system. The program used was developed by Dr. D. B. Hawkins.

Average Pyrite Grain Size vs. Metamorphic Grade

Figure 23

Average grain size based on the detailed analysis of polished sections. Pyrite grains in a particular sample were divided into average large grain size and average fine

grain size. Large grains are typically a groundmass component. Data from all samples was compiled and averaged, and then compared to the Templeman-Kluit (1970) data.

Pyrite Grain Size vs. Percent Total Sulfides

Figure 24

Based on detailed polished analysis. Both average pyrite grain size (includes pyrite porphyroblasts and groundmass pyrite) and percent total sulfides was estimated for each sample.

Frequency Distribution of Pyrite Morphologies

Figure 25

Based on detailed polished section analysis. Semi-quantitative point-count method. Pyrite grains visually divided into cubic, sub-cubic, sub-round, round morphologies. In a given polished section, all pyrite grains in approximately one-half of the section were described and measured. Data from all of the sections was then compiled and plotted as frequency distributions.

X-Ray Method - ChloriteTable 8

Two types of mica mounts were tried in an attempt to get a random orientation of the chlorite.

Type 1: Mica slurry mounted on a glazed glass slide.

Type 2: Dry mica powder blown onto a standard slide coated with petroleum jelly.

Both types of mounts gave nearly identical results when duplicate samples were run.

X-Ray Method - Sphalerite

Standard slurry mount.

REFERENCES

- Barnes, H. L., 1967, *Geochemistry of hydrothermal ore deposits*: Holt, Rinehart and Winston, Inc., New York, 670 p.
- Barton, P. B., and Toulmin, P., 1966, Phase relations involving sphalerite in the Fe-Zn-S system: *Econ. Geol.*, v. 61, p. 815-849.
- Bostrom, K., Farquarson, B., and Eyl, W., 1972, Submarine hot springs as a source of active ridge sediments: *Chem. Geology*, v. 10, p. 189-203.
- Brosge, W. P., and Pessel, G. H., 1977, Preliminary reconnaissance geologic map of the Survey Pass quadrangle, Alaska: U. S. Geol. Survey open-file map OF 77-27.
- Carden, J. R., 1978, The comparative petrology of blueschists and greenschists in the Brooks Range and Kodiak-Seldovia schist belts: unpublished Ph.D. thesis, Univ. of Alaska, Fairbanks, 221 p.
- Davis, G. H., 1972, Deformational history of the Caribou stratabound sulfide deposits, Bathurst, New Brunswick, Canada: *Econ. Geol.*, v. 67, p. 634-655.
- Dillon, J. T., Pessel, G. H., and Veach, N. C., 1980, Middle Paleozoic magmatism and orogenesis in the Brooks Range,

Alaska: Geology, v. 8, p. 338-343.

Engineering and Mining Journal, June, 1978, Exploration round-up section, p. 295.

Forbes, R. B., Turner, D. L., Gilbert, W. G., and Carden, J. R., 1973, Ruby Ridge traverse, southwestern Brooks Range: Alaska Div. of Geol. and Geophys. Surveys, Ann. Rept., p. 34-36.

Franklin, J. M., Lydon, J. W., and Sangster, D. F., 1981, Volcanic-associated massive sulfide deposits: in Econ. Geol., 75th Anniv. Vol., p. 485-627.

Fritts, C. E., 1969, Geology and geochemistry of the southeastern part of the Cosmos Hills Shungnak D-2 quadrangle, Alaska: Alaska Div. of Mines and Geol., Geol. Rept. no. 37, 35 p.

_____, 1970a, Geology and geochemistry of the Angayucham Mountains, western Alaska: Alaska Div. of Mines and Geol., Ann. Rept., p. 1-8.

_____, 1970b, Geology and geochemistry of the Cosmos Hills, Ambler River and Shungnak quadrangles, Alaska: Alaska Div. of Mines and Geol., Geol. Rept. 39, 69 p.

Fritts, C. E., Eakins, G. R., and Garland, R. E., 1972, Geology and geochemistry near Walker Lake, southern Survey Pass

quadrangle, Arctic Alaska: in Alaska Div. Geol. and Geophys. Surveys, Ann. Rept. 1971, p. 19-27.

Gilbert, W. G., Wiltse, M. A., Carden, J. R., Forbes, R. B., and Hackett, S. W., 1977, Geology of Ruby Ridge, southwestern Brooks Range, Alaska: Alaska Div. Geol. and Geophys. Surveys Geol. Rept. 58, 16p.

Grybeck, D. G., 1977a, Map showing known mineral deposits of the Brooks Range, Alaska: U. S. Geol. Survey open-file rept. 77-166-C, 45 p.

_____, 1977b, Map showing geochemical anomalies in the Brooks Range, Alaska: U. S. Geol. Survey open-file rept. 77-166-D, 1 p.

Grybeck, D. G., Beikman, H. M., Brosge, W. P., Tailleur, I. L., and Mull, C. G., 1977, Geologic map of the Brooks Range, Alaska: U. S. Geol. Survey open-file rept. 77-166-B.

Grybeck, D. G., and DeYoung, J. H., Jr., 1978, Map and tables describing mineral resource potential of the Brooks Range, Alaska: U. S. Geol. Survey open-file rept. 78-1-B, 19 p.

Harley, D. N., 1979, A mineralized Ordovician resurgent caldera complex in the Bathurst-Newcastle mining district, New Brunswick, Canada: Econ. Geol., v. 74, p. 786-796.

- Hitzman, M. W., 1978, Geology of the BT claim group, southwestern Brooks Range, Alaska: unpublished M. S. thesis, Univ. of Washington, Seattle, Washington, 80 p.
- Hitzman, M. W., 1980, Geology of the BT claim group, southwestern Brooks Range, Alaska: in Proceedings of the symposium on mineral deposits of the Pacific Northwest, Geol. Soc. America, Cordilleran Section Meeting, Corvallis, Oregon, March 20-21, p. 17-28.
- Hitzman, M. W., Smith, T. E., and Proffett, J. M., 1982, Bedrock geology of the Ambler district, southwestern Brooks Range, Alaska: Alaska Div. of Geol. and Geophys. Surveys, Geol. Rept. 75, 2 plates.
- Jambor, J. L., 1979, Mineralogical evaluation of proximal-distal features in New Brunswick massive sulfide deposits: Canadian Mineralogist, v. 17, p. 649-664.
- Kajiwara, Y., 1973, Chemical composition of ore-forming solution responsible for the Kuroko type mineralization in Japan: Geochem. Jour., v. 6, p. 141-149.
- Kelsey, G. L., 1979, Petrology of metamorphic rocks hosting volcanogenic massive sulfide deposits, Ambler district, Alaska: unpublished M. S. thesis, Arizona State Univ., Tempe, Arizona, 156 p.

- Lambert, I. B., and Sato, T., 1974, The Kuroko and associated ore deposits of Japan: a review of their features and metallogenesis: *Econ. Geol.*, v. 69, p. 1215-1236.
- Lawrence, L. J., 1972, The thermal metamorphism of a pyritic sulfide ore: *Econ. Geol.*, v. 67, p. 487-496.
- MacGeehan, P. J., 1978, The geochemistry of altered volcanic rocks at Matagami, Quebec: a geothermal model for massive sulfide genesis: *Canadian Jour. Earth Sci.*, v. 15, p. 551-570.
- Marrs, C. D., Heatwole, D. A., and Smith, T. E., 1978, Geology of the Sun volcanogenic massive sulfide deposit, Ambler district, Alaska: paper presented to the Northwest Mining Association, Dec., 1978, 12 p.
- Mayfield, C. F., and Grybeck, D. g., 1978, Mineral occurrences and resources map of the Ambler River quadrangle, Alaska: U. S. Geol. Survey open-file rept. 78-120-I.
- Nelsen, C. J., 1979, The geology and blueschist petrology of the western Ambler schist belt, southwestern Brooks Range, Alaska: unpublished M. S. thesis, Univ. of New Mexico, Albq., New Mexico, 123 p.
- Patton, W. W., Jr., Miller, T. P., and Tailleur, I. L., 1968, Regional geologic map of the Shungnak and southern part of

- the Ambler River quadrangles, Alaska: U. S. Geol. Survey misc. geol. inv. map I-554.
- Pessel, G. H., Eakins, G. R., and Garland, R. E., 1972, Geology and geochemistry of the southern Ambler River quadrangle: Alaska Div. of Geol. and Geophys. Surveys, Ann. Rept., p. 7-9.
- Pessel, G. H., and Brosge, W. P., 1977, Preliminary reconnaissance geologic map of the Ambler River quadrangle, Alaska: U. S. Geol. Survey open-file map OF 77-28.
- Riverin, G., and Hodgson, C. J., 1980, Wall-rock alteration at the Millenbach Cu-Zn mine, Noranda, Quebec: Econ. Geol., v. 75, p. 424-444.
- Schmidt, J. M., 1983, Geology and geochemistry of the Arctic prospect, Ambler District, Alaska: unpublished Ph.D thesis, Stanford University, California.
- Simmons, B. D., 1973, Geology of the Millenbach massive sulphide deposit, Noranda, Quebec: Canadian Mining Metallurgy Bull., v. 166, no. 739, p. 67-78.
- Smith, T. E., Proffett, J. M., Heatwole, D. A., Seklemian, R., 1977, Geologic setting of base-metal massive sulfide deposits, Ambler district, northwest Alaska: paper presented to the Alaska Geological Society Symp., April, 1977, 21 p.

- Smith, T. E., Webster, G. D., Heatwold, D. A., Proffet, J. M., Kelsey, G., and Glavinovich, P. S., 1978, Evidence for mid-Paleozoic depositional age of volcanogenic base-metal massive sulfide occurrences and enclosing strata, Ambler district, northwest Alaska: Geol. Soc. American Abs. with Programs, v. 10, no. 3, p. 148.
- Spence, C. D., 1975, Volcanogenic features of the Vauze sulfide deposit, Noranda, Quebec: Econ. Geol., v. 70, p. 102-114.
- Spence, C. D., and de Rosen-Spence, A. F., 1975, The place of sulfide mineralization in the volcanic sequence at Noranda, Quebec: Econ. Geol., v. 70, p. 90-101.
- Spry, A., 1969, Metamorphic textures: 1st ed., Pergamon Press Ltd., 350 p.
- Strauss, G. K., and Madel, J., 1974, Geology of massive sulphide deposits in the Spanish-Portuguese pyrite belt: Geol. Rundschau, v. 63, p. 191-211.
- Tempelman-Kluit, D. J., 1970, The relationship between sulfide grain size and metamorphic grade of host rocks in some strata-bound pyritic ores: Can. Jour. Earth Sciences, v. 7, p. 1339-1345.
- Thorez, J., 1975, Phyllosilicates and clay minerals: Editions G. Lellotte, B 4820 Dison, Belgique, 578 p.

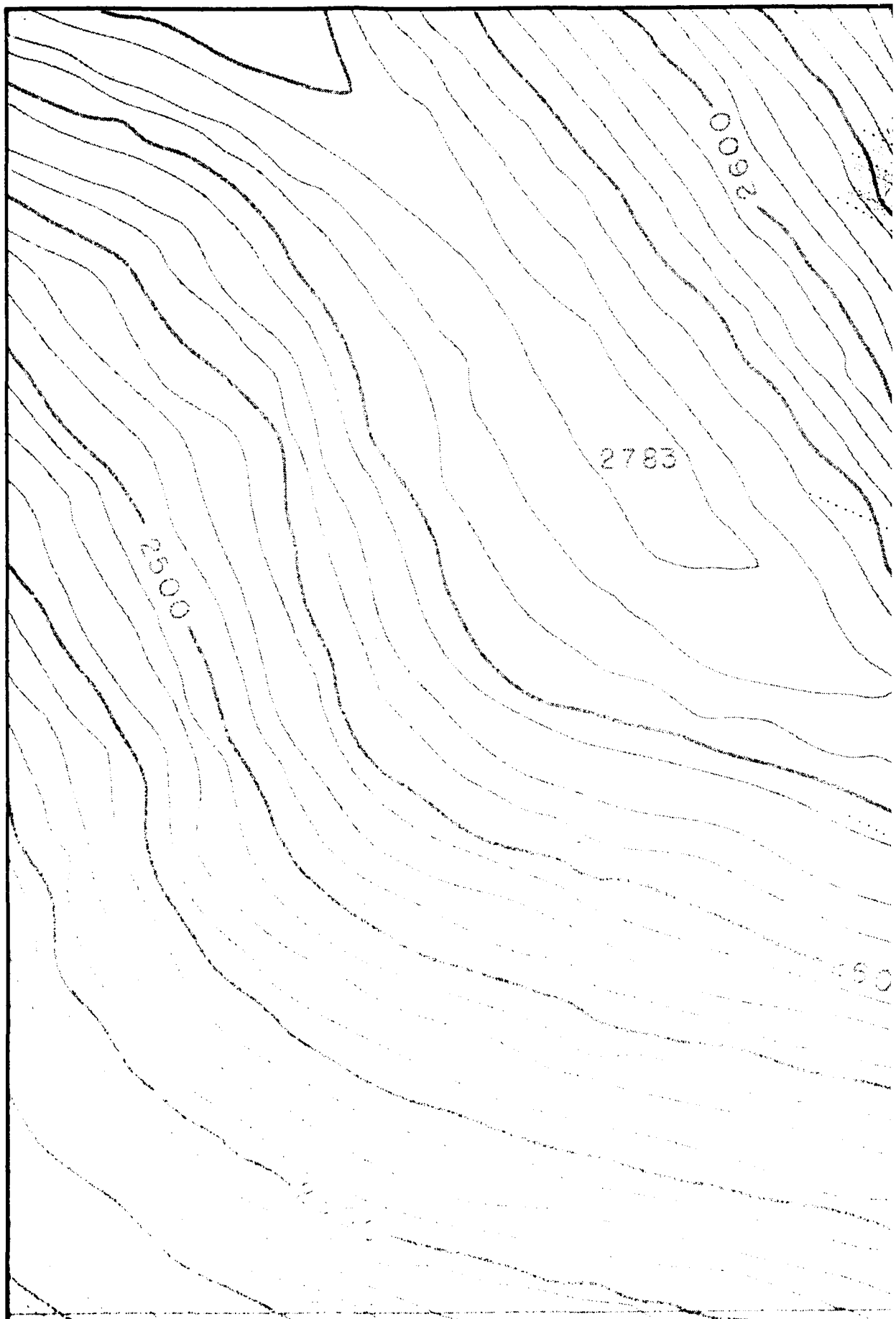
- Turner, D. L., 1973, Geochronology of southwestern Brooks Range metamorphic rocks: Alaska Div. of Geol. and Geophys. Surveys, Ann. Rept., p. 27-30.
- Turner, D. B., Forbes, R. B., and Mayfield, C. F., 1978, K-Ar geochronology of the Survey Pass, Ambler River, and eastern Baird Mountain quadrangles, southwestern Brooks Range, Alaska: U. S. Geol. Survey open-file rept. 78-254, 41 p.
- Turner, F. J., 1981, Metamorphic petrology: Hemisphere Publishing Corporation, McGraw-Hill Book Co., New York, 524 p.
- Ueno, H., 1975, Duration of the Kuroko mineralization episode: Nature, v. 253, 2 p.
- Urabe, T., 1974, Mineralogical aspects of the Kuroko deposits in Japan and their implications: Mineralium Deposita, v. 9, p. 309-324.
- Urabe, T., and Sato, T., 1978, Kuroko deposits of the Kosaka mine, Northeast Honshu, Japan--products of submarine hot springs on Miocene sea floor: Econ. Geol., v. 73, p. 161-179.
- Vokes, F. M., 1969, A review of the metamorphism of sulfide deposits: Earth-Sci. Rev., v. 5, p. 99-143.
- Williams, D., Stanton, R. L., and Rambaud-Perez, F., 1975, The Planes--San Antonio pyritic deposit of Rio Tinto, Spain:

its nature, environment and genesis: Inst. Mining Metallurgy Trans., Sec. B, v. 84, p. B73-B82.

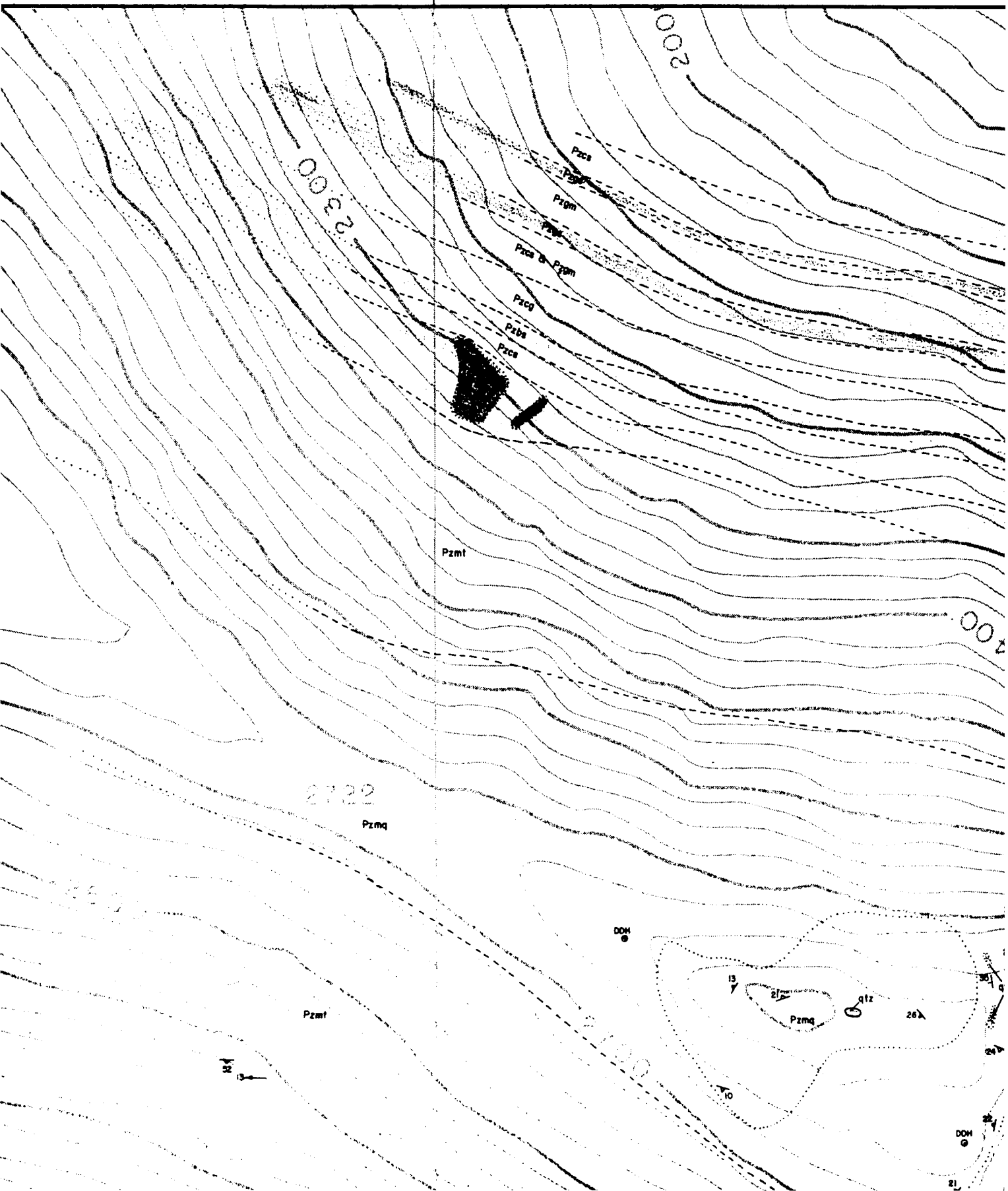
Wiltse, M. A., 1975, Geology of the Arctic Camp prospect, Ambler River quadrangle, Alaska: Alaska Div. of Geol. and Geophys. Surveys, open-file rept. 60, 41 p.

Winkler, H. G. F., 1979, Petrogenesis of metamorphic rocks; Verlag-Springer, New York, 334 p.

Zdepski, J. M., 1980, Stratigraphy, mineralogy and zonal relations of the Sun massive sulfide deposit, Ambler district, northwest Alaska: unpublished M. S. thesis, Univ. of Alaska, Fairbanks, Alaska, 93 p.

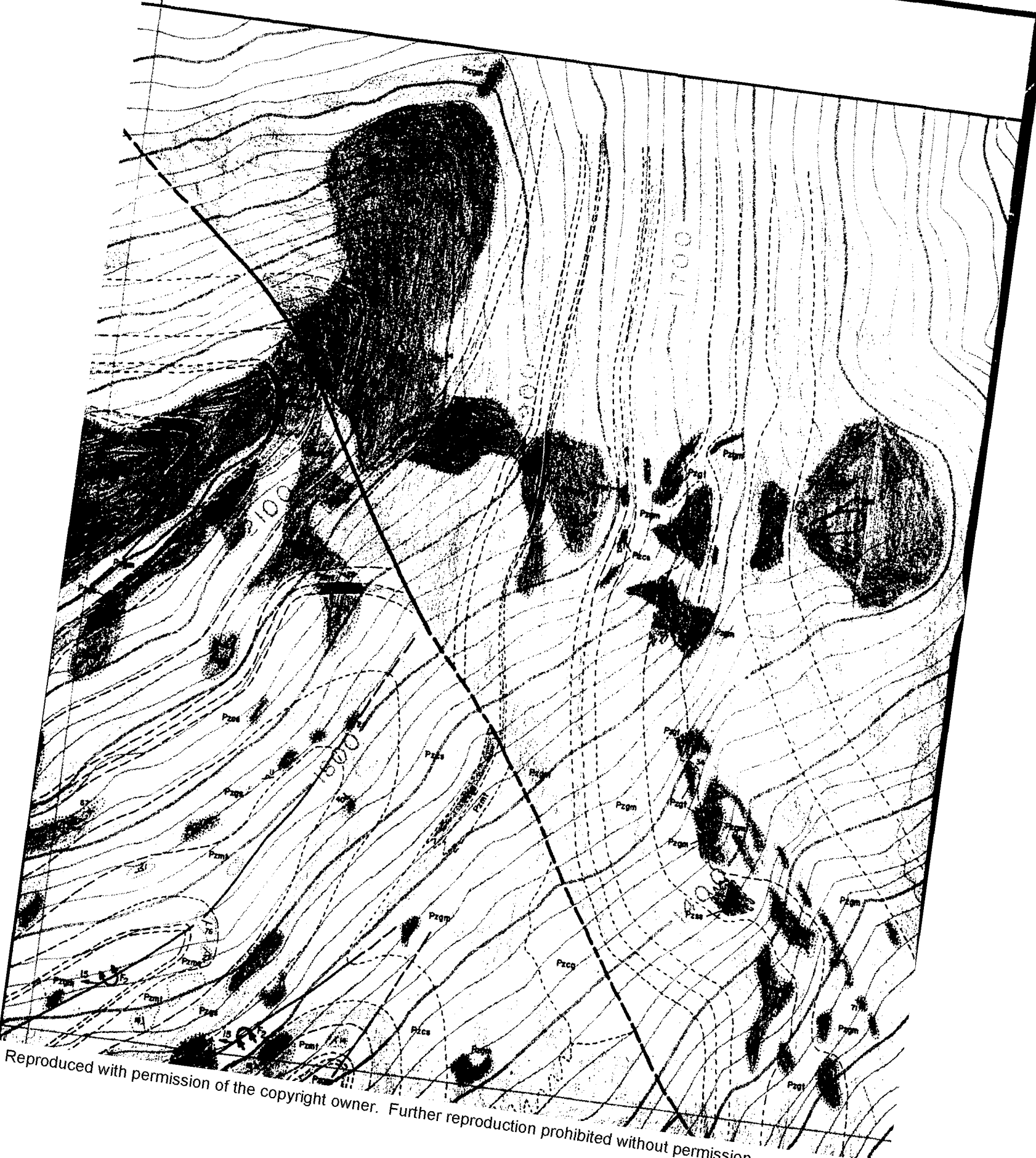


75,000 E

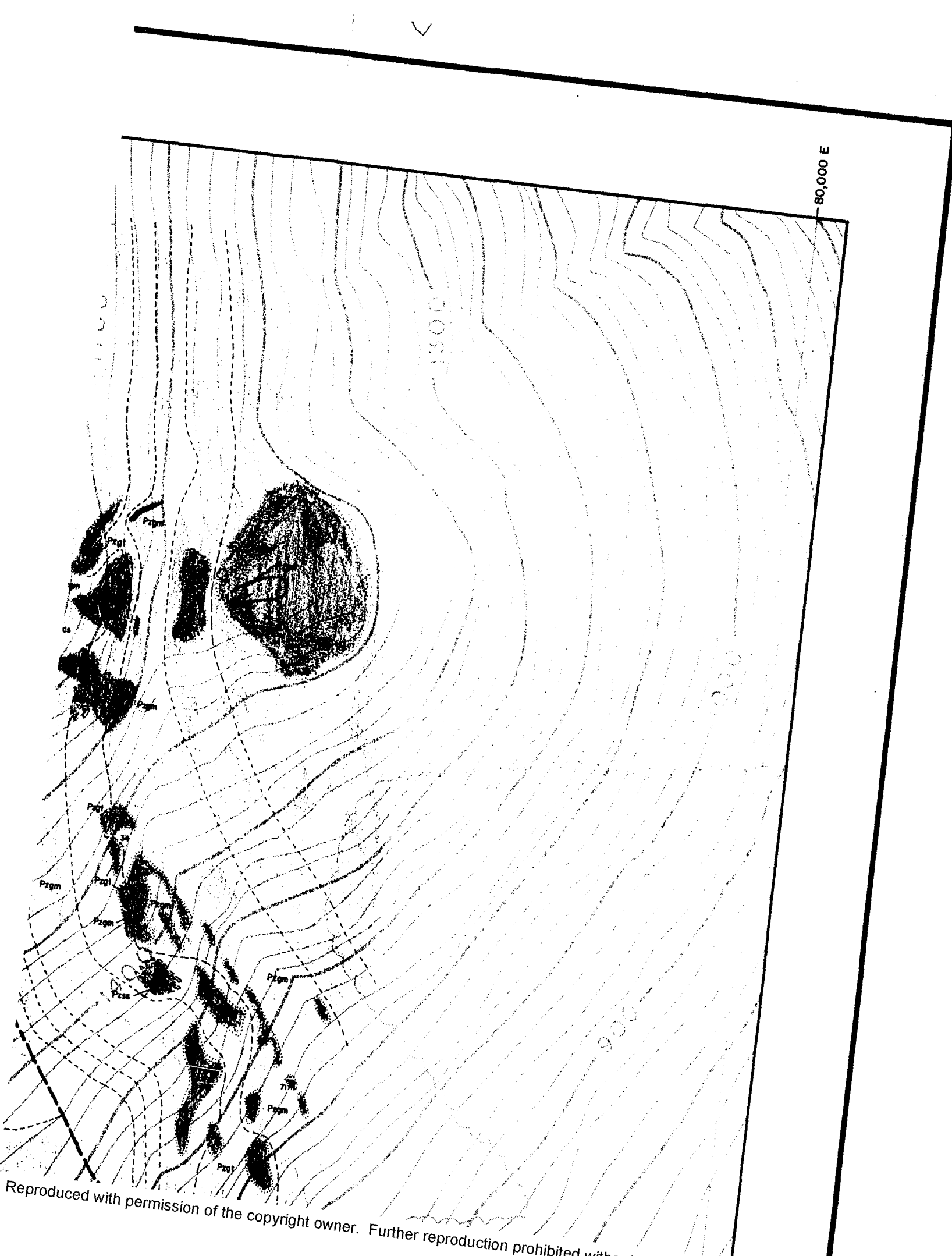




77,500 E

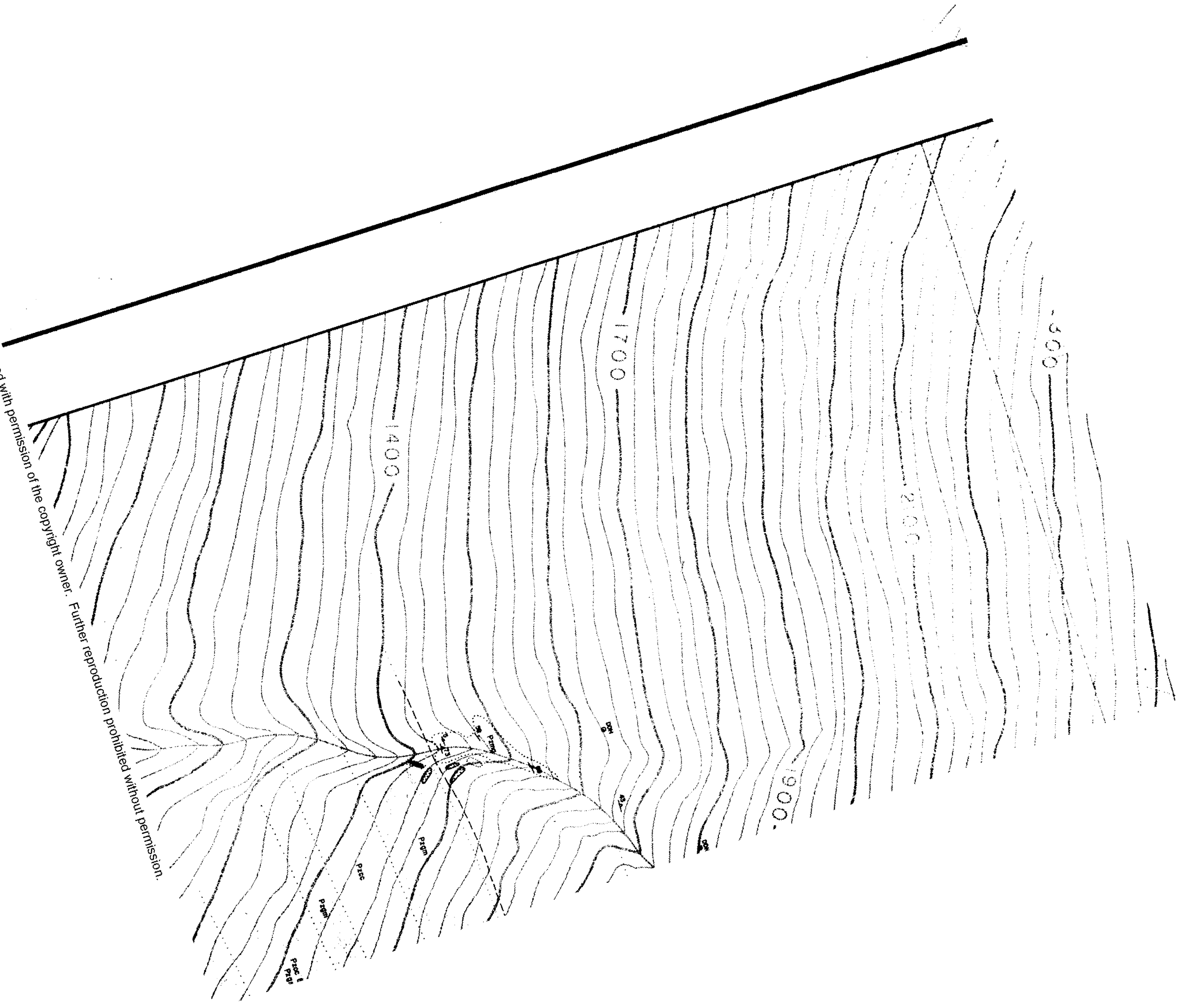


Reproduced with permission of the copyright owner. Further reproduction prohibited without permission.



Reproduced with permission of the copyright owner. Further reproduction prohibited without permission.

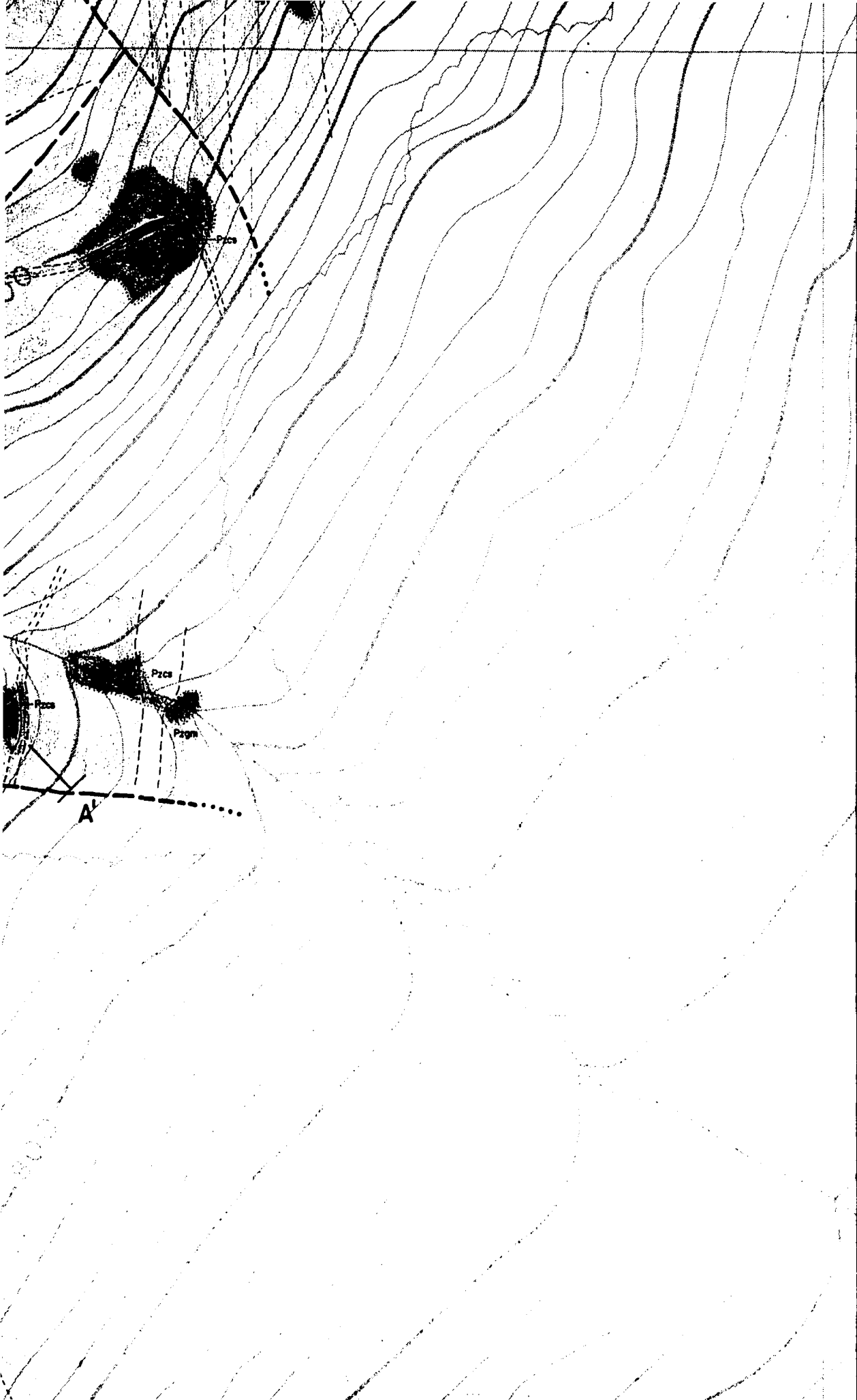
Reproduced with permission of the copyright owner. Further reproduction prohibited without permission.

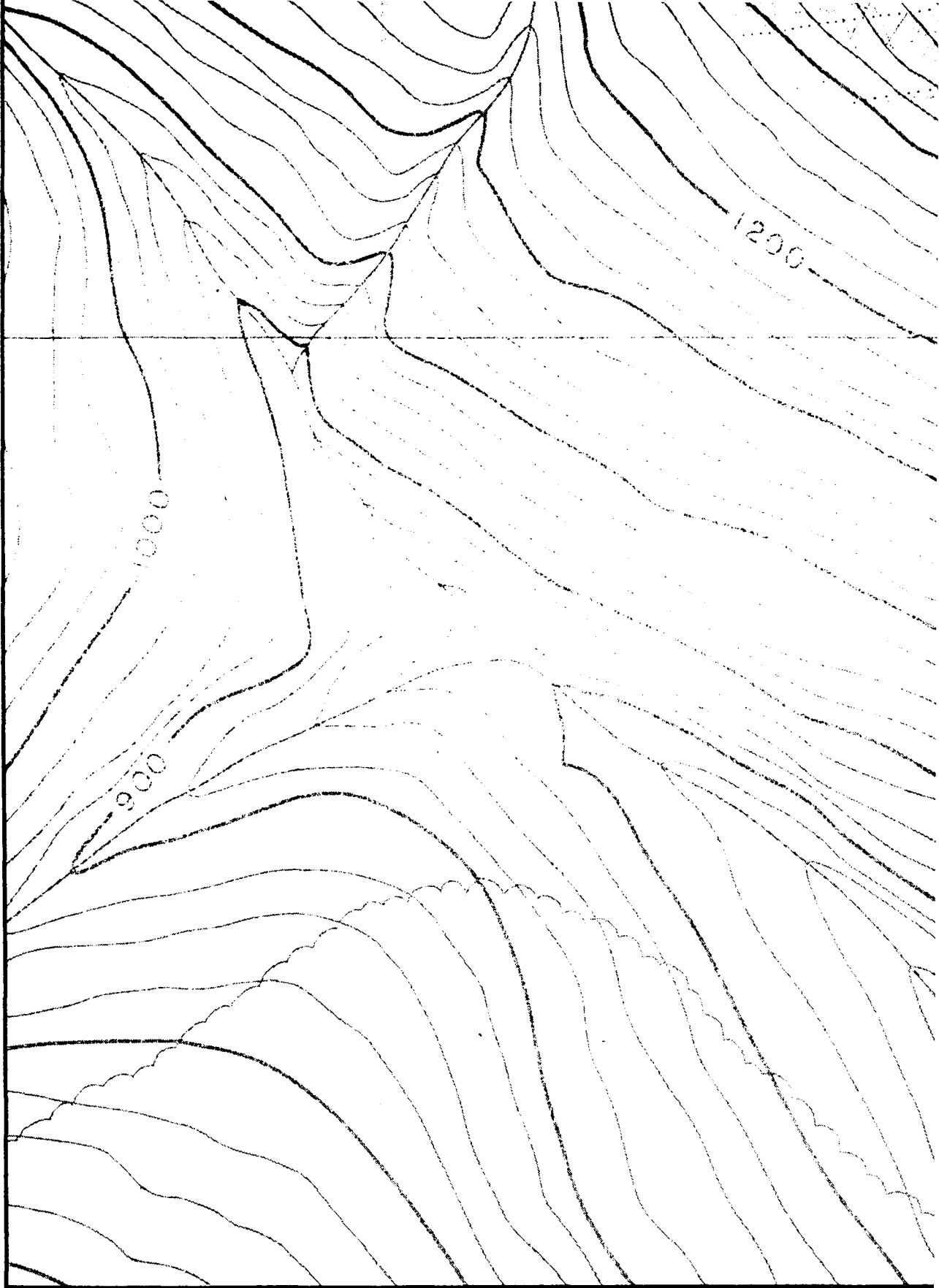




Reproduced with permission of the copyright owner. Further reproduction prohibited without permission.

110,000 N





Pzmt
743

METARHYOLITE TUFF -
(Qz - Mic - Ab - W. Mica)

Pzmq

FELDSPATHIC MICA-QUARTZ SCHIST

745 1/2

FINE TO
GRAPT

GRAPT

GRAPT



FINE TO MEDIUM GRAINED CALCAREOUS AND
GRAPHITIC METASEDIMENTS, Undifferentiated



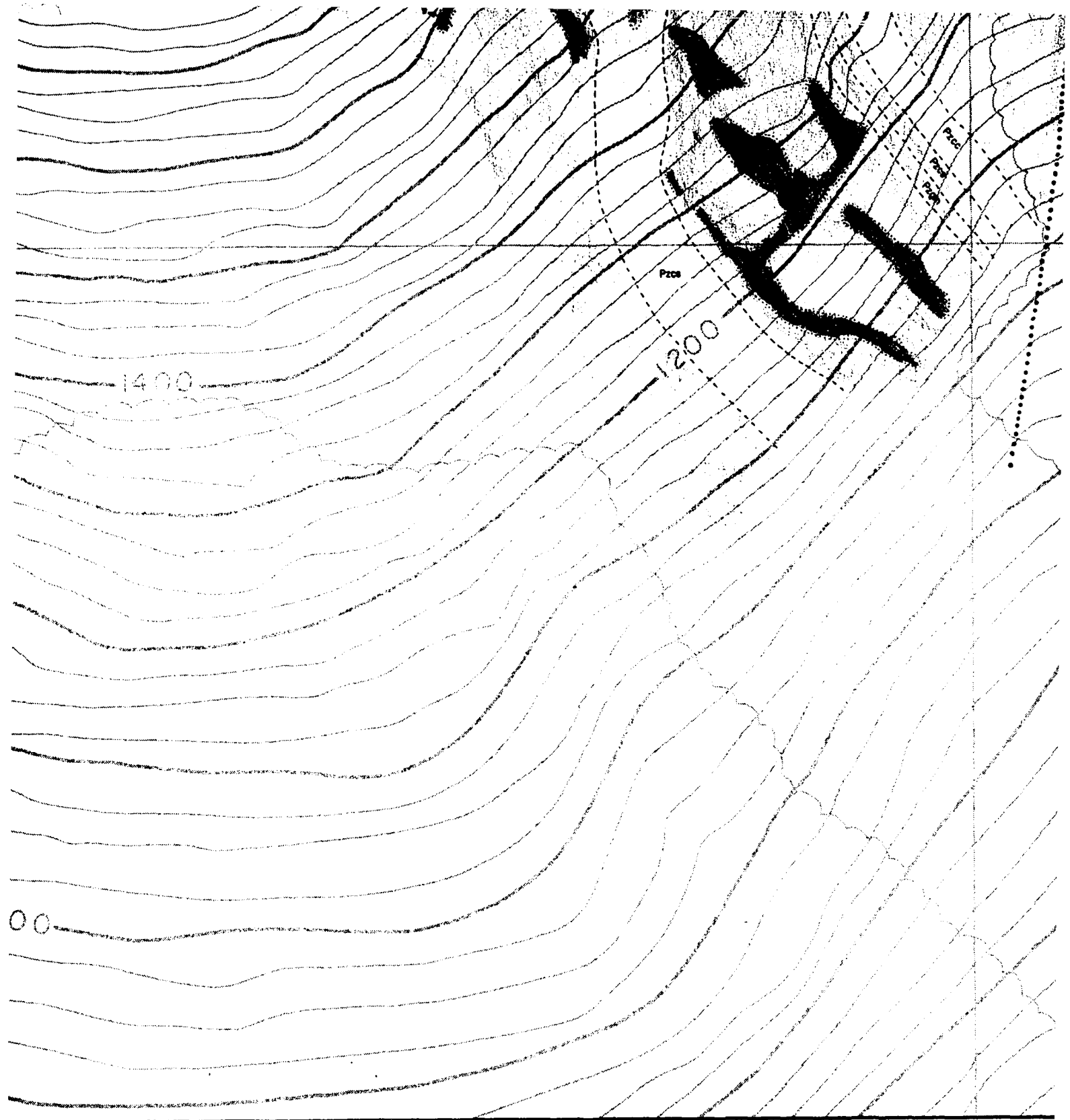
GRAPHITIC - MICA - QUARTZ SCHIST
(G - M - Q)

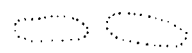
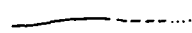



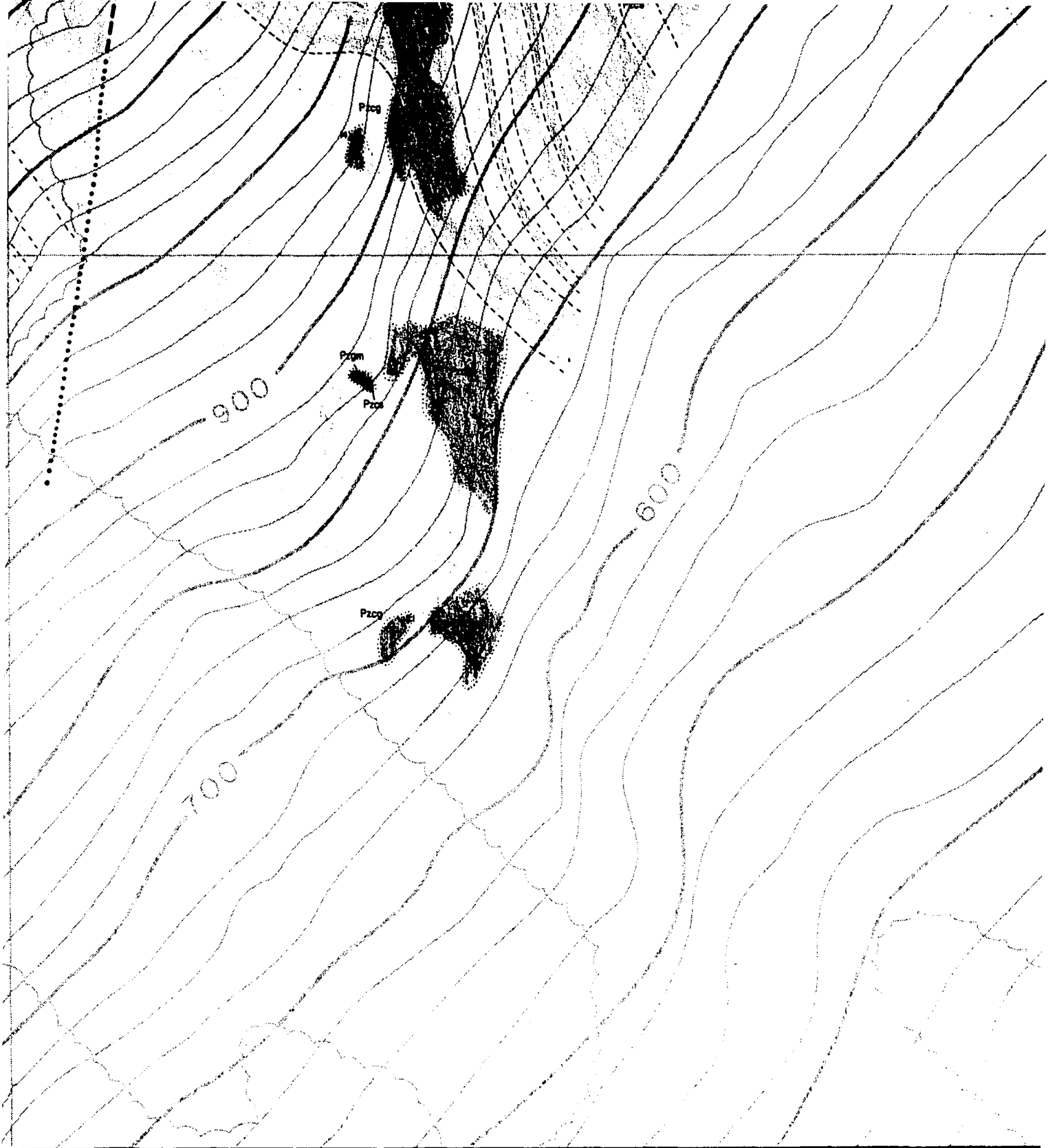
CALC - SILICATE SCHIST -
(Chl - Ab - Act - Cal)


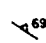

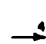


METABASITE -
(Act - Chl - Ab - Gar - Clinz)



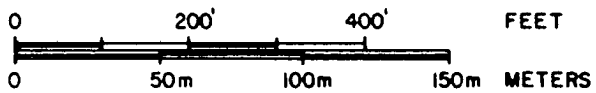
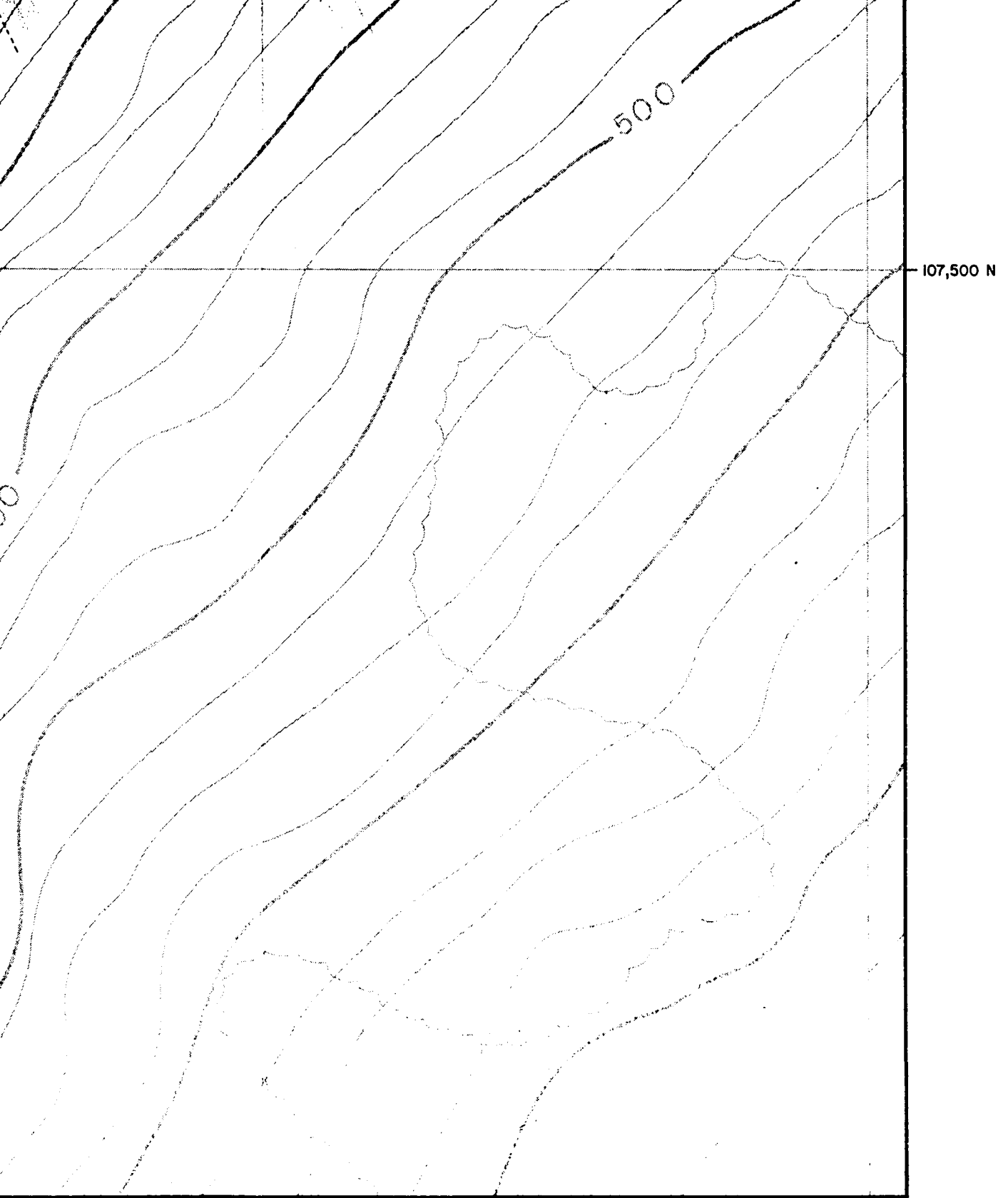
-  LIMIT OF OUTCROP
-  CONTACT ; approximate , inferred
-  FAULT ; approximate , inferred



-  STRIKE AND DIP OF BEDDING
-  STRIKE AND DIP OF S₁ FOLIATION
-  STRIKE AND DIP OF S₂ FOLIATION
-  DIRECTION AND PLUNGE OF L₂ LINEATION

and plunge



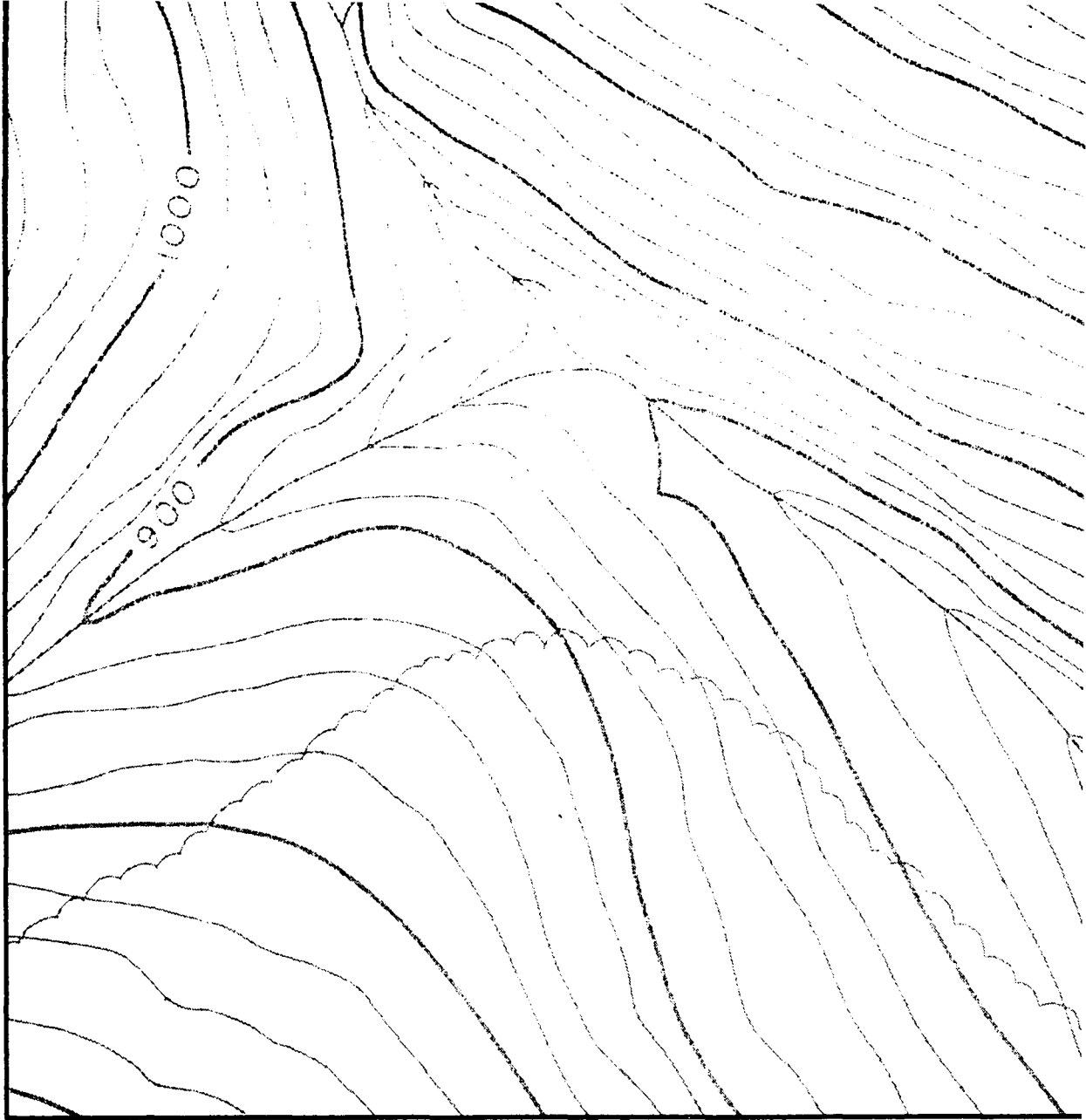


ATION



**GEOLOGIC MAP
OF AMBLER 4 B**

Reproduced with permission of the copyright owner. Further reproduction prohibited without permission.



Pzmt
743

METARHYOLITE TUFF -
(Qz - Mic - Ab - W. Mica)



Pzmq
735 1/2

FELDSPATHIC MICA - QUARTZ SCHIST
(Qz - Ab - W. Mica)



742 1/2

MICROCLINE - MICA - QUARTZ SCHIST
(Qz - Mic - Ab - W. Mica)



745 1/2

**FINE TO
GRAFI**



756

GRAFI
(Qz)



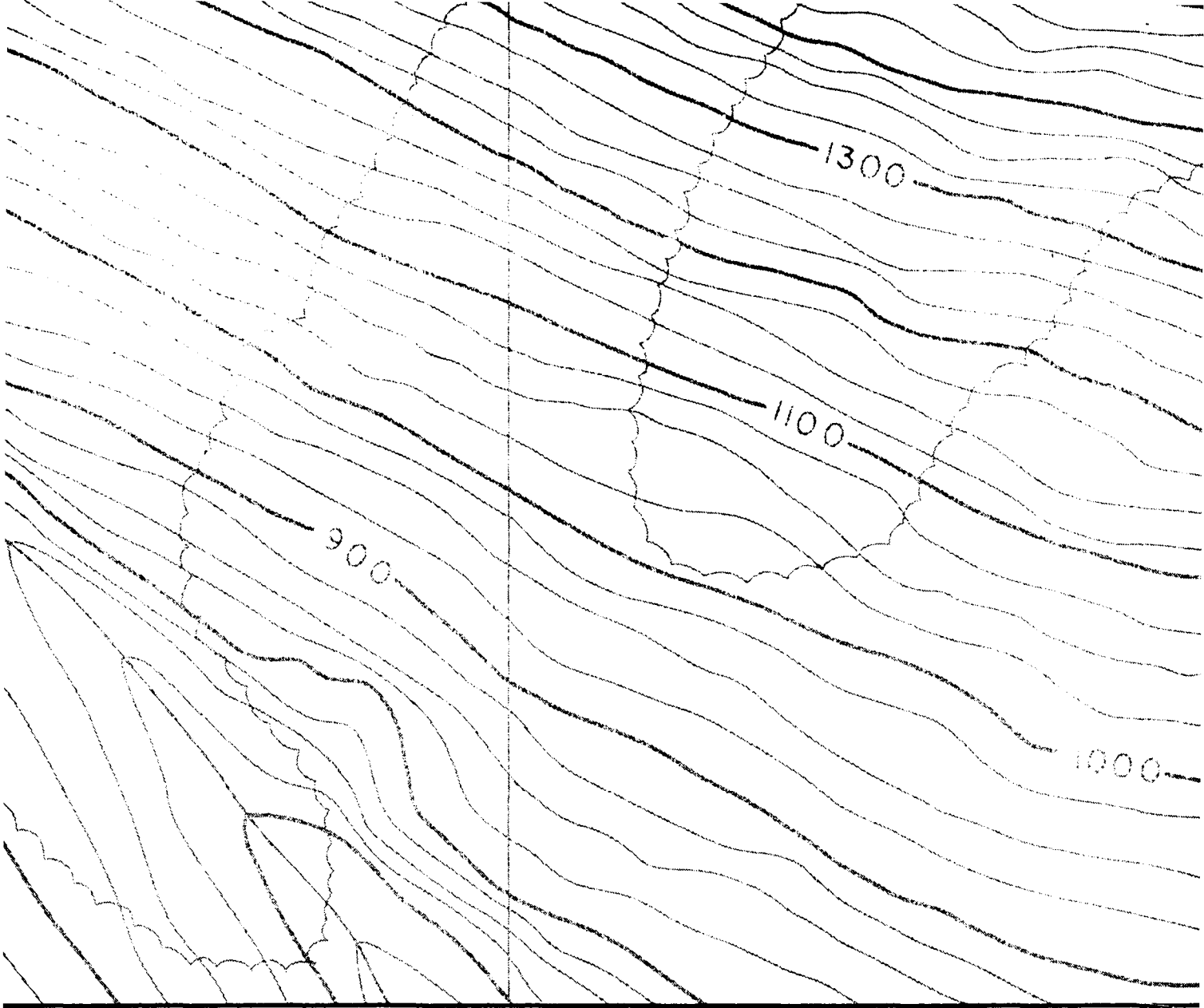
747 1/2

GRAFI
(Qz)




740 1/2

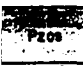
CALC
(Qz)





 FINE TO MEDIUM GRAINED CALCAREOUS AND GRAPHITIC METASEDIMENTS, Undifferentiated
5 1/2

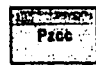
 GRAPHITIC - MICA - QUARTZ SCHIST
(Qz - Ab - W. Mica)
756

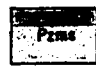
 GRAPHITIC SCHIST -
(Qz - Ab - W. Mica - Graph)
747 1/2

 CALC - SCHIST -
(Qz - Cal - Ab - W. Mica)
740 1/2

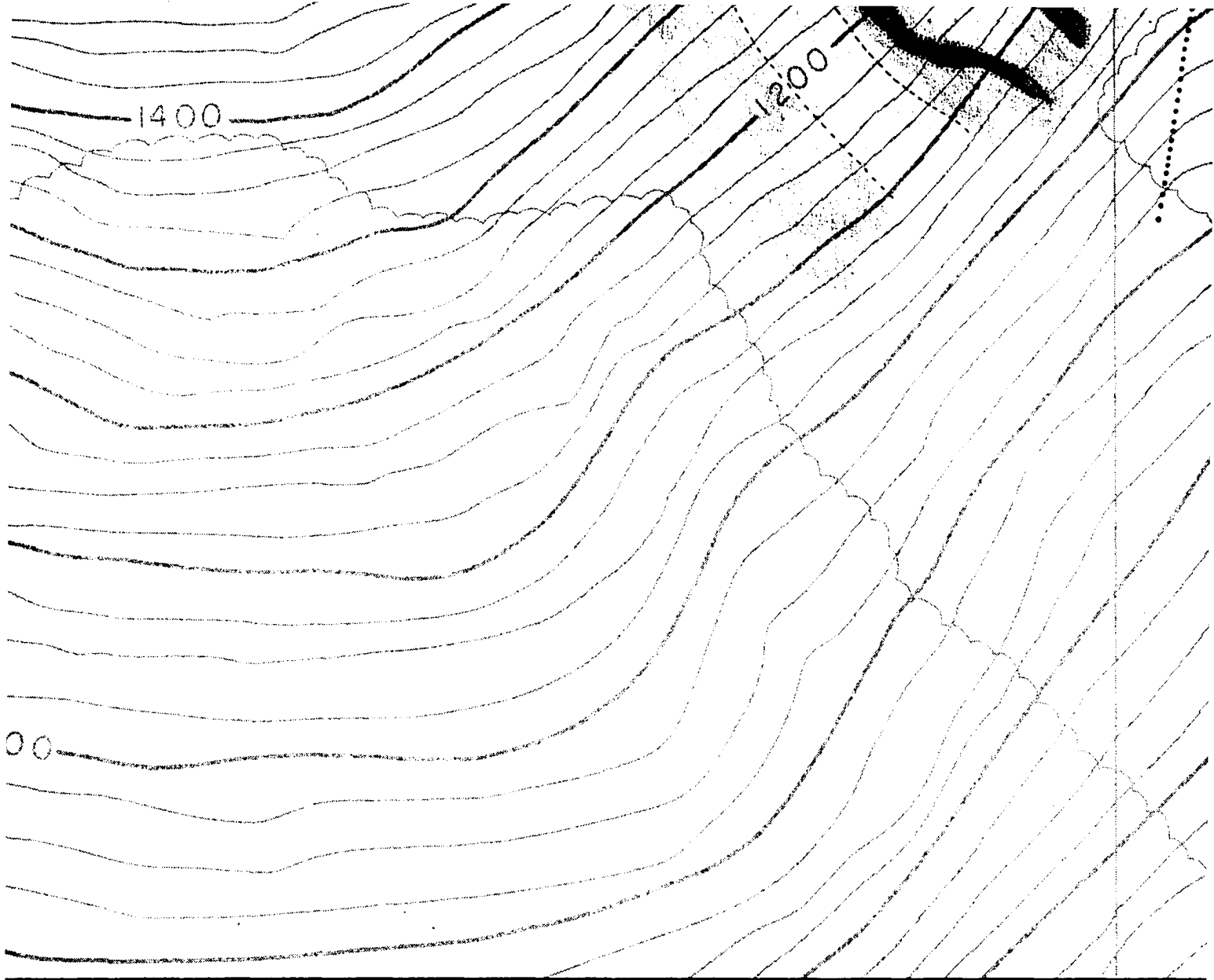
 CALC - SILICATE SCHIST -
(Chl - Ab - Act - Cal)
760

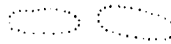



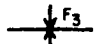
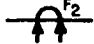
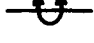
 METABASITE -
(Act - Chl - Ab - Gar - Clnz)
738

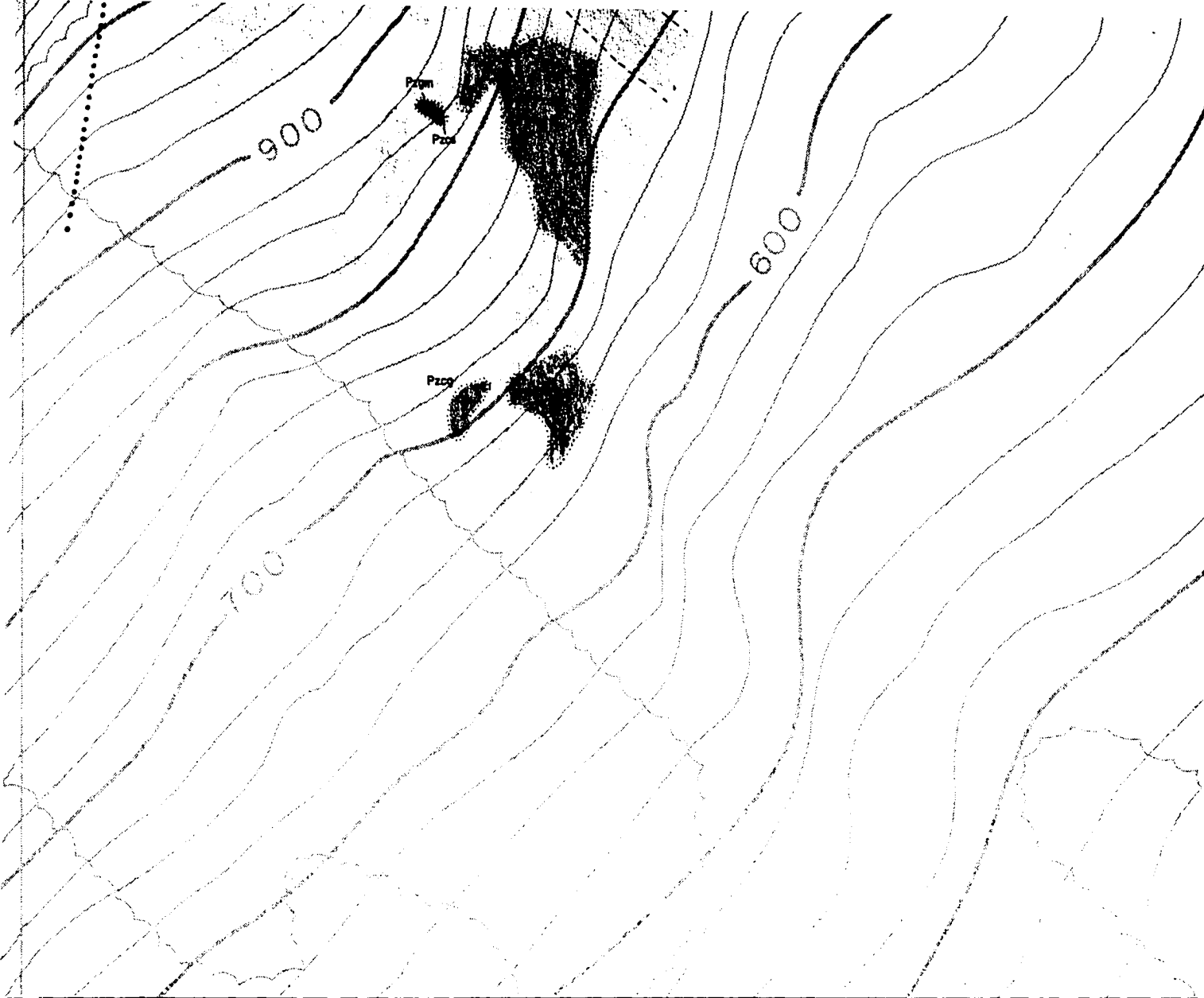
 CALCAREOUS CHLORITE SCHIST -
(Chl - Cal - Qz - W. Mica)
739 1/2

 SEMI - MASSIVE AND MASSIVE SULFIDE -
(Py - Sph - Gn - Cpy)
744

 QUARTZ VEIN
737

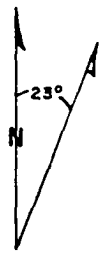


- 
LIMIT OF OUTCROP
- 
CONTACT ; approximate , inferred
- 
FAULT ; approximate , inferred
- 
AXIAL PLANE , showing direction and plunge of fold axis .
- 
SYNCLINE , F₃ indicates 3rd stage folding
- 
OVERTURNED SYNCLINE , F₂ indicates 2nd s
- 
OVERTURNED ANTICLINE



1 and plunge
 ge folding
 indicates 2nd stage folding

- STRIKE AND DIP OF BEDDING
- STRIKE AND DIP OF S₁ FOLIATION
- STRIKE AND DIP OF S₂ FOLIATION
- DIRECTION AND PLUNGE OF L₂ LINEATION
- JOINT
- DIAMOND DRILL HOLE
- TRENCH
- CLAIM CORNER





ATION



GEOLOGIC MAP
 OF AMBLER 4B
PLATE I

SCALE: 1" = 200 ft.

DATE: 4/83

DRAWN BY: JB

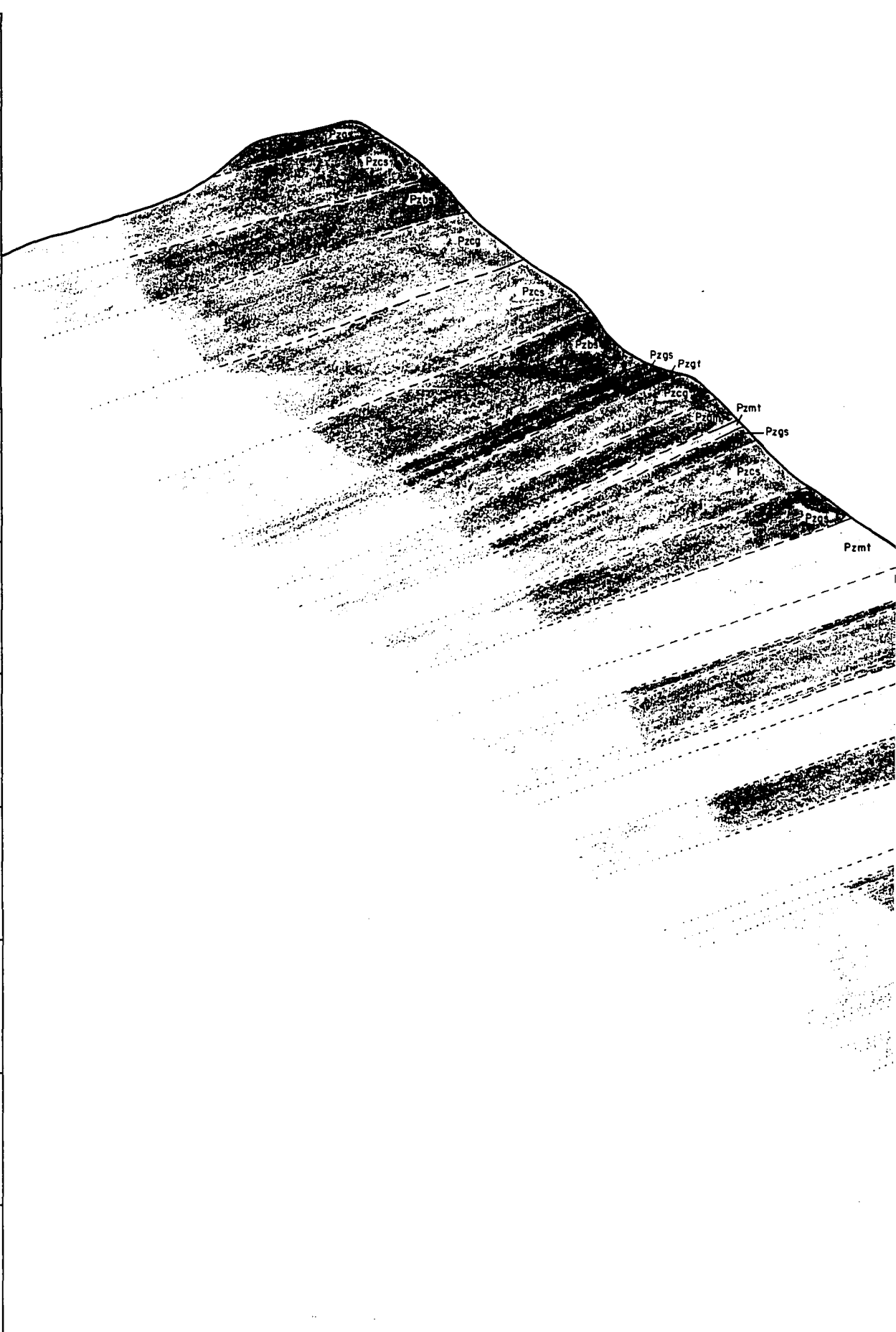
DATA BY: DSIMPSON

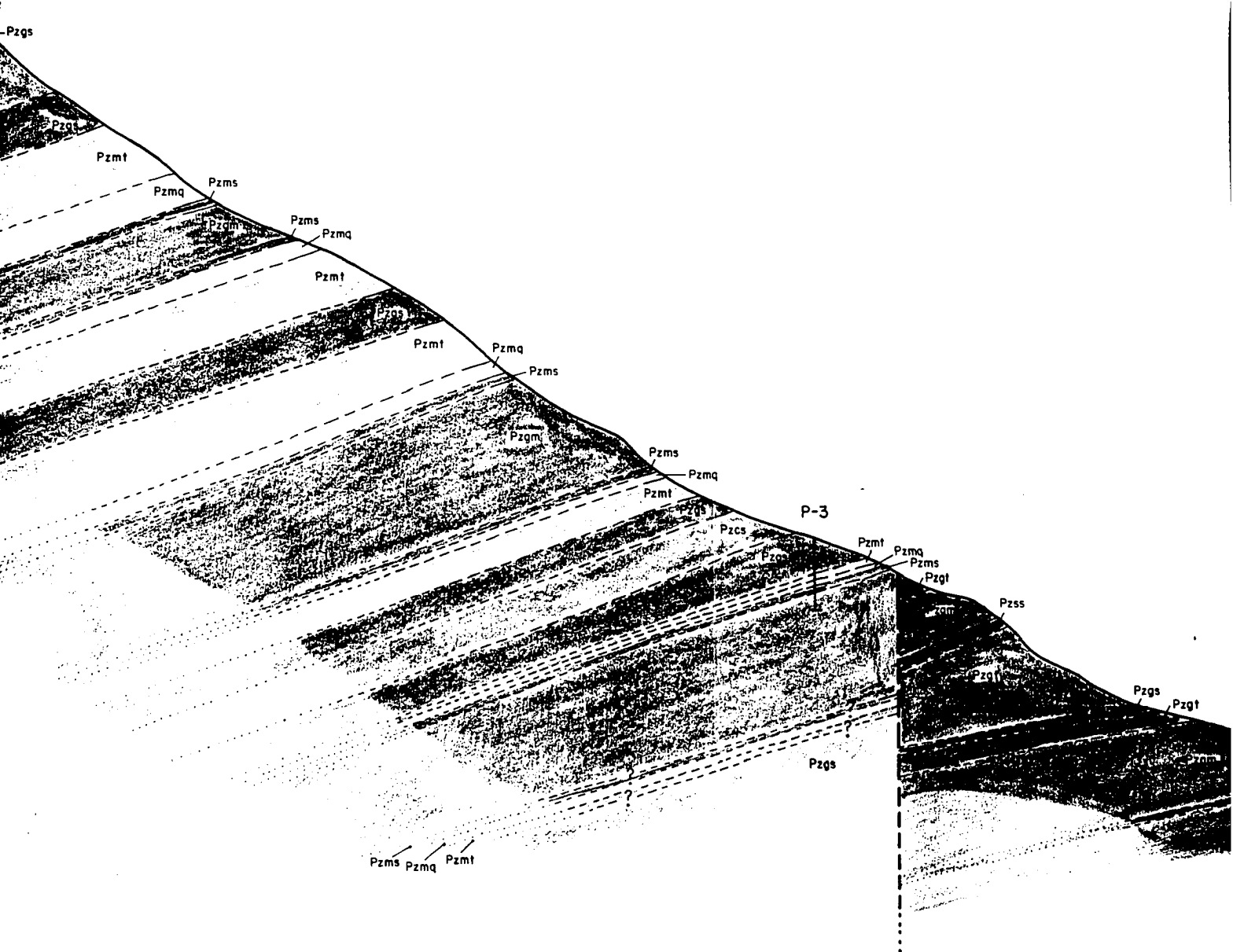
REVISED:

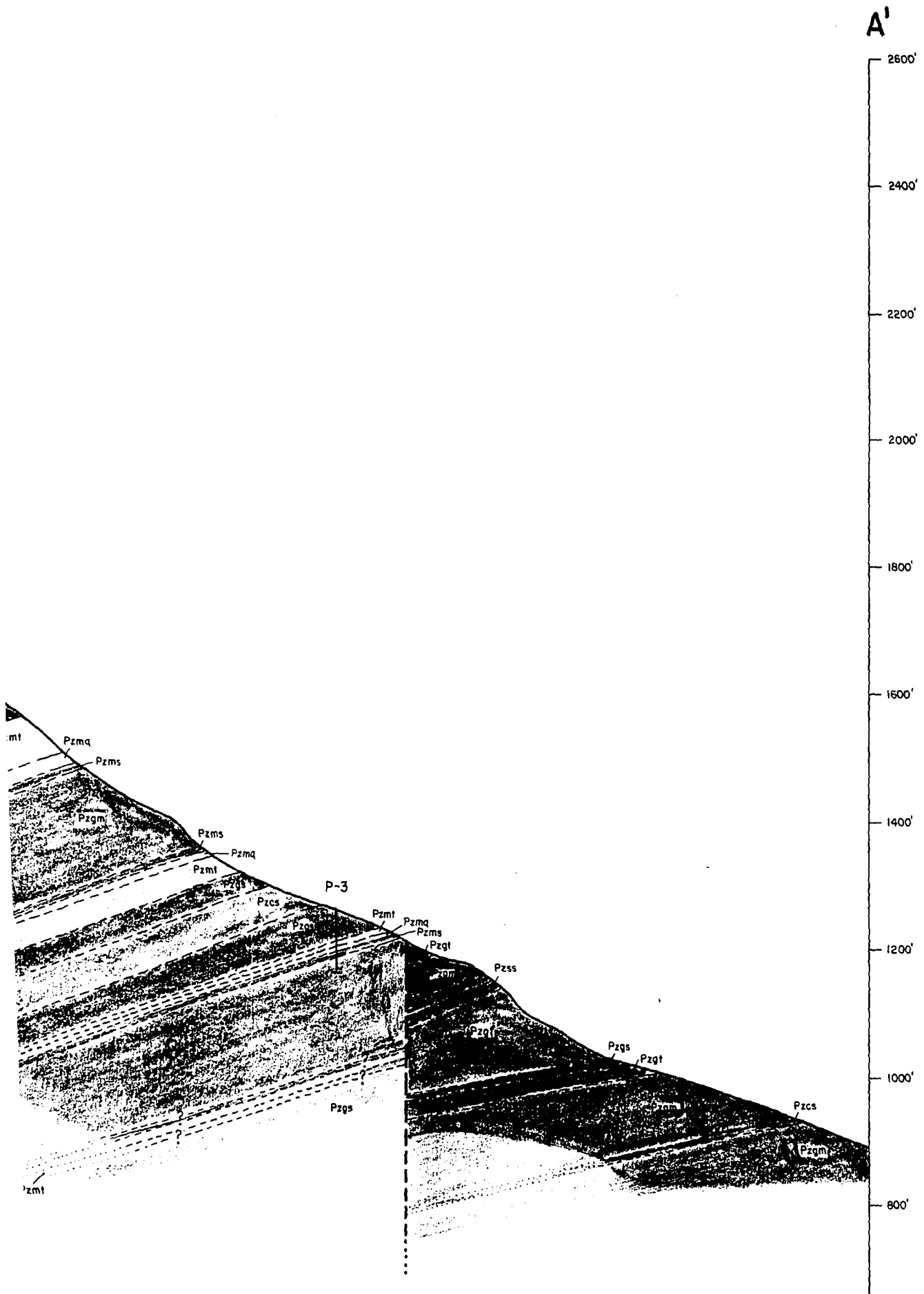
BEAR CREEK
MINING COMPANY
 ALASKA DISTRICT

A

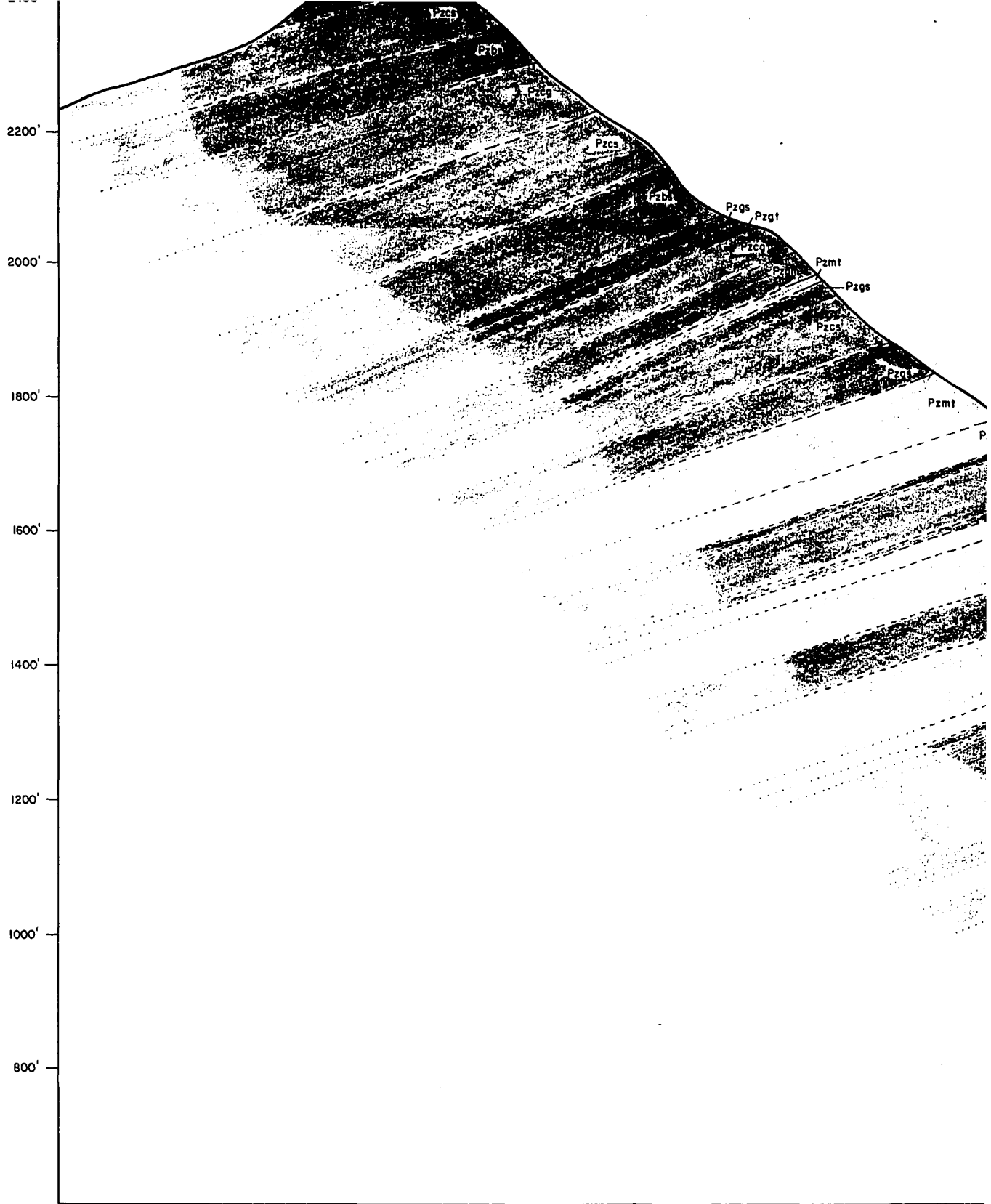
2600'
2400'
2200'
2000'
1800'
1600'
1400'
1200'
1000'
800'







Reproduced with permission of the copyright owner. Further reproduction prohibited without permission.



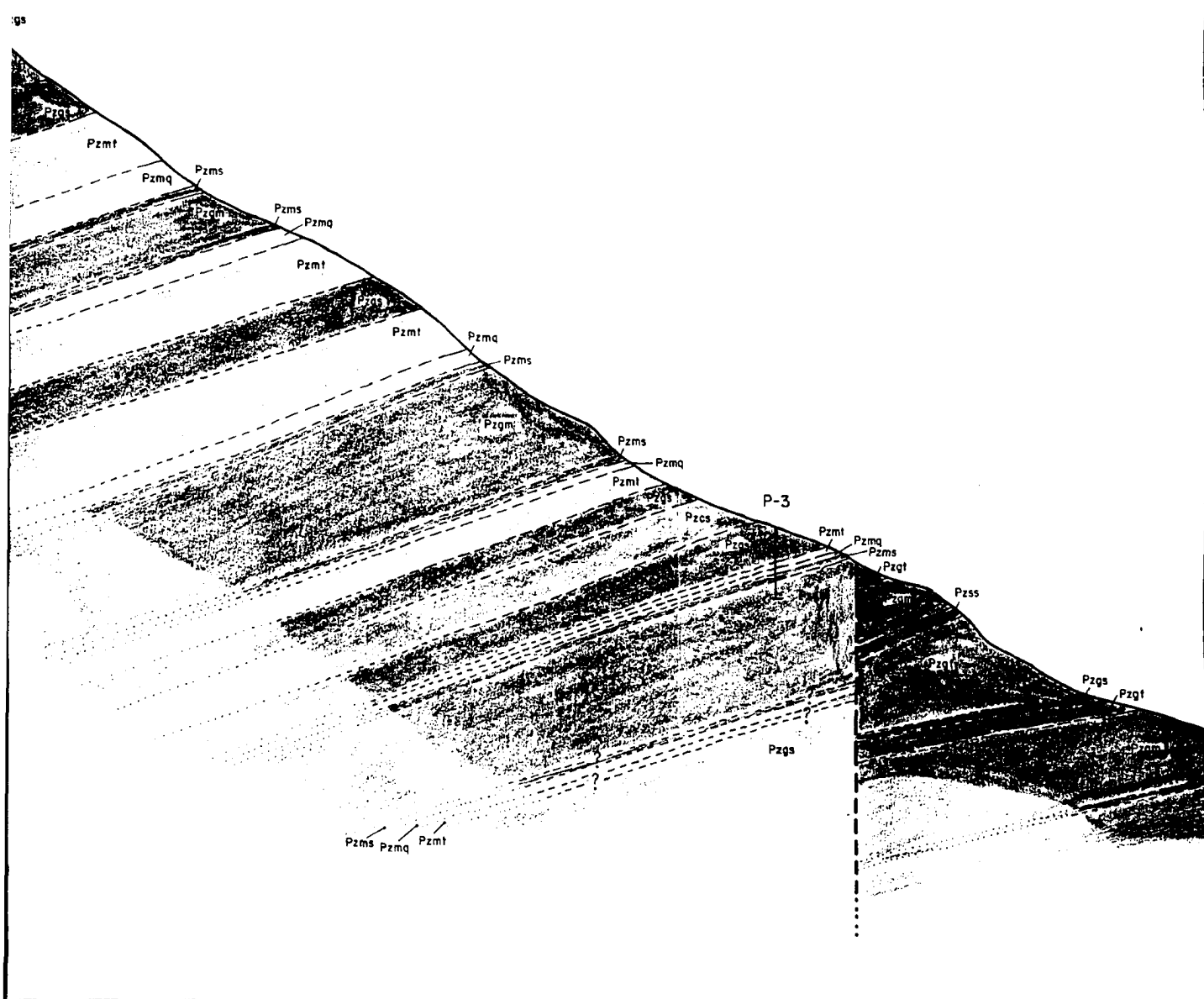


PLATE II

AMBLER 4B - CROSS

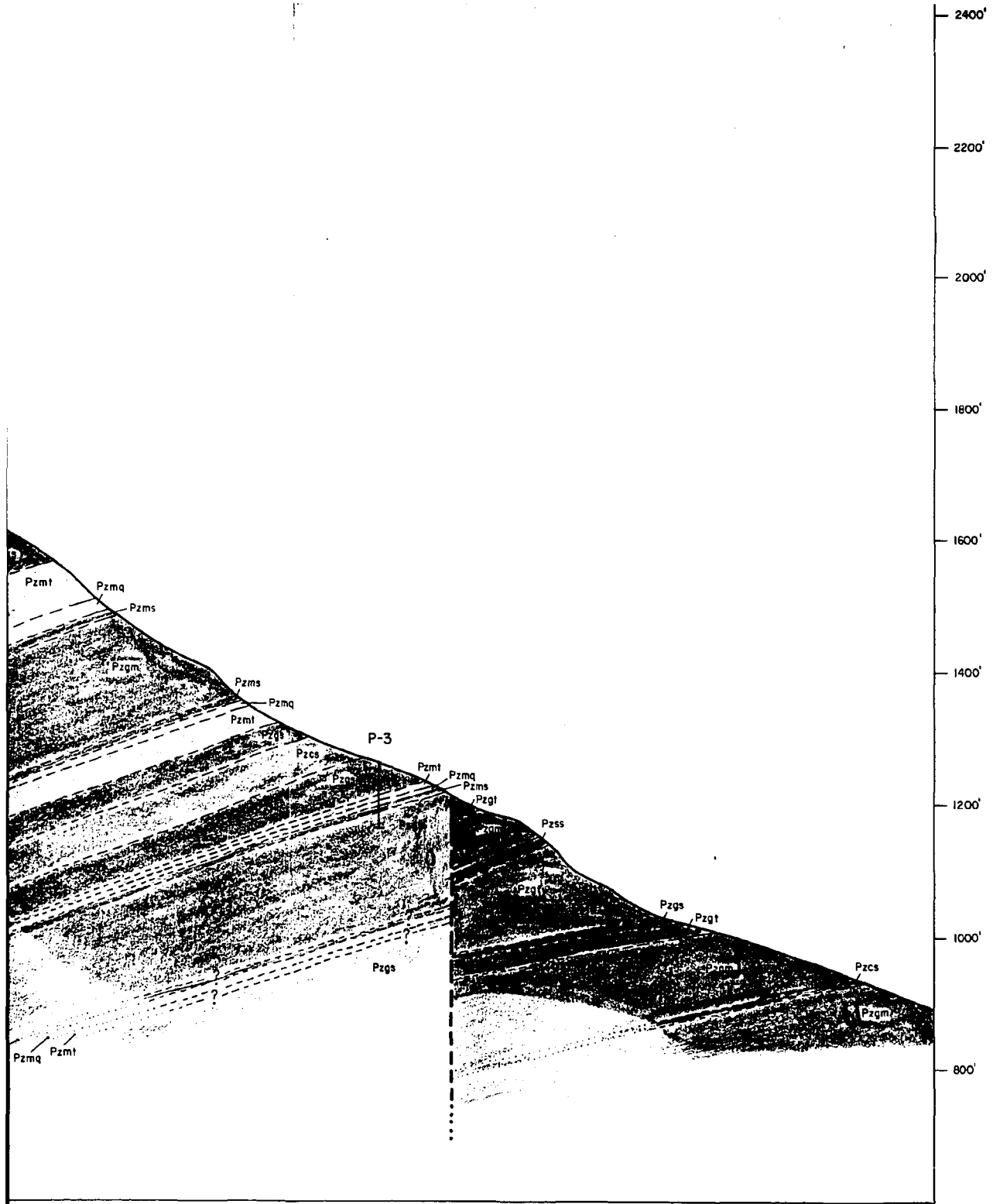


PLATE II

AMBLER 4B - CROSS SECTION